[UCI]I804:24011-200000369422

2021년 2월

박사학위 논문

우주용 전장품의 설계평가를 위한 기판 변형률 기반의 고신뢰도 구조설계 방법론에 관한 연구

조선대학교 대학원

항공우주공학과

박태용

우주용 전장품의 설계평가를 위한 기판 변형률 기반의 고신뢰도 구조설계 방법론에 관한 연구

– A Study on PCB Strain-based Structural Design Methodology for Reliable Design Evaluation of Spaceborne Electronics –

2021 년 2 월 25 일

조선대학교 대학원

항공우주공학과

박태용

우주용 전장품의 설계평가를 위한 기판 변형률 기반의 고신뢰도 구조설계 방법론에 관한 연구

지도교수 오현웅

이 논문을 공학 박사학위 신청 논문으로 제출함.

2020년 10월

조선대학교 대학원

항공우주공학과

박태용

박태용의 박사학위논문을 인준함

위원장	조선대학교	겸임교수	유 영 준 (인)
위 원	조선대학교	교수	오 현 웅 (인)
위 원	조선대학교	교수	안 규 백 (인)
위 원	전북대학교	교수	임 재 혁 (인)
위 원	㈜솔탑	책임연구원	김 홍 래 (인)

2020 년 12 월

조선대학교 대학원

Contents

LIST OF FIGURES

LIST OF TABLES

NOMENCLATURE

Z_{allow}	Allowable displacement of PCB
B	Length of PCB parallel to electronic package
c	Electronic packaging constant
t	Thickness of PCB
r	Relative position factor of package on PCB
$x,\ y$	In-plane distances of package from edges of PCB
$X,\ \ Y$	In-plane lengths of PCB
L	Length of electronic package
L	Length of package body
FoS_{m}	Factor of safety for MoS calculation
MoS	Margin of safety
ϵ_c	Critical in-plane principal PCB strain
$\dot{\epsilon}$	Strain rate of PCB
ζ	Allowable in-plane principal PCB strain
$\epsilon_{\mathrm{p_{max}}}$	Maximum in-plane principal PCB strain
$\epsilon_{\mathrm{x_{rms}}},\ \epsilon_{\mathrm{y_{rms}}}$	RMS in-plane normal strains of PCB
$\epsilon_{\mathrm{xy_{rms}}}$	RMS in-plane shear strains of PCB

σ_a	Volumetric-averaged stress
$\sigma_\mathrm{VM,e}$	Element von-mises stress
V_e	Element volume
σ'_f	fatigue strength coefficient of solder material
N_f	Number of cycles to failure
f_n	1st eigenfrequency of PCB
N	Number of cycles to failure
S	Stress of solder joint
T	Exposure time to random vibration
G	Acceleration
Z	Displacement
b	Fatigue exponent for solder material
TTF_req	Required time to failure for survival of solder joint
$T_\mathrm{x\ dB}$	0 dB equivalent exposure time during a single vibration test
t_test	Duration of a single vibration test
t_lnch	Duration of launch random vibration excitation
G_ratio	Ratio of RMS input test level to the 0 dB input
$\sum T_\mathrm{C-Q}$	Total 0 dB equivalent exposure time with respect to a set of random vibration test at component level

$\sum T_{\mathrm{S/S-A}}$	Total 0 dB equivalent exposure time with respect to a set of random vibration test at satellite system (S/S) level
$\sum T_{\mathrm{L}}$	Total 0 dB equivalent exposure time with respect to launch random vibration excitation
FoS_{ttf}	Factor of safety for time to failure
DF	Design factor for MoS calculation
N_{org}	Original criterion (2×10^7 cycles) used in the previous methodologies
N_{req}	Total number of fatigue life cycles required for survival in test and launch processes

초 록

우주용 전장품의 설계평가를 위한 기판 변형률 기반의 고신뢰도 구조설계 방법론에 관한 연구

박 태 용
지도교수: 오 현 웅
항공우주공학과
조선대학교 대학원

우주용 전장품은 임무 기간동안 위성 시스템이 필요로 하는 기능을 제공하는 역할을 수행한다. 우주용 전장품의 경우 발사 시 극심한 랜덤진동환경 하에서의 솔더접합부의 파손이 주요 임무 실패원인 중 하나이며, 성공적인 임무를 위해 솔더 접합부에 대한 구조건전성이 보장되도록 설계되어야 한다.

현재까지 우주산업 분야에서는 랜덤진동환경 하에서 전장품의 구조건전성 보장을 위한 구조설계 방법론으로 1970 년대에 제안된 Steinberg 의 피로파괴 이론이 가장 폭넓게 적용되어 왔다. Steinberg 이론은 진동환경 하에서의 전자기판 (Printed Circuit Board, PCB)의 최대 동적변위가 Steinberg 의 경험식으로부터 산출된 허용변위를 초과하지 않도록 설계될 경우, 랜덤진동에 대해 2,000 만 주기의 피로수명을 보장한다. 그러나 위의 경험식은 PCB 가 사각형이며 각 가장자리가 단순지지되어 PCB 가 반 정현파 (Half Sine)의 모드 형상을 갖는다는 가정조건

하에서 수립되었다. 이로 인해 PCB 가 비대칭적인 형상, 불규칙적인 구속 점 위치 및 보강재 적용 등에 의해 모드 형상이 복잡해질 경우, Steinberg 의 가정조건에서 벗어나 산출된 허용변위에 오차가 발생하여 솔더 접합부 평가 결과의 신뢰성 보장 측면에서 문제점이 존재한다. 특히 전자 패키지가 PCB 의 가장자리에 위치하는 등의 경계조건에 따라서는 실제 솔더부의 피로수명 대비 과도하게 긍정적인 방향으로 안전여유가 예측되는 등 부정확한 결과가 도출된다. 또한, 전술한 2,000 만 주기의 설계기준은 실제 전장품의 진동시험 및 발사 과정에서 누적되는 피로주기 대비 과도하게 많은 마진을 부여하여 전장품이 구조적으로 과잉 설계 (Overdesign)가 이뤄지는 문제가 있다. 즉, Steinberg 이론은 경우에 따라 솔더부 평가결과가 과도하게 긍정적임에 따라 충분한 보수성이 반영되지 못할 수 있으며, 이와 반대로 설계기준은 실제 필요한 설계수명 대비 과도하게 보수적일 수 있다는 것이다. 그러나 이러한 한계점에도 불구하고 대체 이론의 부재로 인해 현재까지 Steinberg 이론이 우주용 전장품 설계에 그대로 적용되고 있는 실정이다.

Steinberg 이론 외에도 선행연구에서는 다양한 솔더부 피로수명 예측 이론이 제안되었다. 그러나 상기 이론들은 수명예측을 위해 전자 패키지 및 솔더부의 실제 형상이 구현된 상세 유한요소모델 (Finite Element Model, FEM)을 필요로 하며, 이는 솔더의 응력 또는 변형률을 정확하게 예측함에 있어서는 유효하나, 다양한 전자 패키지가 다수 장착된 전장품 전체에 대한 상세 FEM 을 구축하는 것 자체가 작업자의 시간과 노력을 과도하게 소모하는 문제점이 있다. 또한 각 전자 패키지 별로 정확한 기하학적인 형상 및 재료 물성치를 수집하는 것 또한 현실적으로 어려우며 많은 시간을 필요로 하는 작업이다.

우주용 전장품 설계에 있어서 구조설계 방법론이 보다 실용적으로 활용되기 위해서는 Steinberg 이론 대비 솔더부 구조건전성 평가 결과의 신뢰도가 향상되면서도, 상세 유한요소모델에 기반한 과거의 수명예측 기법과 비교하여 신속한 FEM 구축 및 구조해석 수행이 가능해야 한다. 이를 위해 본 연구에서는 발사 랜덤진동환경 하에서 우주용 전장품의 구조건전성 평가에 있어서 전술한 한계점 극복이 가능한 새로운 개념의 PCB 변형률 기반 구조설계 방법론을 제안하였다. 제안된 이론은 솔더 응력, 변형률 또는 PCB 변위를 이용하는 전술한 기법들과 달리 PCB 변형률에 대한 설계여유 (Margin of Safety, MoS) 계산에 기반하여 랜덤진동 하 솔더부의 구조적 안전성을 평가하는 방식이며, 특히 PCB 변형률을 이용함으로서 Steinberg 이론에서 나타나는 이론적 한계점 극복이 가능함에 따라 보다 신뢰성 있는 구조 건전성 평가가 가능한 장점을 갖는다. 또한 제안된 이론은 기존 Steinberg 이론에서 적용되던 2,000 만 주기의 설계기준이 아닌, 전장품의 지상시험 단계에서 실제 발사 시까지 누적되는 피로주기에 기반한 MoS 산출이 가능함에 따라 설계수명에 대해 과도하게 보수적인 마진이 부여되는 문제점 극복이 가능하다. 또한, 본 연구에서는 전장품의 구조설계에 있어서 고신뢰도이면서도 신속한 구조건전성 평가를 위한 전자 패키지의 FEM 모델링 기법을 제안하였으며, 이에 대한 유효성을 검토하였다. 이 FEM 모델링 기법을 포함하여 본 연구에서 제안된 구조설계 방법론을 “Oh-Park 방법론”으로 명명한다.

제안 구조설계 방법론의 유효성 입증을 위해 다양한 경계조건의 PCB 상에 전자 패키지가 장착된 PCB 시편을 제작하였으며, 솔더 접합부의 피로수명 평가를 위해 제작된 시편을 랜덤진동환경에 노출시켰다. 또한, 제안 방법론을

이용하여 시험이 이뤄진 전자 패키지의 솔더접합부에 대한 구조건전성 평가를 수행하였다. 본 연구에서는 설계 방법론 평가를 위해 Plastic Ball Grid Array (PBGA), Ceramic Column Grid Array (CCGA) 및 Quad-Flat Package (QFP)의 다양한 패키지를 대상으로 실험 검증을 수행하였다. 본 연구에서 제시된 모든 분석-시험간 비교검토 결과는 Oh-Park 방법론이 우주용 전장품의 구조설계에 있어서 신속하면서도 보다 고신뢰도의 평가를 위한 설계 방법론으로서 유효함을 입증하였다.

Key Words: 우주용 전장품, 랜덤진동, 솔더접합부, 구조건전성, 구조설계 방법론

ABSTRACT

A Study on PCB Strain-based Structural Design Methodology for Reliable Design Evaluation of Spaceborne Electronics

by Park, Tae-Yong
Advisor: Prof. Oh, Hyun-Ung, Ph. D.
Department of Aerospace Engineering
Graduate School of Chosun University

The role of the spaceborne electronics is to provide the functions required for operating the satellite system during on-orbit mission. For a successful space mission, ensuring a mechanical safety on the solder joint under a severe launch random vibration environment is important because it is one of the major causes of failure in spaceborne electronics.

In space engineering field, Steinberg's fatigue failure theory has been widely used as a structural design methodology for spaceborne electronics under a launch vibration environment. This theory guarantees the fatigue life on solder joint more than 2×10^7 cycles for random vibration if the maximum printed circuit board (PCB) displacement is limited to the allowable value estimated by Steinberg's empirical formula. However, this theory has theoretical limitations as it was created under assumption of rectangular PCB with simply supported boundary conditions on the edges of the board. This leads to less reliable results of mechanical safety evaluation on solder joint caused by the inaccurate estimated allowable displacement when PCB exhibits complex mode shapes owing to asymmetric board configurations, irregular constraints, or presence of stiffeners. In particular, the inaccuracy in

allowable board displacement incurs excessively positive evaluation results in case when the package is located at the position closer to the edge of the board. In addition, design criterion of 2×10^7 cycles for the random vibration provides an excessive margin compared with the accumulated damage during on-ground vibration tests and launch of the electronics. These drawbacks have led to structural overdesign of electronics by providing excessive margins on the fatigue life of solder joints. To sum up, it is very unlikely that the Steinberg's theory provides reasonable evaluation results on solder joint in some cases of PCB configuration, whereas it's design criterion could provide too conservative margin on the fatigue life of solder joint much more than necessary. However, the Steinberg's theory has been inevitably used for the electronics design because there was no alternative solution thus far.

In addition to the Steinberg's theory, various life prediction theories were also proposed and investigated for reliable prediction of fatigue life of solder joints under random vibration environment. However, these theories require a detailed finite element model (FEM), which reflects the actual configurations of the package and solder joints. The use of detailed FEM, of course, is effective to accurately estimate the solder stress or strain response under given vibration loading. However, the construction of the detailed FEM would be extremely time and effort-consuming for implementing the analysis model of entire electronics with various types of packages. Collecting information on the geometries and material properties of each package is also difficult and exhausting task.

For the structural design methodology to be practically used for the design of spaceborne electronics, it shall provide more reliable results on the mechanical safety on solder joint compared with the Steinberg's theory. In addition, it requires much more rapid FEM construction and analysis compared with the detailed FEM used for the conventional life prediction theory. Therefore, in this study, a novel concept of a PCB strain-based structural design methodology was proposed to make up for the drawbacks of the conventional Steinberg

theory. The proposed methodology is based on the margin of safety (MoS) calculation with respect to the PCB strain, which thus enables to eliminate the theoretical limitations of Steinberg's theory. This ensures the reliable evaluation on the mechanical safety of solder joint under random vibration. In addition, the proposed methodology calculates the MoS based on the number of fatigue cycles accumulated during test and launch phases, which thus can solve the problem of excessively conservative margin on the fatigue life. In this study, the FEM modeling technique of electronic package, which provides a reliable and rapid solution to the structural design of electronics, was proposed and investigated. The structural design methodology proposed in this study, including the package modeling technique, is named as "Oh-Park methodology".

To validate the effectiveness of the proposed structural design methodology, we fabricated the sample PCB assemblies with electronic packages mounted on various boundary conditions of the boards. The fabricated samples were exposed to the random vibration environment to assess the fatigue life of solder joints. In addition, the mechanical safety on the solder joint of the tested samples were evaluated through the analysis using the proposed methodology. Moreover, the effectiveness of the proposed methodology was also evaluated with respect to various types of packages such as plastic ball grid array (PBGA), ceramic column grid array (CCGA) package and quad-flat package (QFP). All of the comparisons between the test and analysis results presented in this study indicated that the proposed Oh-Park methodology is effective as reliable and rapid solution on the structural design of spaceborne electronics.

Key Words: Spaceborne Electronics, Random Vibration, Solder Joint, Mechanical Safety, Structural Design Methodology

I. Introduction

The advances in semiconductor and electronic packaging technologies have driven the trends in space engineering, as other fields such as automotive, home electronics, and medical engineering [1-2]. As a result, the mission capability of a satellite has been continuously advancing. In addition, the bulky packages developed in earlier generation have been replaced with highly integrated electronic packages, because launch cost is proportional to the total mass of a satellite. Surface mount-type packages, such as a ball grid array (BGA) and small outline package (SOP) shown in Fig. I-1, are typical examples of these packages, and they have been widely used for various space missions [3-6]. These packages have higher component density and many more electrical connections within a smaller package size compared to conventional through-hole mounting-type packages. Therefore, they enable the implementation of a higher functional performance, and efficiently use the accommodation area of the printed circuit board (PCB) installed in the electronics.

Figure I-2 shows the typical launch and ascent process of the launcher. Spaceborne electronics experience severe mechanical loads during lift off [7]. These loads involve a steady-state acceleration owing to engine thrust, sinusoidal vibration caused by engine cutoff, and self-excited vibration called the pogo effect owing to the combustion instability of the launcher, random vibration caused by noise of the thrust, and mechanical shock caused by the separation of the launcher stage and spacecraft. Among these effects, electronics are particularly susceptible to failure under random vibration because a relative displacement between the package and PCB due to the repetitive bending behavior of the PCB incurs a fatigue fracture on the solder joint of electronic packages, which connects the package to the PCB [8]. In addition, highly integrated electronic packages such as ball grid array (BGA) and column grid array (CGA) packages have been increasingly applied to enhance the functionality and performance of spaceborne electronics. However, it is known that the solder joint configurations of these packages are more vulnerable to fatigue failure compared with former developed packages such as pin grid array (PGA) and dual in-line packages (DIP). Therefore, a suitable structural design for spaceborne electronics, using a reliable design methodology, is crucial for successful missions.

Various methodologies have been proposed to predict the mechanical reliability of the fatigue life of a solder joint under random vibration [10-29]. Most of them are based on a finite-element analysis (FEA) to determine the stress and strain responses from the critical solder joint under the given mechanical load condition, and a theoretical approach to estimate its fatigue life. Figure I-3 shows the example of fatigue life prediction approach using detailed FEM. Yu et al. [10] developed a methodology to evaluate the fatigue life on SAC305 and SAC405 solder joints of a BGA package under random vibration based on the vibration tests and FEA. The results of fatigue life prediction on the solder joint using rainflow cycle counting and Miner's rule agreed with the experimental results. Wong et al. [11] developed a fatigue life prediction model for a BGA solder joint under random vibration using the empirical formula derived from the universal slopes produced by high-cycle fatigue test data. To consider different levels of acceleration response during random vibration, this formula was combined with a three-band technique derived from a Gaussian distribution. Wu et al. [12] developed a methodology for estimating the fatigue life of a BGA solder joint under random vibration by using Basquin's power-law fatigue damage model and a linear superposition method of Miner's rule. Its effectiveness was validated by comparison of the fatigue life prediction results with the results obtained using a commercialized software of CALCE PWA. By using a similar method, Mathew et al. [13] performed fatigue life assessment on the electronic unit of a solid rocket booster for space shuttle under random vibration, to determine the number of future mission in which the unit can be used without failure. For the assessment, they used vibration time history obtained during the actual flight as an input data of FEA. In all, considerable researches on the fatigue life prediction theories on the solder joint have been performed.

However, these previously proposed methodologies have some limitations in terms of reliability prediction on the PCB of the spaceborne electronics. This is because the construction of a detailed finite-element model (FEM) requires increased time and effort as the number of electronic packages increases. This makes it extremely difficult to construct a PCB assembly with various types of packages. However, they required a detailed FEM of the package that reflects the actual configuration of the package body and solder joint. It is extremely time-consuming and requires considerable effort to construct and analyze the FEM, even for a single package. As such, the analysis of entire electronics with several PCBs and packages might be difficult in the extent of nearly impossible. Collecting information on the detailed geometry and material properties for various types of packages might be also difficult and exhausting task in many cases.

In addition to the fatigue life prediction methodologies, a commercial reliability and life prediction tool of Sherlock [30] has been recently utilized for evaluating the solder joint safety under vibration environments. Fig. I-4 shows the design and analysis process of Sherlock tool. This physics of failure-based tool is effective to predict the fatigue life of the electronics under the vibration environment by using the reliable life prediction methodology based on the PCB strain and solder and lead stresses. One of the advantageous function of the Sherlock is that it reduces the time and effort required to construct the FEM of a complex electronic PCB by using its design file such as Gerber or ODB++ files. In addition, the inherent failure mechanism of the electronics can be rapidly predicted based on the physics of the failure approach. However, even the Sherlock tool requires considerable time to construct the FEM, because the detailed geometry and material information of the electronic packages are needed. In particular, these PCB design files can be obtained only after the design has progressed to some extent, rendering the use of the Sherlock tool less efficient in the initial design stage of the electronics.

Due to the limitations of conventional methodologies described above, Steinberg's fatigue failure theory [8], proposed in the 1970s, has been also widely used as a structural design methodology for spaceborne electronics. This theory was developed to ensure more than 2×10^7 fatigue cycles for solder joints under random vibrations if the maximum displacement of a printed circuit board (PCB) is limited to the allowable value estimated by the Steinberg's empirical formula. A major advantage of this theory is that the board displacement can be estimated with reasonable accuracy even if the finite element model (FEM) of electronic package with solder joints is simplified using equivalent beam or rigid link element [31-32]. This is an efficient approach in terms of the time and effort required to construct and analyze the FEM of electronics, especially when numerous tradeoff studies are required to determine the final design. Therefore, several previous studies evaluated electronics using Steinberg's theory with finite element-based structural analysis [32-38]. Jung et al. [32] evaluated the mechanical reliability on a remote drive unit under launch random vibration based on Steinberg's theory. In addition, this theory was used for investigating the mechanical reliability of electronic PCBs for CubeSat applications [33] and the electronics for military applications [34]. In all, many studies have presented the analysis results on the mechanical safety or fatigue life of solder joint under vibration using Steinberg's theory. However, some recent study [39] reported the theoretical limitations of Steinberg's theory, which lead to difficulties in reliable evaluation of electronics. Steinberg's empirical formula was established based on the assumption of a simply supported rectangular PCB having an ideal mode shape of a half-sine wave. This assumption simplified the formula derivation; however, it caused an error in the estimated allowable displacement as the package mounting position was closer to the edge of the board. In addition, this formula cannot represent the complex mode shape of the PCB due to the presence of stiffeners on the board, an asymmetric board shape, or irregular locations of board fixation points. These drawbacks have made the Steinberg's theory to be inevitably used in space programs, despite its theoretical limitations, as no alternative solution have been provided thus far.

Another limitation of the conventional Steinberg's theory in its application as a practical design methodology for spaceborne electronics is that the design criterion in the MoS calculation provides too much margin on the fatigue life of solder joints. This problem has arisen due to the fact that the criterion of 2×10^7 cycles was not established specifically for the spaceborne electronics but for the automotive, defense or other applications. In general, spaceborne electronics are exposed to random vibrations not only in the launch phase but also in the on-ground vibration tests prior to launch. Nevertheless, the total number of fatigue cycles accumulated on the solder joint during both the test and launch phases could be much smaller than the design criterion of 2×10^7 cycles used in the previous methodologies. The problem is that the above criterion is still being used in the previous methodologies without modification. This is a significant factor for the excessive margin on the fatigue life, which leads to structural overdesign of electronics.

A recent new space trend has driven the development of small satellites weighing less than 500 kg to ensure cost-effective space programs [40-44]. The increased demand for LEO-based services, earth observation imagery and analytics facilitates growth of small satellite market as shown in Fig. I-5. To develop a low-cost small satellite, a crucial factor is the reduction in mass and volume of on-board instruments, most of which would be electronics. For this, the development of a design methodology that contributes to preventing the structural overdesign of electronics might be necessary. In addition, one of the important factors associated with the satellite development cost is the fabrication of multiple development models to enable strict design validation prior to the actual flight. An engineering-qualification model (EQM) of electronics is typically not used as a flight model (FM) owing to the stress accumulated on the hardware during the qualification level of the environmental tests [45]. However, the applicability of an EQM as FM could be favorably considered if the structural safety of the solder joint considering the total amount of fatigue damage accumulated during the tests as well as the flight is ensured by a reliable design methodology. If this is realized, it could be a feasible development approach for implementing low-cost satellites in new space era; these are the commencing points of this study.

In this study, to make up for the drawbacks of the conventionally used Steinberg's theory, we proposed a novel PCB strain-based structural design methodology that enables more reliable evaluation on the mechanical safety of solder joint in the initial structural design stage of spaceborne electronics. The failure mode evaluated by the methodology proposed in this study involves the fatigue failure of solder or lead frame induced by the random vibration excitation. The proposed methodology evaluates the mechanical safety of a solder joint based on the margin of safety (MoS) calculation with respect to the PCB strain occurred at the mounting location of electronic package. To validate the effectiveness of the proposed methodology, we fabricated the PCB samples with BGA and SOP packages mounted on the various locations of the board. These samples were exposed to the random vibration environment to evaluate the solder joint fatigue life. The effectiveness of the PCB strain-based methodology was validated by comparing the fatigue life of the tested packages and MoS of solder joints estimated from various analysis approaches. These works were first step of this study.

The second step of this study is to solve the problem of excessive margin on the fatigue life due to the design criterion proposed by Steinberg. For this, we also proposed a methodology to calculate the MoS in accordance with respect to the required time to failure (TTF_{req}) for solder joint survival during on-ground test and launch phases. The proposed approach prevents the structural overdesign of electronics by the original criterion used in previous methodologies.

In this study, the FEM modeling technique for electronic package based on the strain-based theory, which provides a reliable and rapid solution to the structural design of electronics, was also investigated for application in the proposed methodology.

The structural design methodology proposed in this study, including the FEM modeling technique, is named the Oh-Park methodology. To validate the effectiveness of the proposed methodology, sample packages mounted on the PCBs with various boundary conditions were exposed to a random vibration environment to assess the fatigue life of solder joints. These test results were compared with the MoS calculated using the proposed methodology with various FEM modeling techniques. In this study, to ensure the reliability of the proposed methodology, the validation was performed with respect to various types of packages such as plastic ball grid array (PBGA), ceramic column grid array (CCGA) package and quad-flat package (QFP). These validation results indicated that the Oh-Park methodology proposed in this study is effective for reliable and rapid evaluation on the structural design of spaceborne electronics under launch random vibration environment.

The present study describes the validation results of the “A Novel PCB Strain-based Structural Design Methodology for Reliable and Rapid Design Evaluation of Spaceborne Electronics” and proceeded as followings:

The chapter II describes the limitations of conventional Steinberg’s theory in evaluating the structural design of spaceborne electronics.

The chapter III introduces the PCB strain-based structural design methodology and differences in comparison with the conventional Steinberg’s theory. In addition, the validation results of the proposed methodology based on the fatigue life test results of PCB samples with PBGA388 packages are described.

The chapter IV introduces the PCB strain-based structural design methodology for rapid design evaluation of spaceborne electronics and its validation results based on the test results of PCB samples with PBGA388 packages. In addition, the validation results with respect to the other types of electronic packages are described.

The chapter V provides concluding remarks of this study.

The chapter VI describes the future works for practical use of the proposed structural design methodology in actual space programs.

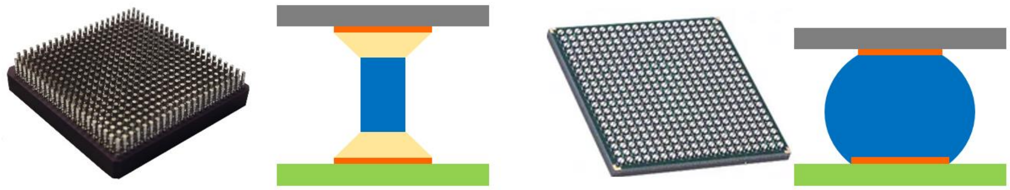

Column Grid Array (CGA) *Ball Grid Array (BGA)*

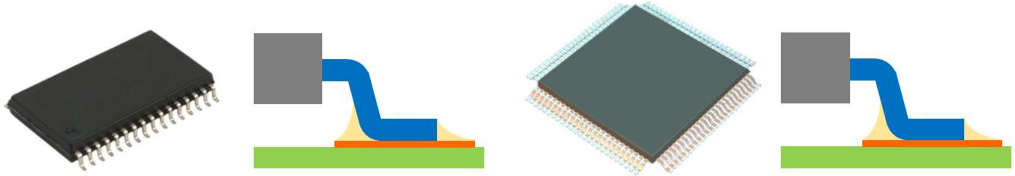

Small Outline Package (SOP) *Quad Flat Package (QFP)*

Fig. I-1 Various types of integrated electronic packages

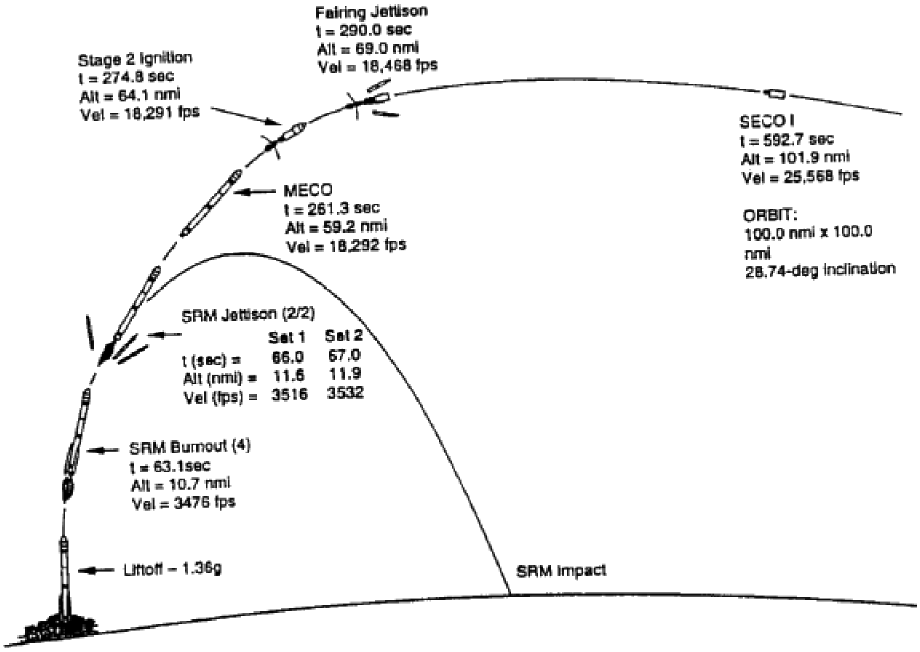

Fig. I-2 Typical launch and ascent process of launcher [9]

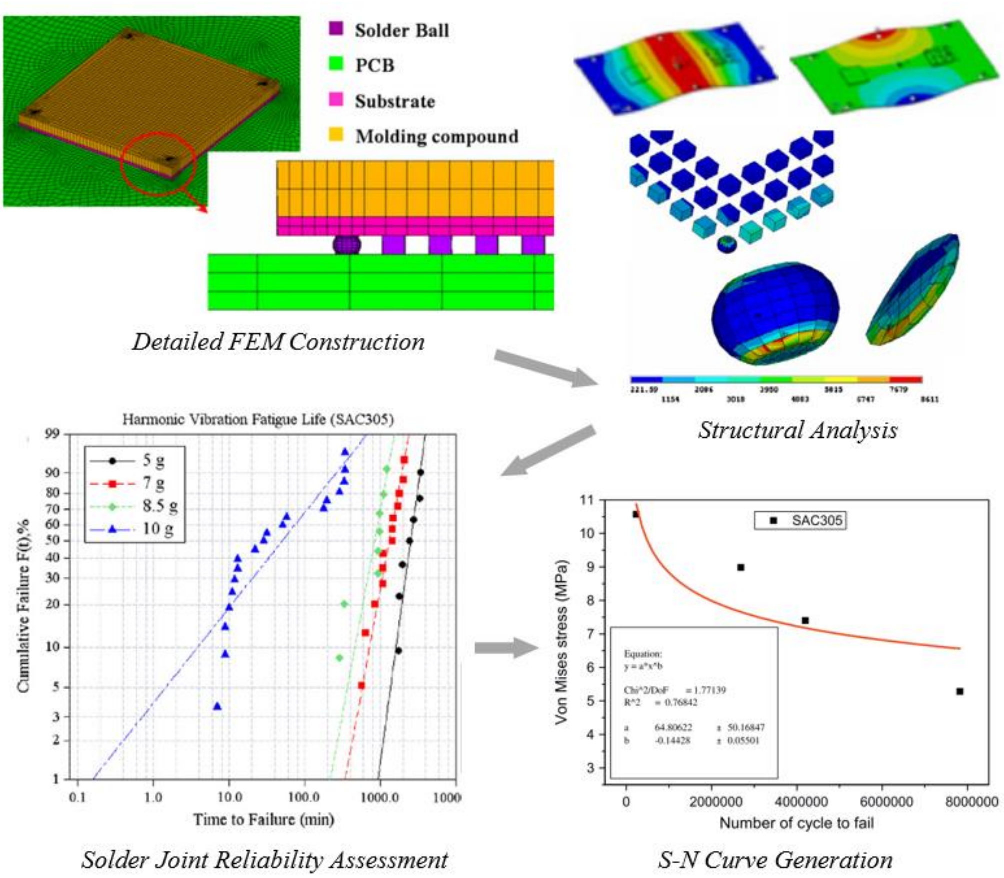

Fig. I-3 Conventional fatigue life prediction approach for solder joint under vibration [10]

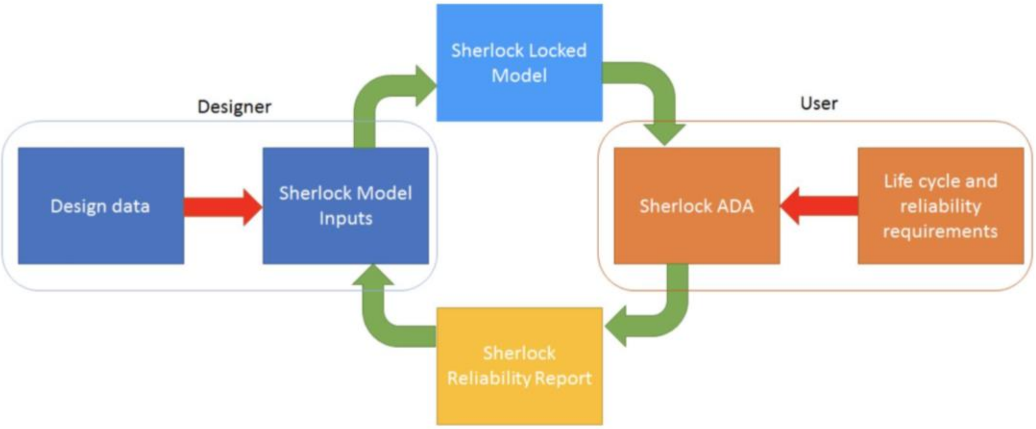

Fig. I-4 Fatigue life prediction approach using Sherlock tool [30]

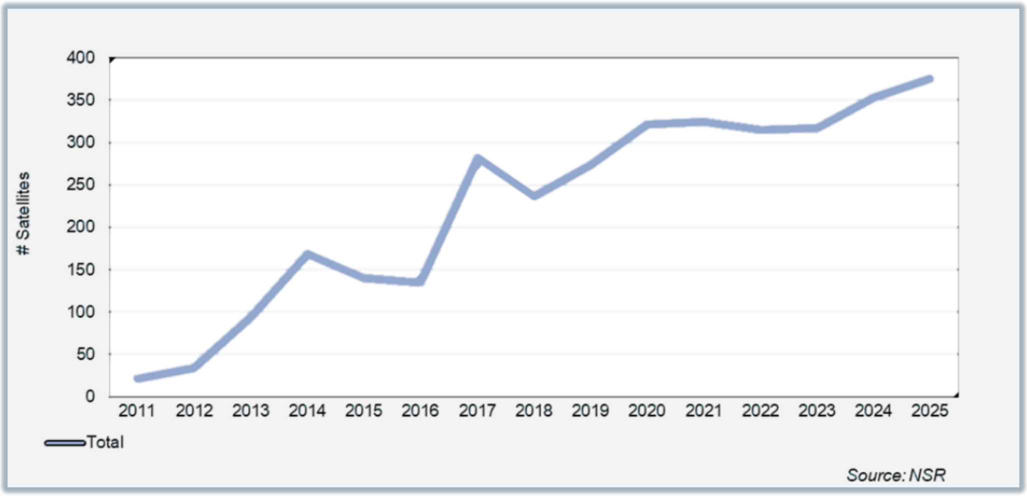

Source: NSR

Fig. I-5 Number of small satellite development in 2000-2020 [46]

II. Research Background

A. Limitation of Conventional Steinberg's Theory

Since the development of Steinberg's theory in the 1970s, it has been widely used in space programs for evaluating the solder joint mechanical safety under a launch random vibration environment [8]. Steinberg proposed an empirical formula to estimate the allowable PCB displacement, Z_{allow}, as follows:

$$Z_{\mathrm{allow}} = \frac{0.00022B}{Ctr\sqrt{L}} \tag{II-1}$$

where B is the length of the PCB parallel to the electronic package; C is a constant for different types of electronic packages, which was developed through numerous analyses and tests; t is the thickness of the PCB; and L is the length of the package. r is a relative position factor of the package mounted on the board, which is calculated as follows.

$$r = \sin\left(\frac{x}{X}\right) \times \sin\left(\frac{y}{Y}\right) \tag{II-2}$$

where X and Y are the lengths of the PCB along the in-plane directions; and x and y are the distances from the edge of the PCB to the center of the package, as shown in Fig. II-1. Steinberg established the design criterion as that the solder joint can endure more than 2×10^7 fatigue cycles for random vibration if the maximum board displacement (3-sigma displacement), Z_{max}, is limited to be lower than Z_{allow} estimated using Eq. (II-1). The MoS of the solder joint with regard to this criterion is described as follows.

$$MoS = \frac{Z_{\mathrm{allow}}}{FoS_{\mathrm{m}} \times Z_{\mathrm{max}}} - 1 > 0 \tag{II-3}$$

where FoS_{m} is the factor of safety for the MoS.

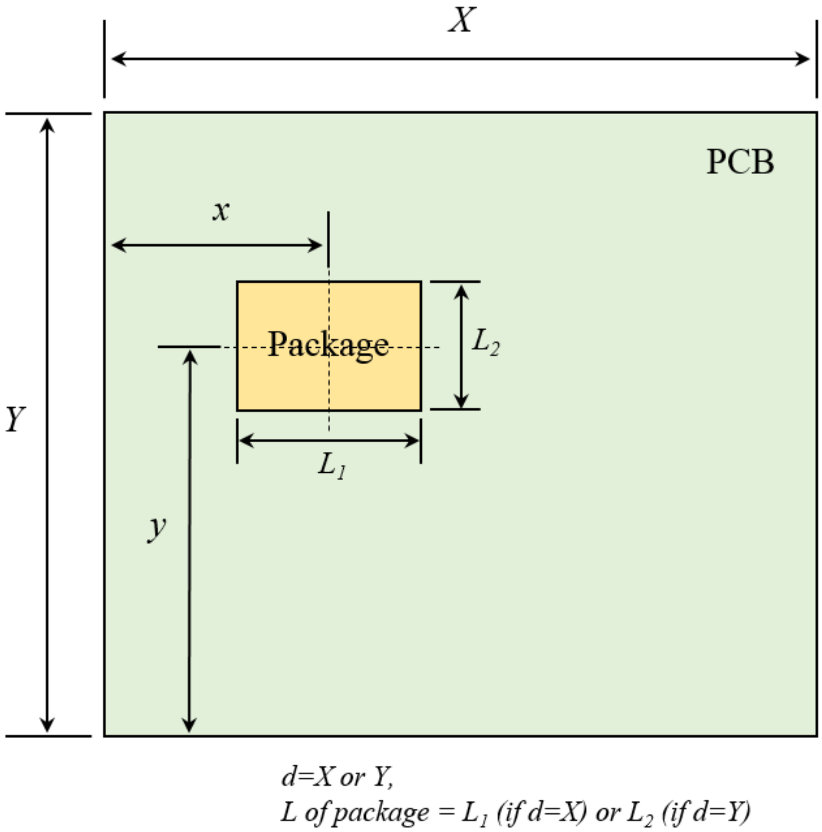

Fig. II-1 Geometrical factors for Steinberg's empirical formula (Eq. (II-1))

However, the theoretical limitations of Steinberg's theory have created several technical problems in evaluation of electronics [39]. These limitations primarily result from the empirical formula of Eq. (II-1), which was established based on the assumption of a simply supported rectangular PCB having a mode shape of an ideal half-sine wave. This is because the assumption makes it difficult to represent the dynamic deflection of a PCB having a non-half-sine mode shape. However, the PCB often presents complicated mode shapes owing to the asymmetric shape of the board, irregular locations of fixation points, and the presence of stiffeners, as the example shown in Fig. II-2. The difference between these complicated mode shapes and that assumed in Steinberg's theory leads to a calculation error in Z_{allow}. The factor r is also a major cause of the error because Z_{allow} can be over-estimated as the mounting position of the package is getting closer to the edge of the board. In addition, determining the values for B and r in Eq. (II-1) becomes ambiguous if the PCB exhibits a non-half-sine mode as the example shown in Fig. II-3. Moreover, the local strain effect acting on the package, which can be caused by the presence of adjacent packages, connectors, or mechanical fixations, is ignored if the evaluation is performed based on the board displacement using Steinberg's theory.

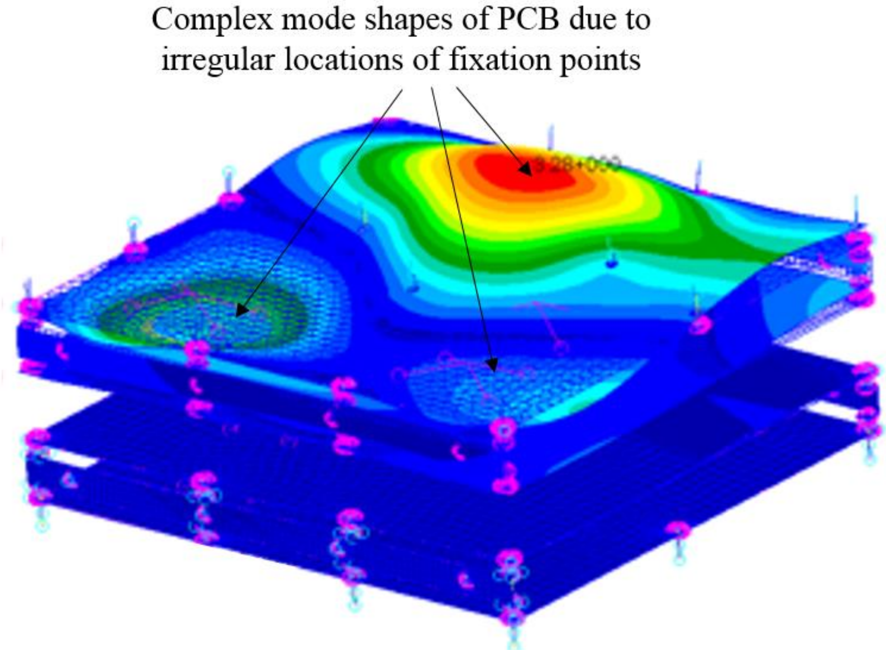

Complex mode shapes of PCB due to irregular locations of fixation points

Fig. II-2 Example of complex mode shapes of PCB

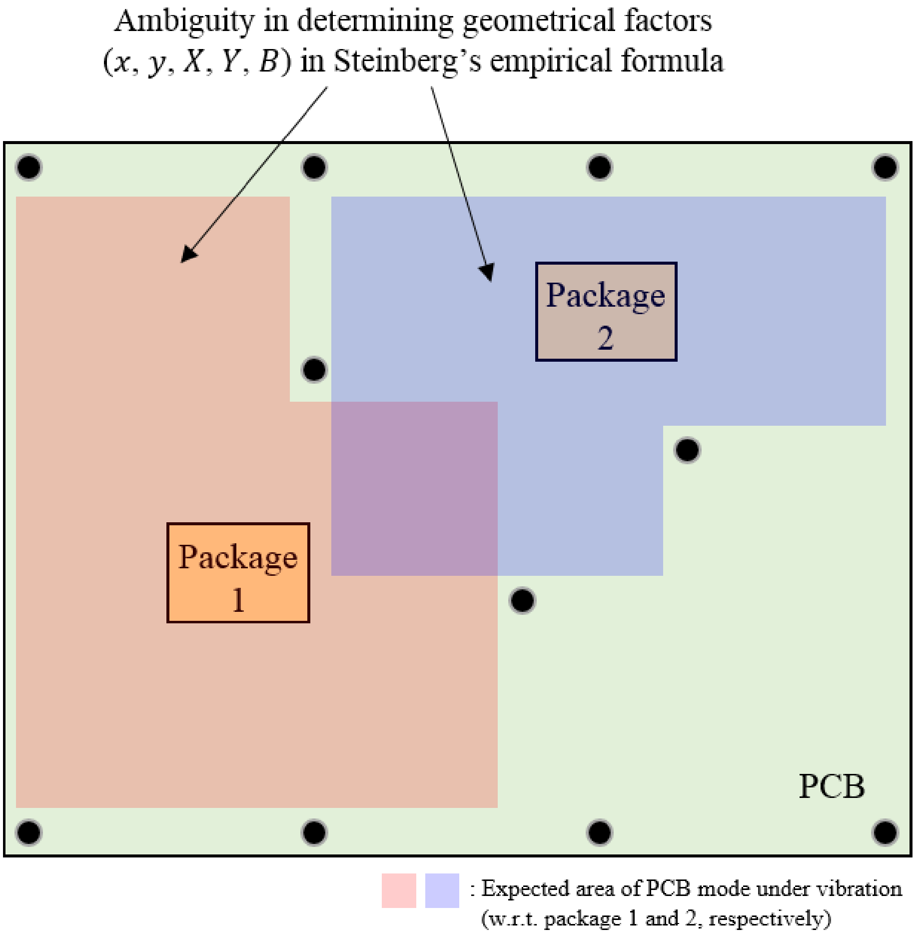

Fig. II-3 Example of PCB with irregular fixation points, making ambiguous to determine geometrical factors used for Steinberg's empirical formula

B. Limitations of Fatigue Life Prediction Methodologies

In case of an FEM for the structural analysis of the electronics, a detailed FEM that includes the actual configuration of the solder interface is effective for predicting the dynamic responses of the PCB. However, constructing such FEM requires much time and effort, especially in the case of high-density packages with BGA, SOP, and ceramic column grid array (CCGA). In addition, the computation time increases with an increased number of finite-element meshes by modeling the detail configuration of the solder interface. Therefore, the use of detailed FEM has some limitations when many trade-off studies are required to verify the effectiveness of the structural design of electronics in its initial design stage. If the package is simplified into a rigid beam and 0D mass elements, the time and effort required to develop the FEM can be saved. However, this incurs an unavoidable change in natural frequency and displacement response of the PCB. In particular, this change increases with the package size, which is one of the limitations in predicting the dynamic responses of a PCB for the mechanical safety evaluation based on Steinberg’s theory. Therefore, a more practical methodology is needed to evaluate the mechanical safety on the entire electronic unit including many integrated PCBs with various electronic packages.

Regarding the above limitation, the Sherlock tool is more applicable for FEM construction and reliability prediction of the electronics as compared to general FEA tools. This physics of failure is effective for predicting the fatigue life of the electronics under the vibration environment by using the reliable life prediction methodology based on the PCB strain. Therefore, the Sherlock tool can be applied to detect the inherent failure mechanism of the designed electronics and establish a relevant mitigation plan in its early design stage. In addition, this tool readily constructs the FEM of the electronics based on the ODB++ or Gerber design files with its internal database of various electronic packages. However, even the

Sherlock tool faces limitations in terms of saving the time and effort required for FEM construction, because a detailed geometry and material information of the packages are required to obtain proper analysis results. In addition, these PCB design files are typically available only when the design has progressed to some extent. Therefore, the Sherlock tool might be less efficient for reliability evaluation at the initial structural design stage of the electronics.

III. PCB Strain-based Structural Design Methodology

A. Description of Design Methodology

To overcome the theoretical limitations of conventional Steinberg’s theory and life prediction approaches, we proposed the use of a critical strain theory as a structural design methodology for evaluating the mechanical safety of solder joints in spaceborne electronics. The design methodology proposed in this study is called as “PCB strain-based methodology”. This methodology evaluates solder joint safety in a manner similar to Steinberg’s theory described above; however, the MoS is calculated with respect to the PCB strain and this is important difference with the conventional Steinberg’s theory. First, a critical value of the in-plane principal strain of the PCB with respect to the package, ϵ_{c}, is estimated using the formula modified from Eq. (II-1) as follows [47].

$$\epsilon_{\mathrm{c}} = \frac{\zeta}{C\sqrt{L}} \tag{III-1}$$

where C and L are the same parameters as those used in Eq. (II-1); and ζ is an allowable in-plane principal PCB strain, which replaces r and B in Eq. (II-1) to eliminate the theoretical limitations of Steinberg’s theory. ζ is calculated as follows.

$$\zeta = \sqrt{\frac{2.35}{t}} \times \{1900 - 300 \times \log(\dot{\varepsilon})\} \tag{III-2}$$

where $\dot{\varepsilon}$ is the strain rate of the PCB; $\dot{\varepsilon} = 50{,}000$, derived from the IPC-WP-011 document [48]. $\varepsilon_{\mathrm{p}_{\mathrm{max}}}$ is the three-sigma value of the root mean square (RMS) in-plane principal strain based on the Gaussian probability distribution of random vibration, which is described as follows [49]:

$$\varepsilon_{\mathrm{p_{max}}} = 3 \times \left(\frac{\varepsilon_{\mathrm{x_{rms}}} + \varepsilon_{\mathrm{y_{rms}}}}{2} + \sqrt{\left(\frac{\varepsilon_{\mathrm{x_{rms}}} - \varepsilon_{\mathrm{y_{rms}}}}{2} \right)^2 + \left(\varepsilon_{\mathrm{xy_{rms}}} \right)^2} \right) \qquad \text{(III-3)}$$

where $\varepsilon_{\mathrm{x_{rms}}}$ and $\varepsilon_{\mathrm{y_{rms}}}$ are the root mean squares (RMS) in-plane normal strains, and $\varepsilon_{\mathrm{xy_{rms}}}$ is the RMS in-plane shear strain. The multiplication factor of three is applied in Eq. (III-3) and corresponds to the three-sigma value of the RMS principal strain, considering the probability of response occurrence based on the Gaussian distribution under random vibration [8]. The MoS with regard to the PCB strain to meet the solder joint survival criterion, i.e., 2 × 10^7 random vibration cycles, can be calculated as follows.

$$MoS = \frac{\epsilon_{\mathrm{c}}}{FoS_{\mathrm{m}} \times \varepsilon_{\mathrm{p_{max}}}} - 1 \qquad \text{(III-4)}$$

The Eq. (III-4) is a core formula associated with the novelty of the proposed design methodology which has not been proposed previously.

B. Methodology Validation (PBGA324 & TSSOP48)

1. Description of PBGA388 PCB Sample

In this study, the validation of proposed PCB strain-based methodology was conducted through the comparison of the calculated MoS with the experimental results. Thus, we fabricated a PCB sample with PBGA packages and TSSOPs with the configuration shown in Fig. III-1. The numbers and locations of each package are also shown in the figure. Five 324-pin PBGA packages (U1, U4, U5, U6 and U9) and four 48-pin TSSOPs (U2, U3, U7 and U8) were mounted on the PCB, which was formed of FR-4. The total mass of the assembled PCB was 65.6 g and the dimensions were 121 mm × 107.3 mm × 1.65 mm. The boundary conditions on the PCB included a total of 10 holes for M3 screws. In addition, a solder material of eutectic Sn-Pb37 was used to mount these packages on the PCB considering the space heritages. Table III-1 lists the specifications of input random vibration for the sample test, which corresponds to the qualification level for the spaceborne electronics.

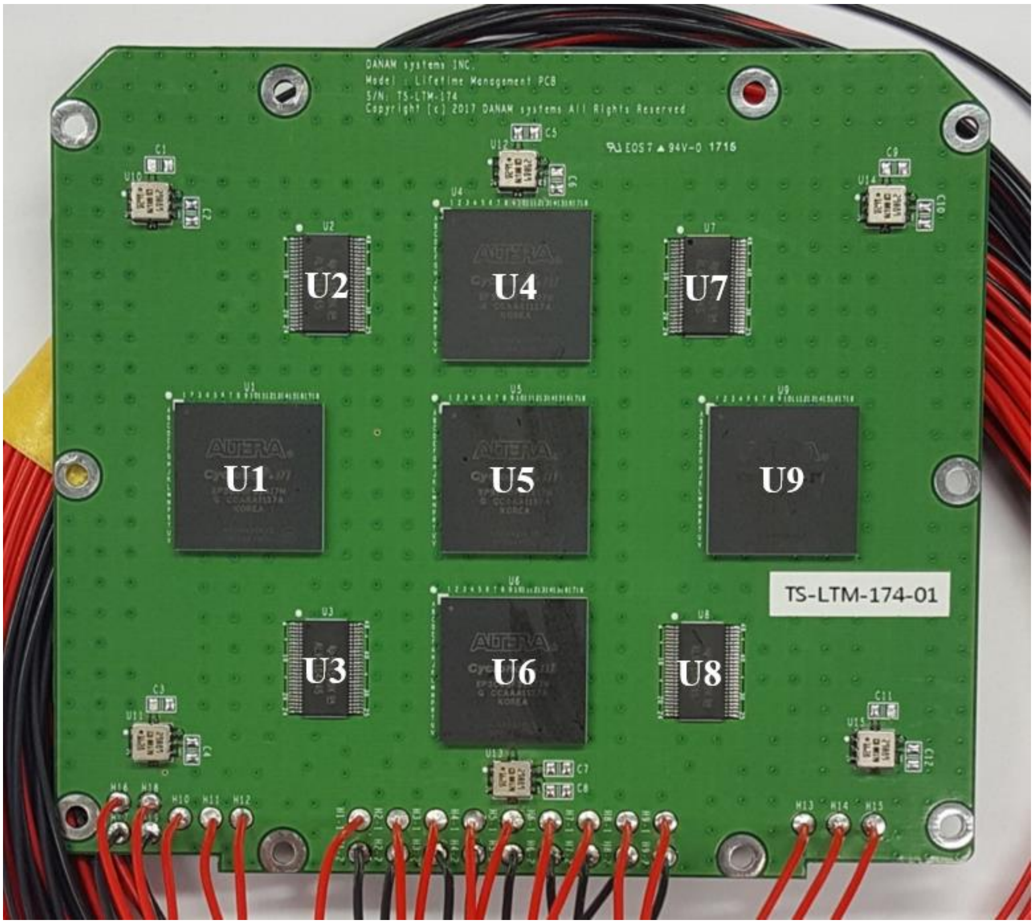

Fig. III-1 Configuration of PCB sample with PBGA packages and TSSOPs

Table III-1 Specifications of PBGA324 & TSSOP48 packages

Package no.	Configuration	Properties
U1, U4, U5, U6, U9	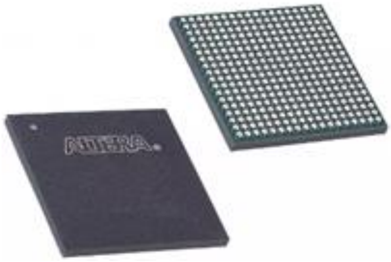	Package type: PBGA Pin count: 324 Mount type: Surface mount Size (mm): 19×19×1.6 Mass (gr): 1.4 Solder Material: Sn-Pb37
U2, U3, U7, U8		Package Type: TSSOP Pin Count: 48 Mount Type: Surface mount Size (mm): 12.5×6.1×1.1 Mass (g): 0.283 Lead material: Copper Solder material: Sn-Pb37

2. Fatigue Life Tests

Prior to the random vibration test, non-destructive inspections of the PCB samples were conducted to check the manufacturing status on the solder joint. Figures III-2 and III-3 show the representative X-ray and micro-optical inspection results for the U5 and U3 packages, respectively. The results indicated that the qualities of all solder joints were acceptable and did not any unexpected voids and initial cracks.

In the fatigue test, two PCB samples were used for guaranteeing the reliability of the test results. Figure III-4 shows a test set-up for the random vibration fatigue test of the PCB sample. An electrodynamic shaker (IMV, J260/SA78M) was used to implement the random vibration level specified in Table III-2. To measure the time to failure of each package during the tests, we used the in-situ resistance monitoring method based on the daisy-chain circuit, which connects the solder joints in series. Figures III-5 and III-6 show the daisy-chain circuit applied on the PBGA package and TSSOP, respectively. A data acquisition equipment (National Instruments, NI-9219) was used to monitor the resistance of each package at a speed of 50 samples/s. Considering the measurement error range of the equipment, the initial resistance of each packages was set to approximately 50 Ω by adding additional resistors at the end of the electrical circuit. In the test, the failure criterion on the solder joint were defined as when the daisy-chain resistance exceeded 10.5 kΩ, which is the maximum measurement limit of the test equipment.

Figures III-7 and III-8 show the test results of time histories for daisy-chain resistances for the PCB samples of cases 1 and 2. The first PCB sample of case 1 was exposed to the random vibration environment specified in Table III-2 for 7.67 h. The resistance value of the U5 package was gradually increased after 5.89 h of random excitation, and reached 10.5 kΩ, which was defined as a failure on the solder joint after 7.42 h. The resistance value of the U6 package, was increased to 1.1 kΩ during the test. To increase the reliability of the test results, the second PCB sample of case 2 was tested for 16 h. The results of Fig. III-8 indicated that the U5 package reached to failure after 6.89 h of excitation. This is almost similar to the results obtained in case 1, with a difference of 7.14%, although the resistance variation was observed after 3.02 h. In addition, the U6 package reached failure after 12.04 h. During the test, the other seven packages of both PCB samples did not show any resistance variation.

Figures III-9~III-14 show the representative SEM cross-section micrographs of the corner-most solder joints of the tested PBGA package and TSSOPs on the second PCB sample of case 2, respectively. None of the four TSSOPs showed any crack on the solder joints even after 16 h of excitation, as shown in Fig. III-9. In contrast, in the case of U5 and U6 packages, full cracks were observed along the boundary between the solder ball and solder pad at the package side, as shown in Fig. III-10~III-14. In addition, partial cracks occurred at the U1, U4, and U9 solder joints, although no resistance variations of those packages were observed during the test. This is because the resistance measurement equipment with limited accuracy could not detect the slight variation in resistance due to the micro-crack. To determine the time to failure on the solder joints of the tested packages, the SEM inspections were also conducted for the case 1 sample.

Table III-3 summarizes these results and the fatigue life on each package or both case 1 and 2 samples. The results indicated that both samples showed the same crack propagation states on the solder joint of each package, except for the U6 package, which did not reach failure criterion in the case 1 sample. The solder cracks of U1, U4, and U9 packages were initiated at some point within 7.67 h of the test. In case of the U5 package, the solder crack was initiated after 3.02 h in case 2. These results will be considered for the mechanical safety evaluation based on the MoS calculation using various methodologies proposed in this study.

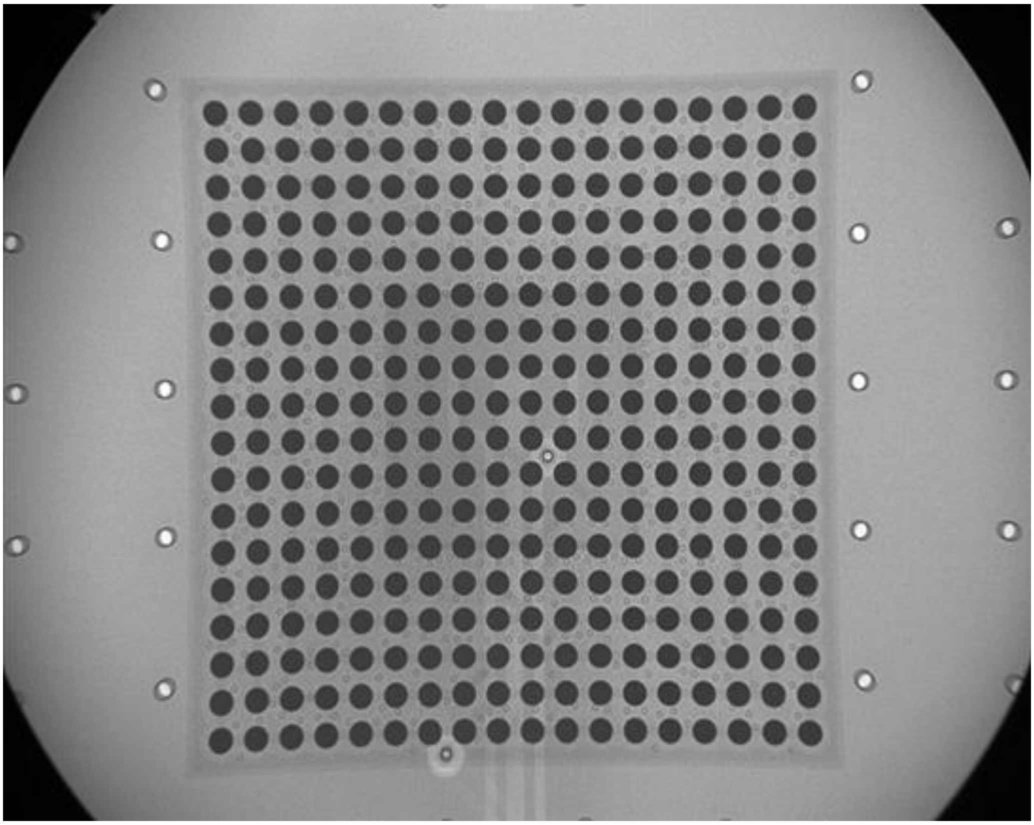

Fig. III-2 Representative X-ray inspection results on U5 BGA solder joints

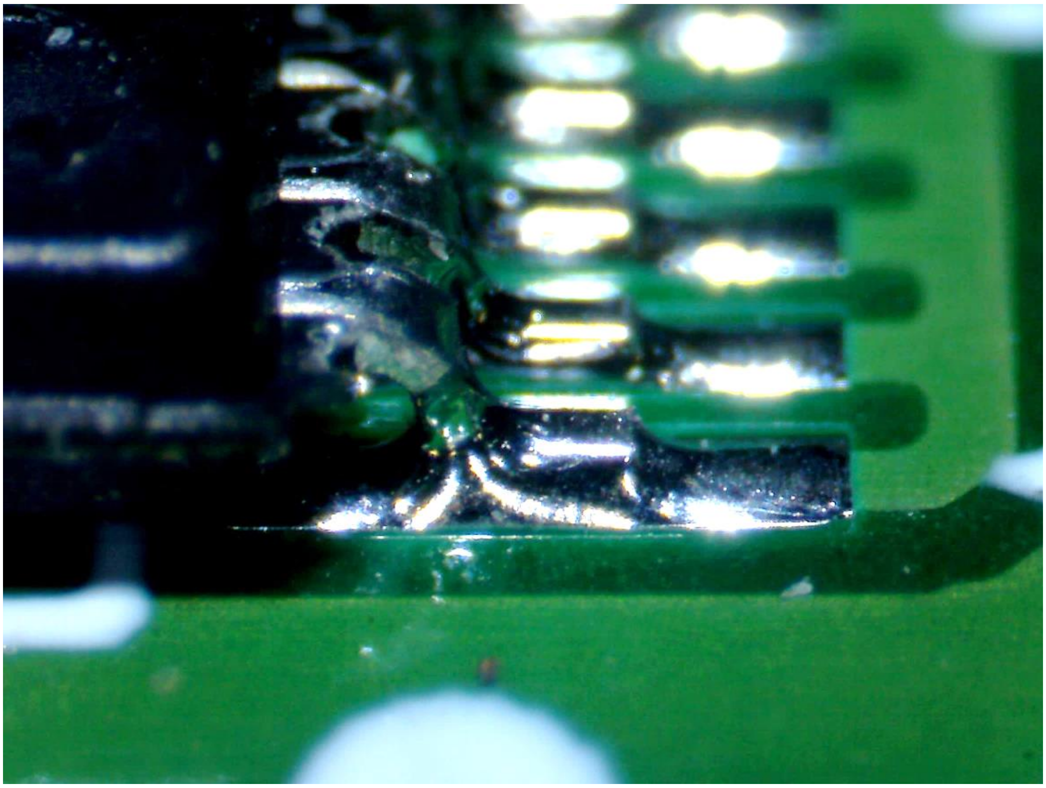

Fig. III-3 Representative optical inspection results on U3 TSSOP solder joints

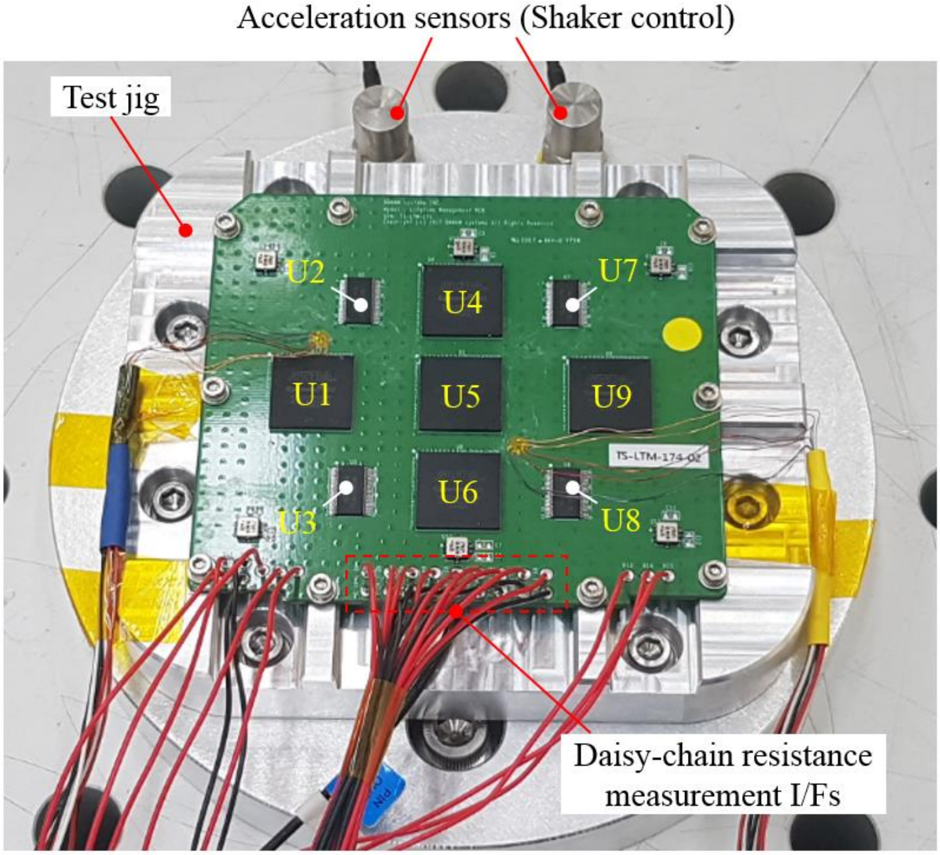

Fig. III-4 Random vibration fatigue test set-up

Table III-2 Specifications of random vibration (20 G_{rms})

Frequency (Hz)	**PSD acceleration (PSD, g^2/Hz)**
20~60	+3dB/oct
60~1,000	0.273
1,000~2,000	-6dB/oct
Overall	20 G_{rms}

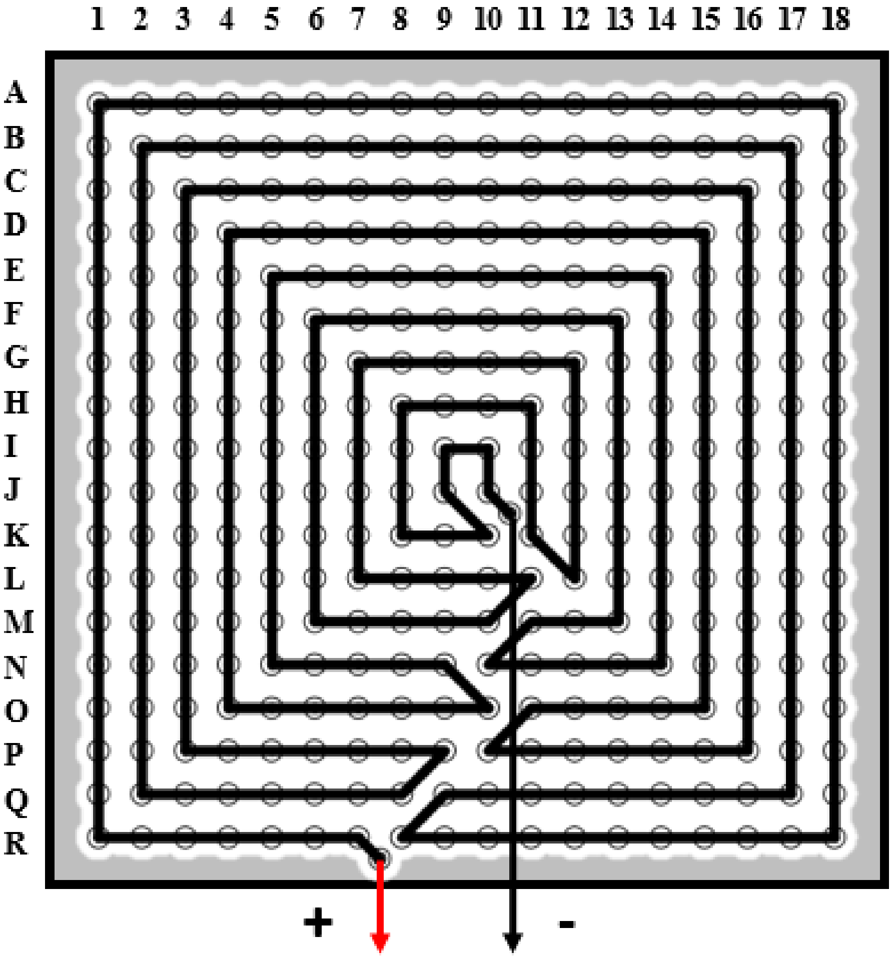

Fig. III-5 Configuration of daisy-chain circuit for PBGA324 package

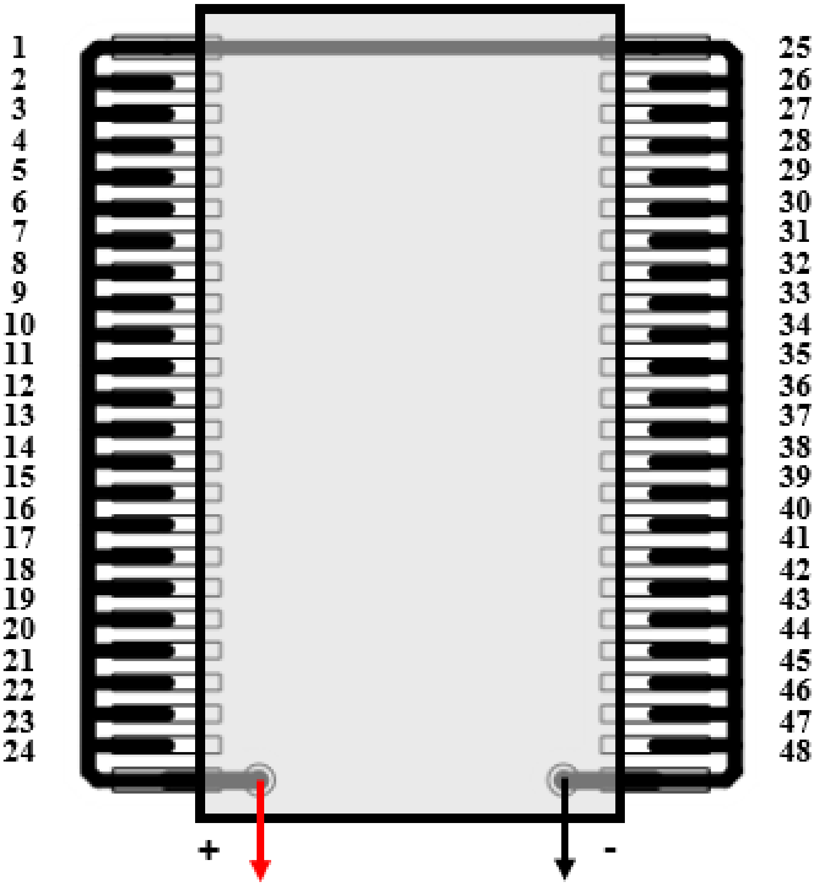

Fig. III-6 Configuration of daisy-chain circuit for TSSOP48

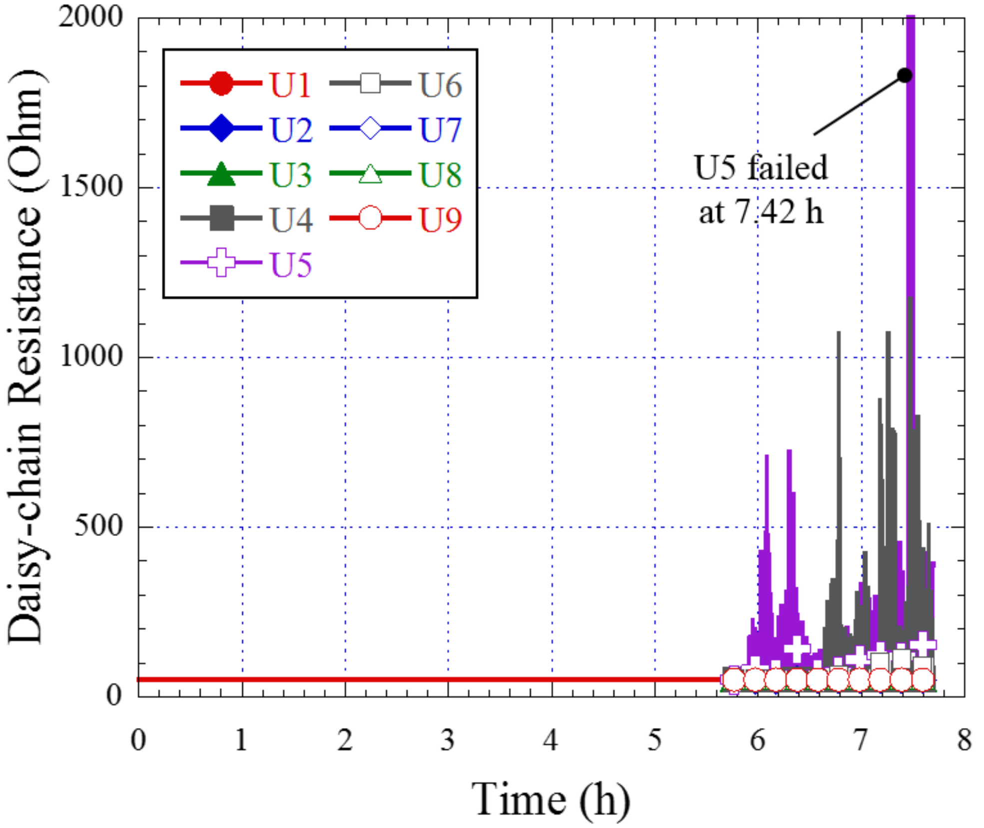

Fig. III-7 Time profiles of daisy-chain resistance on each packages of PBGA324 & TSSOP48 PCB sample #1

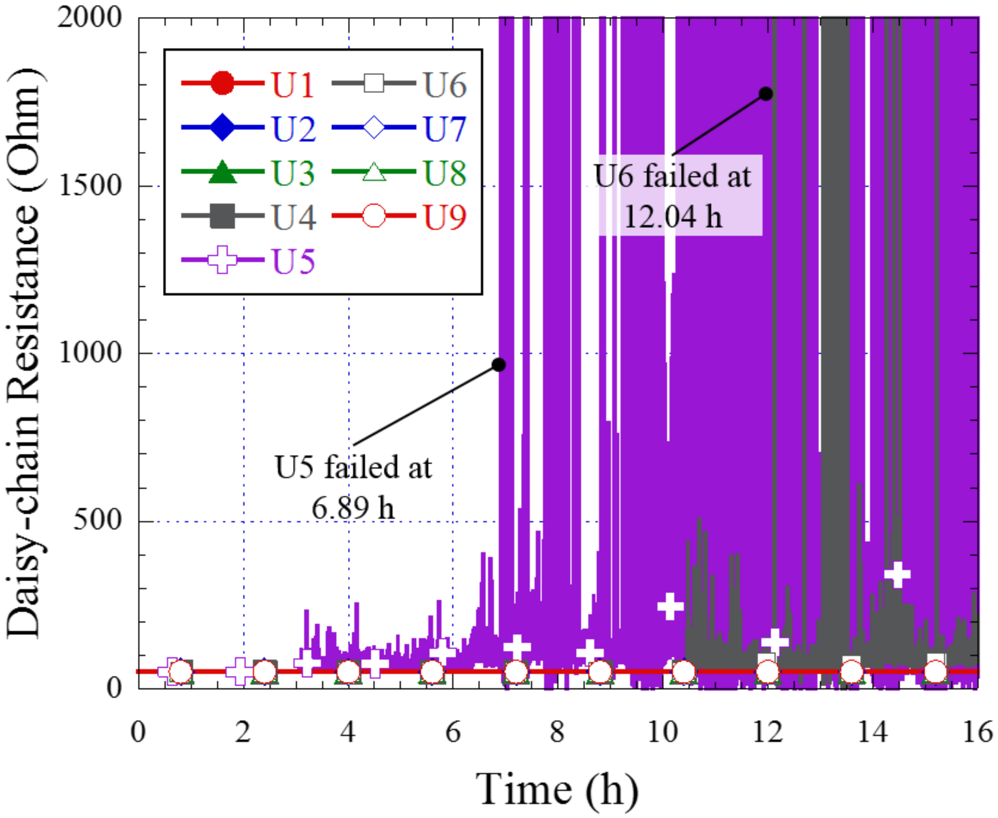

Fig. III-8 Time profiles of daisy-chain resistance on each packages of PBGA324 & TSSOP48 PCB sample #2

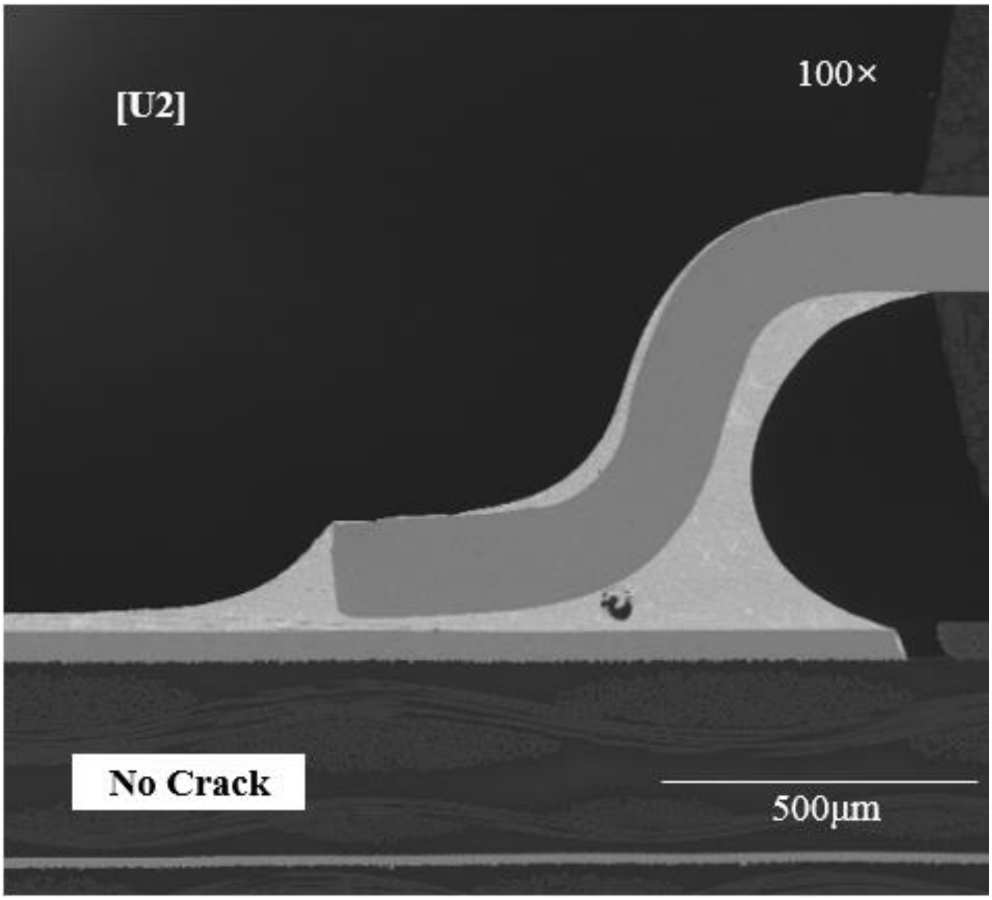

Fig. III-9 SEM micrographs on solder joint of U2 package of PCB sample #2

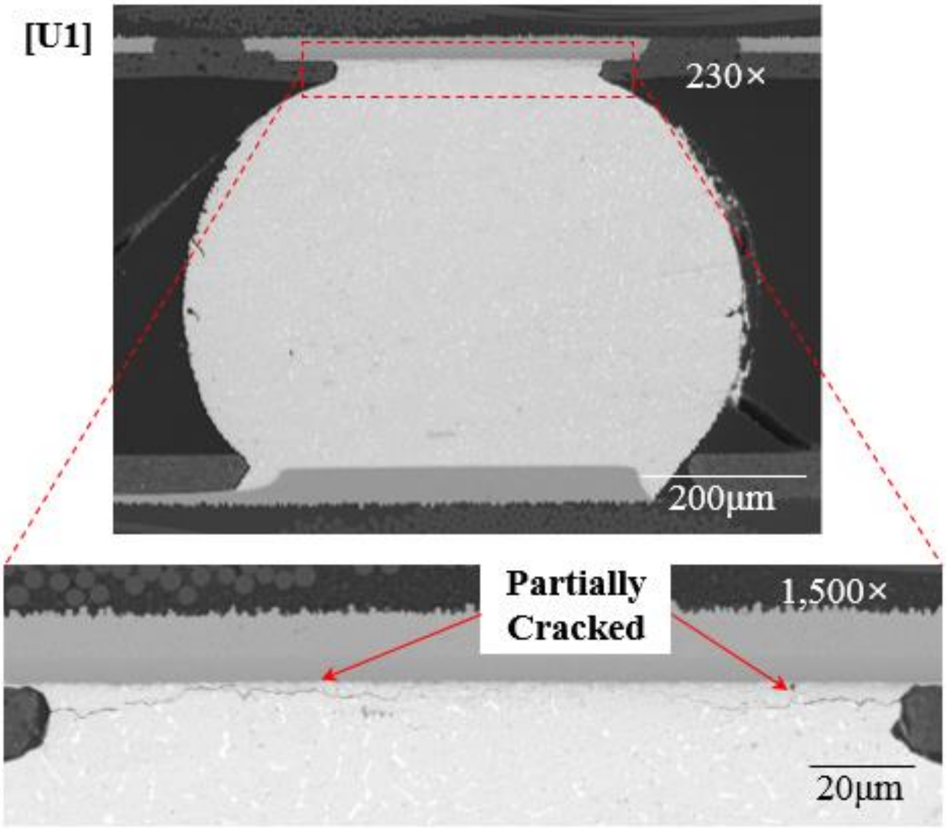

Fig. III-10 SEM micrographs on solder joint of U1 package of PCB sample #2

[U4]

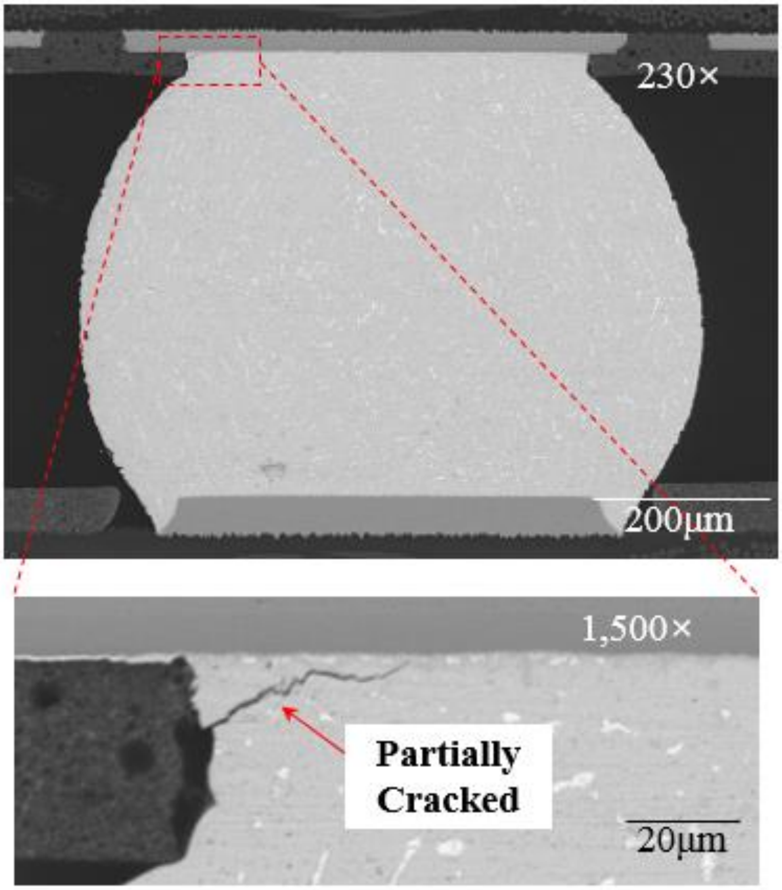

Fig. III-11 SEM micrographs on solder joint of U4 package of PCB sample #2

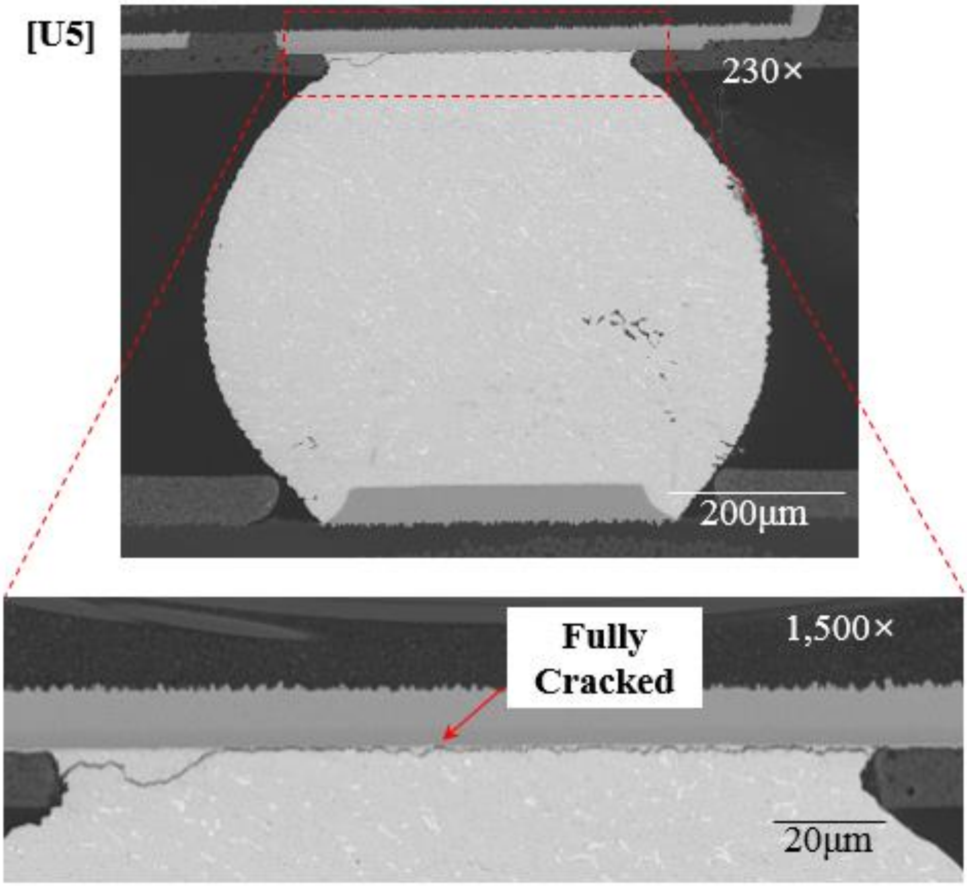

Fig. III-12 SEM micrographs on solder joint of U5 package of PCB sample #2

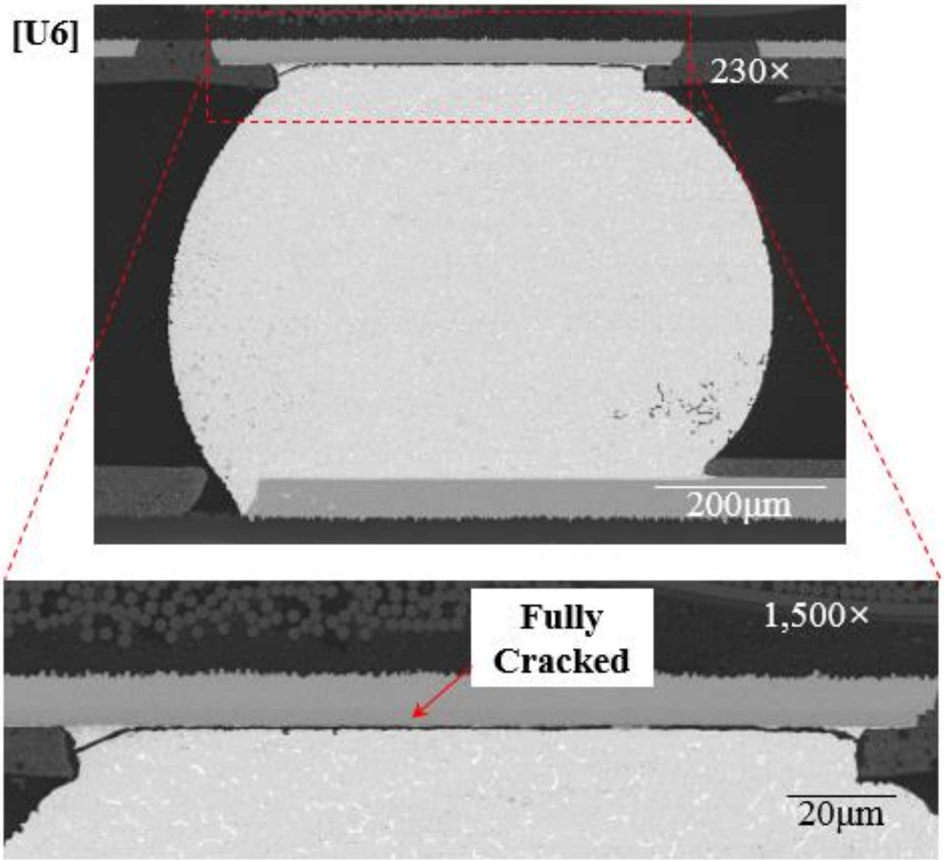

Fig. III-13 SEM micrographs on solder joint of U6 package of PCB sample #2

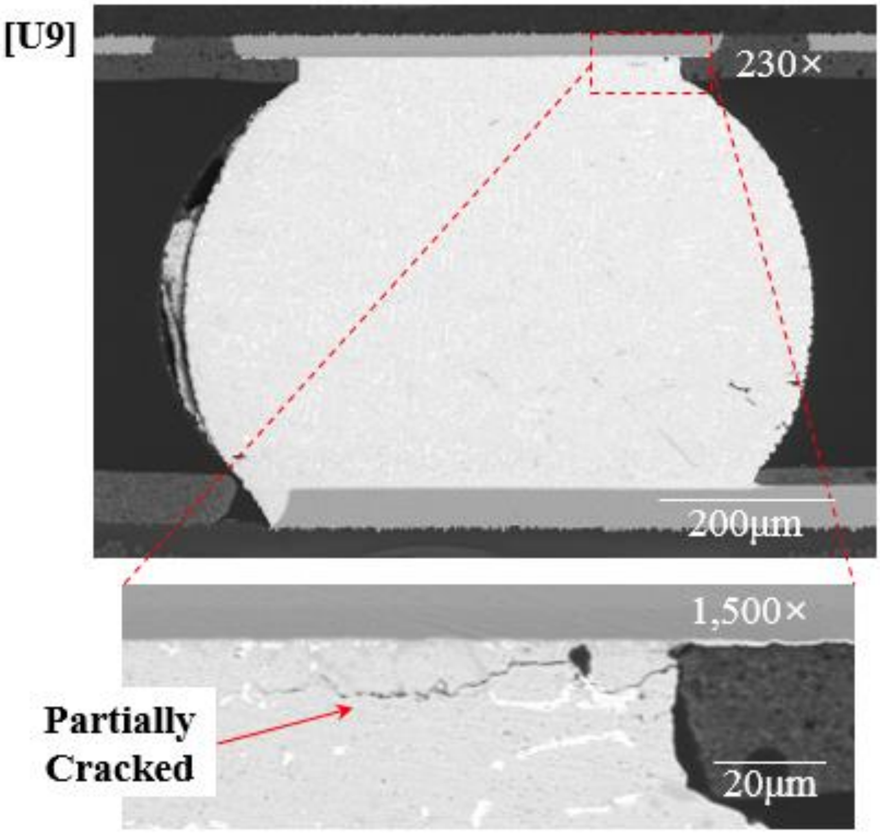

Fig. III-14 SEM micrographs on solder joint of U9 package of PCB sample #2

Table III-3 Summary of crack propagation state and time to failure on each package

Package no.	**Case 1**		**Case 2**	
	Crack propagation	***TTF* (h)**	**Crack propagation**	***TTF* (h)**
U1	Partial crack	< 7.67	Partial crack	< 16
U2	No crack	> 7.67	No crack	> 16
U3	No crack	> 7.67	No crack	> 16
U4	Partial crack	< 7.67	Partial crack	< 16
U5	Full crack	7.42	Full crack	6.89
U6	Partial crack	< 7.67	Full crack	12.04
U7	No crack	> 7.67	No crack	> 16
U8	No crack	> 7.67	No crack	> 16
U9	Partial crack	< 7.67	Partial crack	< 16

C. Mechanical Safety Evaluation

To find a more practical structural design methodology for electronics in the structural design phase, we proposed evaluation approaches to assess the mechanical safety on the solder joint of various packages as shown in Fig. III-15; these were derived from the MoS calculation based on Steinberg's theory and the PCB strain-based methodology, respectively. In this study, FoS_{m}=1.11 was used for the MoS calculation. This value is equivalent to a safety factor of 2.0 in the fatigue life for the Sn-Pb37 solder [8].

As a first step for evaluating the effectiveness of our proposed methodologies, we constructed a detailed FEM for the PCB sample, as shown in Fig. III-16. The MoS of each package was calculated based on the displacement and strain responses predicted from the random vibration analysis with the random input profile specified in Table III-2. In addition, the calculated MoS was compared with the fatigue test results described in Table III-3. Here, the methodologies based on Steinberg's theory and the PCB strain-based methodology are named as STT-RV-1 and CST-RV-1, respectively.

In the analysis, the detailed FEM reflects the actual configuration of the package, solder, solder pad and lead frame. The model consists of 738,995 nodes, 496,906 CPENTA elements, 84,764 CHEXA elements, and 20 rigid link elements. As the boundary condition, six degrees of freedom (DOFs) were constrained on the screw holes of the PCB. Table III-4 lists the material properties used for the detailed FEM. Fig. III-17 shows the representative mode shapes of the PCB sample. The modal analysis results indicated that the first eigenfrequency was 641.53 Hz.

Table III-5 summarizes MoS of each package calculated using the STT-RV-1 and CST-RV-1 methodologies. The calculated MoS values showed positive margin with respect to all

TSSOPs. In case of the PBGA packages, the MoS values obtained using the STT-RV-1 methodology showed a positive margin for the U1 and U9 packages, although these packages showed partial crack on the solder joint in the fatigue tests, as shown in Fig. III-10~III-14. On the other hand, the results obtained using the CST-RV-1 methodology showed negative margin for all PBGA packages. This well represents the fatigue test results which showed cracks on the solder joints of the PBGA packages. These results indicate that the CST-RV-1 methodology, based on the PCB strain-based methodology, is more effective for evaluating mechanical safety on the solder joint as compared to the STT-RV-1 methodology, based on Steinberg's theory.

We proposed another design approach that calculates MoS based on the quasi-static analysis. For this, we derived the random equivalent quasi-static load of 83.45 G_{rms} calculated by the Mile's equation as follows [9].

$$G_{\mathrm{rms}} = \sqrt{\left(\frac{\pi}{2}\right)(f_{\mathrm{n}})(Q)\left(PSD_{\mathrm{f_n}}\right)} \qquad \text{(III-5)}$$

where Q indicates the amplification factor and PSD_{f_n} is the input PSD acceleration at the first eigenfrequency of f_n.

By applying this methodology, the mechanical safety on the solder joint can be more simply evaluated while reducing the computation time as compared to the previous methodologies based on the random vibration analysis. Here, the methodologies based on Steinberg's theory and PCB strain-based methodology are named as STT-QS-1 and CST-QS-1, respectively. The MoS values calculated using these methodologies are summarized in Table III-6. The results indicated that only the U5 package showed a negative margin from the STT-QS-1 methodology. In contrast, the results based on CST-QS-1 methodology indicated a negative margin with respect to all PBGA packages. This also represents the fatigue test results well which showed cracks on the solder joint of PBGA packages. In addition, these results are similar to those obtained using the CST-RV-1 methodology although there are some differences in the calculated MoS values. This indicates that the CST-QS-1 methodology is also effective in evaluating the mechanical safety on the solder joint, similar to the CST-RV-1 methodology, even though the analysis method is much simpler than that of random vibration analysis.

However, the construction of a detailed FEM of the entire package shown in Fig. III-16 requires much time and effort. In addition, the use of such a large-sized FEM for the analysis at the electronic box level requires a significantly longer computation time. Therefore, in this study, the detailed FEM was simplified using 0D lumped masses and rigid link elements to model the masses of the package and solder joint, as shown in Fig. III-18, respectively. The first eigenfrequency calculated from this model was 611.06 Hz, which showed a difference of only 4.75% compared to that of the detailed FEM. The random equivalent static load of 80.46 G_{rms} was used for the quasi-static analysis. Here, the methodologies based on Steinberg's theory and the PCB strain-based methodology are named as STT-QS-2 and CST-QS-2, respectively.

Table III-7 summarizes the results of MoS calculation based on the STT-QS-2 and CST-QS-2 methodologies. The results indicated that only the U5 package showed negative margin when calculating the MoS based on the STT-QS-2 methodology. This is similar to those based on the STT-QS-1 methodology. In case of the CST-QS-2 methodology, the MoS results showed negative margin with respect to all PBGA packages, which well represents the fatigue test results of PBGA packages shown in Fig. III-10~III-14. These results indicate that the CST-QS-2 methodology is more effective for the mechanical safety evaluation than the STT-QS-2 methodology. Further, the simplified FEM is effective for evaluating the mechanical safety on the solder joint as the detailed FEM shown in Fig. III-16. Moreover, the time to failure on the solder joint, estimated by dividing the 20 million critical fatigue cycles into the first eigenfrequency of PCB, was approximately 9.09 h. Therefore, the calculated MoS well represents the fatigue test results shown in Table 4 because all PBGA packages actually failed within 7.67 h of excitation.

Table III-8 summarizes the computation time of modal, random vibration and quasi-static analyses for each methodology. By using the simplified FEM and quasi-static analysis approach, the CST-QS-2 methodology needs much less computation time compared to the CST-RV-1 methodology. Therefore, it can be applied methodology for the mechanical safety evaluation of electronics including many integrated PCB with various packages.

To validate the effectiveness of the CST-QS-2 methodology for evaluating the mechanical safety on the ceramic column grid array (CCGA) package, we also performed an additional fatigue test on the PCB sample under random vibration excitation. In addition, the test results were compared with the MoS calculated from the CST-QS-2 methodology. The PCB sample used in this study was formed of FR-4 with a dimensions of 100 mm × 100 mm × 2 mm and a total mass of 51.08 g. A daisy-chained 624-pin CCGA package with dimensions of 32.5 mm × 32.5 mm × 4.88 mm and a mass of 13.28 g was mounted at the PCB center. The materials of solder and solder column were Sn-Pb37 and Sn-Pb90, respectively. Figure III-19 shows the fatigue test set-up. In the tests, the PCB sample was exposed to 28 G_{rms} of the random vibration for 20 min. In-situ monitoring of the daisy-chain resistance of the CCGA package was performed during the test. The failure criterion on the solder joint was same as that used in the test shown in Fig. III-4. Figure III-20 shows the time history of daisy-chain resistances for the PCB sample. The CCGA package rapidly reached a resistance value of 10.5 kΩ, defined as a failure on the solder joint, after approximately 5.38 min. The optical microscope inspection results shown in Fig. III-21 indicate full cracks on several solder columns located at the corner of the package.

A simplified FEM was constructed in the form shown in Fig. III-18. The f_n analyzed by this FEM was 350 Hz. The equivalent static load calculated from PSD_{f_n} of 0.404 G^2/Hz was 64.47 G_{rms}. Since the variable C for the CCGA package has not been developed so far, we used a value of 1.75 to calculate ε_c in Eq. (III-1). This value was originally used for the BGA package [8]. The calculated MoS shown in Table III-9 indicated a negative margin. Therefore, these well represent the test results of cracks on the solder joint. These results indicate that the CST-QS-2 methodology proposed in this study is also effective for evaluating mechanical safety on the solder joint of the CCGA package.

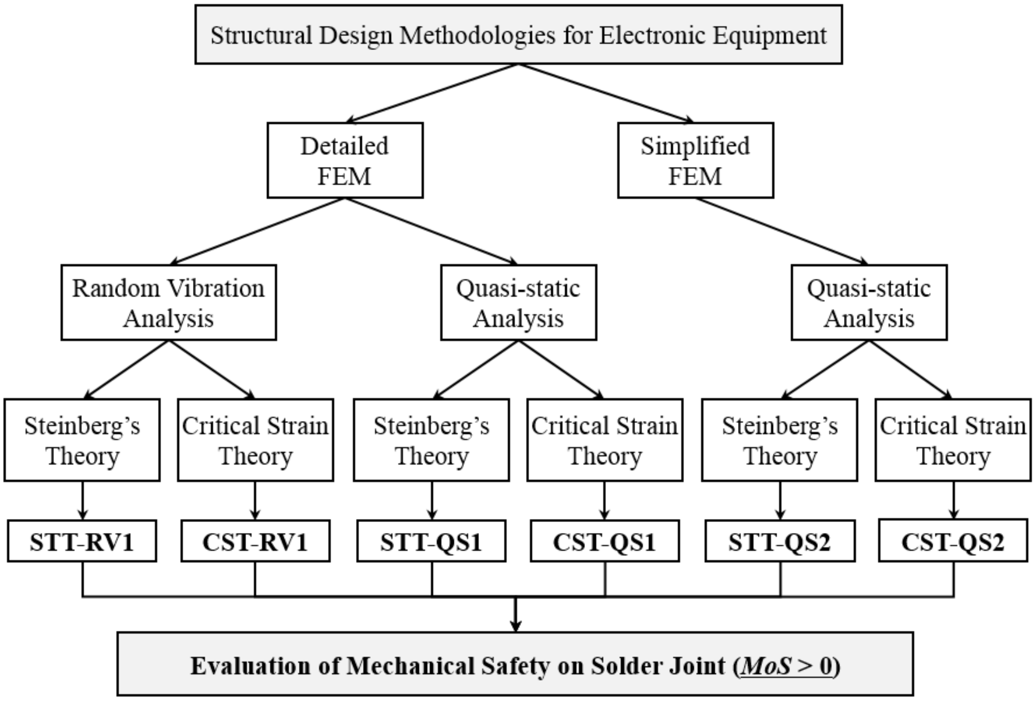

Fig. III-15 Evaluation scheme for structural design methodology (w.r.t PBGA324 & TSSOP48 PCB)

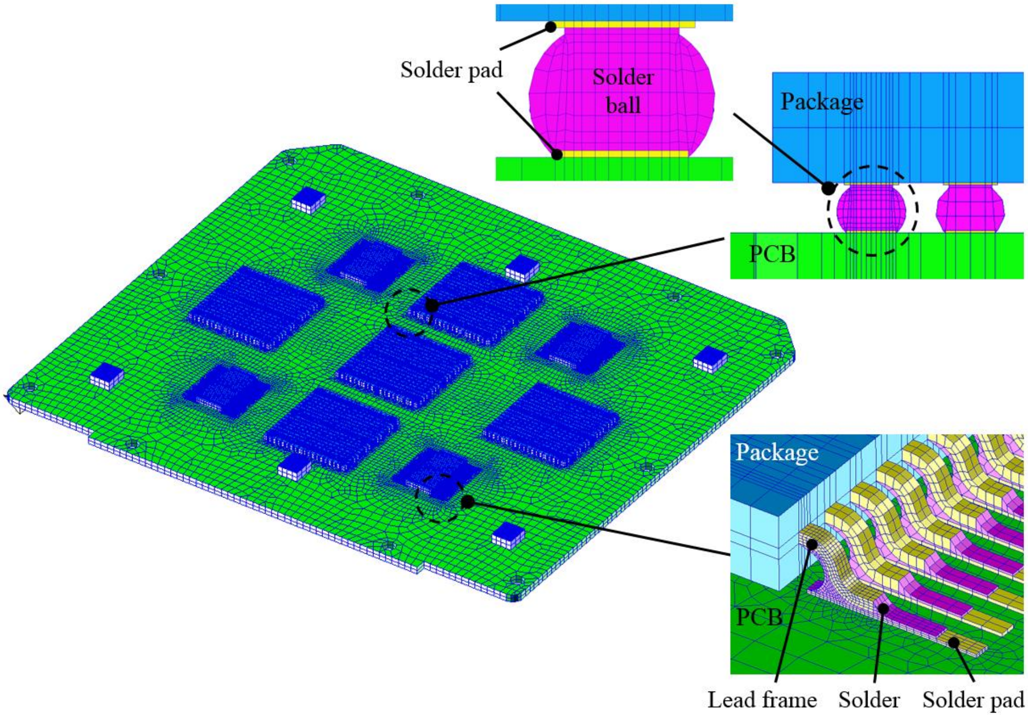

Fig. III-16 Configuration of detailed FEM of PBGA324 & TSSOP48 PCB sample

Table III-4 Material properties used for analysis

Material		Elastic modulus (MPa)	Shear modulus (MPa)	Poisson Ratio	Density (kg/m^3)
PCB (FR-4)		31,893	13,866	0.15	2,477
PBGA package	Component	15,168	6,320	0.2	1,900
TSSOP	Component	11,700	4,500	0.3	2,940
	Lead (Copper)	113,000	42,164	0.34	8,900
Solder (Sn-Pb37)		29,379	10,801	0.36	8,490

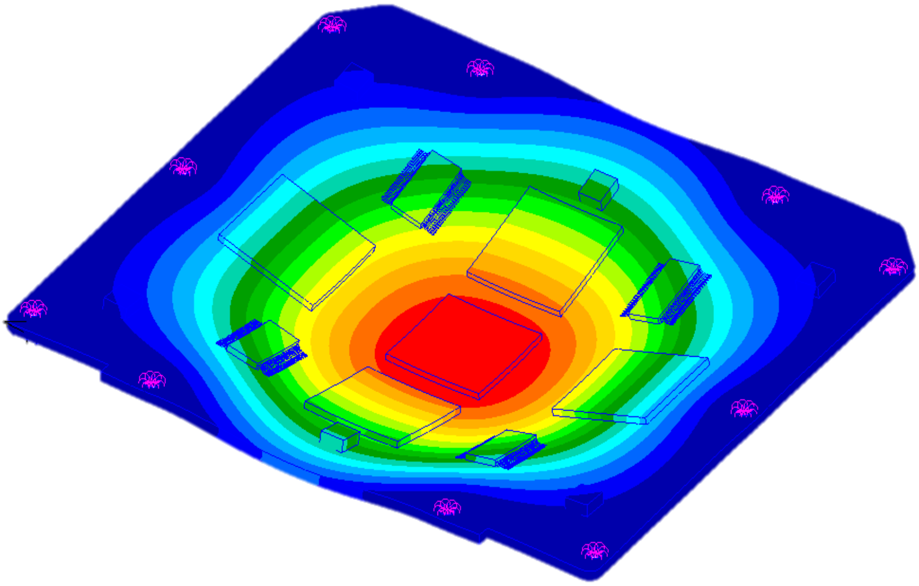

(a)

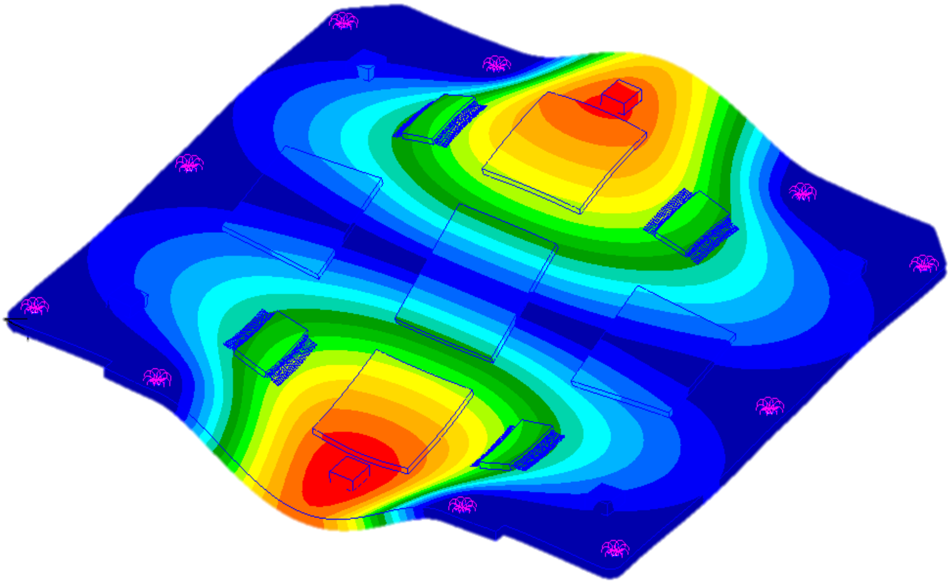

(b)

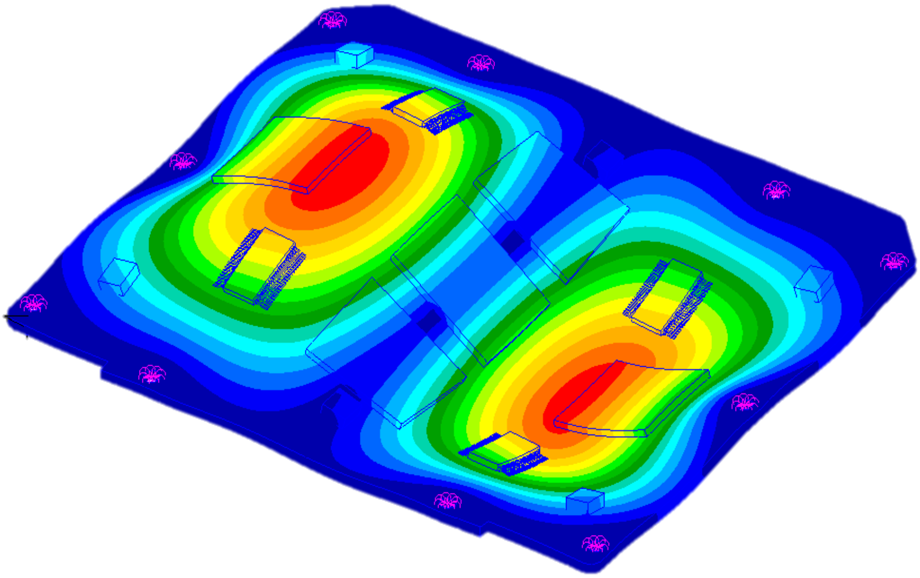

(c)

Fig. III-17 Representative mode shapes of PCB sample

Table III-5 Comparison of *MoS* calculated using STT-RV-1 and CST-RV-1 methodologies

No.	Type	STT-RV-1			CST-RV-1		
		Z_{allow} (mm)	Z_{max} (mm)	MoS	ε_c (μ-strain)	ε_{max} (μ-strain)	MoS
U1	PBGA	0.379	0.184	0.65	387	445	-0.31
U2	TSSOP	0.737	0.19	2.11	662	208	1.55
U3	TSSOP	0.739	0.193	2.06	662	211	1.51
U4	PBGA	0.313	0.272	-0.08	387	503	-0.39
U5	PBGA	0.22	0.379	-0.54	387	582	-0.47
U6	PBGA	0.314	0.278	-0.10	387	514	-0.40
U7	TSSOP	0.689	0.19	1.90	662	208	1.55
U8	TSSOP	0.688	0.193	1.85	662	211	1.51
U9	PBGA	0.378	0.184	0.65	387	446	-0.31

Table III-6 Comparison of *MoS* calculated using STT-QS-1 and CST-QS-1 methodologies

No.	Type	STT-QS-1			CST-QS-1		
		Z_{allow} (mm)	Z_{max} (mm)	*MoS*	ε_c (μ-strain)	ε_{max} (μ-strain)	*MoS*
U1	PBGA	0.379	0.122	1.49	387	509	-0.39
U2	TSSOP	0.737	0.129	3.57	662	165	2.21
U3	TSSOP	0.739	0.129	3.58	662	166	2.19
U4	PBGA	0.313	0.17	0.47	387	615	-0.50
U5	PBGA	0.22	0.231	-0.24	387	650	-0.52
U6	PBGA	0.314	0.184	0.36	387	635	-0.51
U7	TSSOP	0.689	0.129	3.27	662	165	2.21
U8	TSSOP	0.688	0.129	3.27	662	165	2.21
U9	PBGA	0.378	0.122	1.48	387	509	-0.39

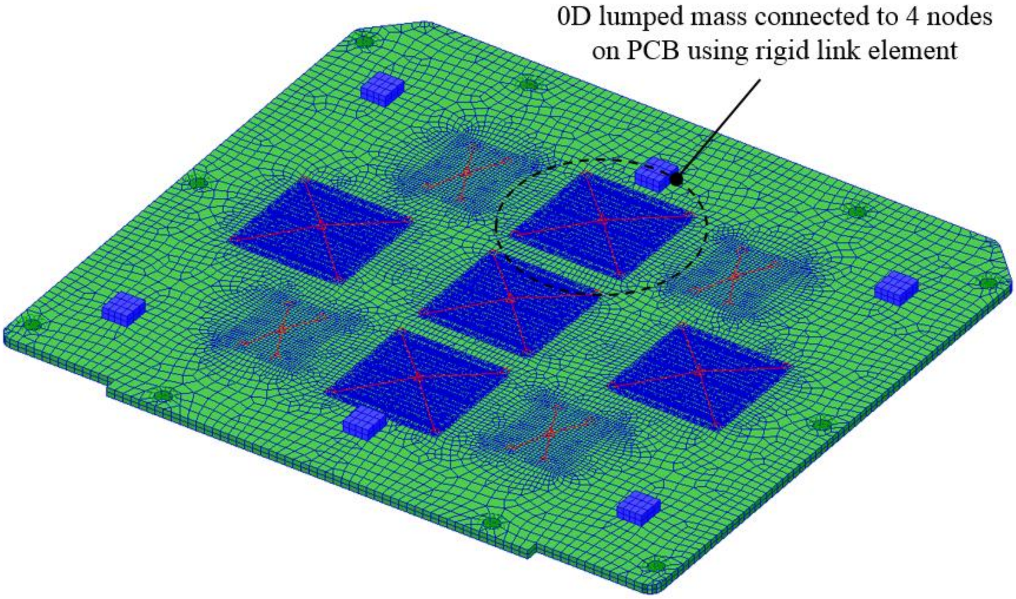

Fig. III-18 Configuration of simplified FEM of PBGA324 & TSSOP48 PCB sample

Table III-7 Comparison of MoS calculated using STT-QS-2 and CST-QS-2 methodologies

No.	Type	STT-QS-2			CST-QS-2		
		Z_{allow} (mm)	Z_{max} (mm)	MoS	ε_c (μ-strain)	ε_{max} (μ-strain)	MoS
U1	PBGA	0.379	0.127	1.39	387	531	-0.42
U2	TSSOP	0.737	0.135	3.37	662	381	0.39
U3	TSSOP	0.739	0.135	3.38	662	348	0.52
U4	PBGA	0.313	0.203	0.23	387	748	-0.59
U5	PBGA	0.22	0.254	-0.31	387	907	-0.66
U6	PBGA	0.314	0.203	0.24	387	769	-0.60
U7	TSSOP	0.689	0.135	3.08	662	351	0.51
U8	TSSOP	0.688	0.135	3.08	662	340	0.56
U9	PBGA	0.378	0.127	1.38	387	531	-0.42

Table III-8 Comparison of computation time between various methodologies

Methodology	Modal analysis (min)	Random Vibration analysis (min)	Quasi-static analysis (min)	Remarks
CST-RV-1	6.28	38.47	-	Detailed FEM
CST-QS-1	6.28	-	9.52	Detailed FEM
CST-QS-2	1.47	-	1.12	Simplified FEM

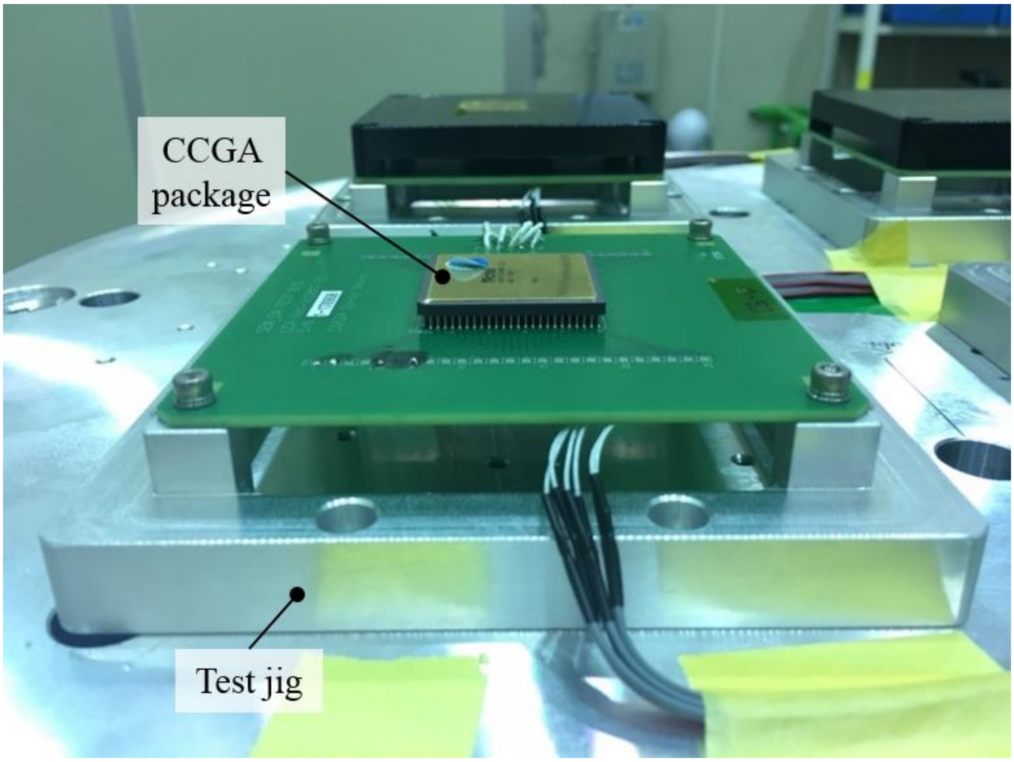

Fig. III-19 Random vibration fatigue test set-up of PCB sample with CCGA package

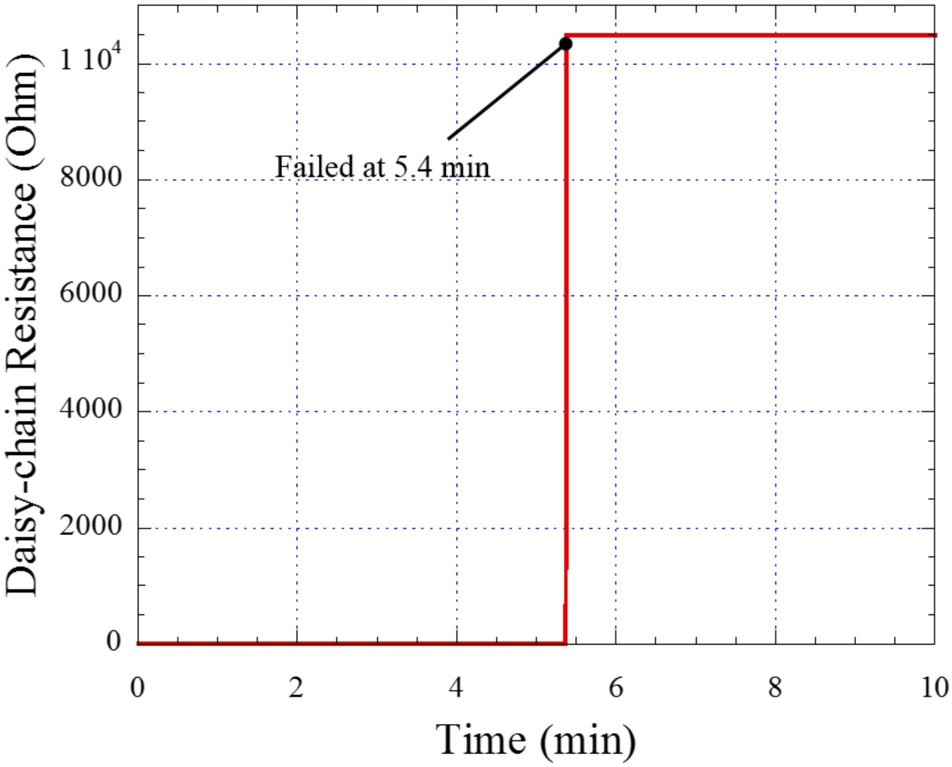

Fig. III-20 Time profile of daisy-chain resistance of CCGA package

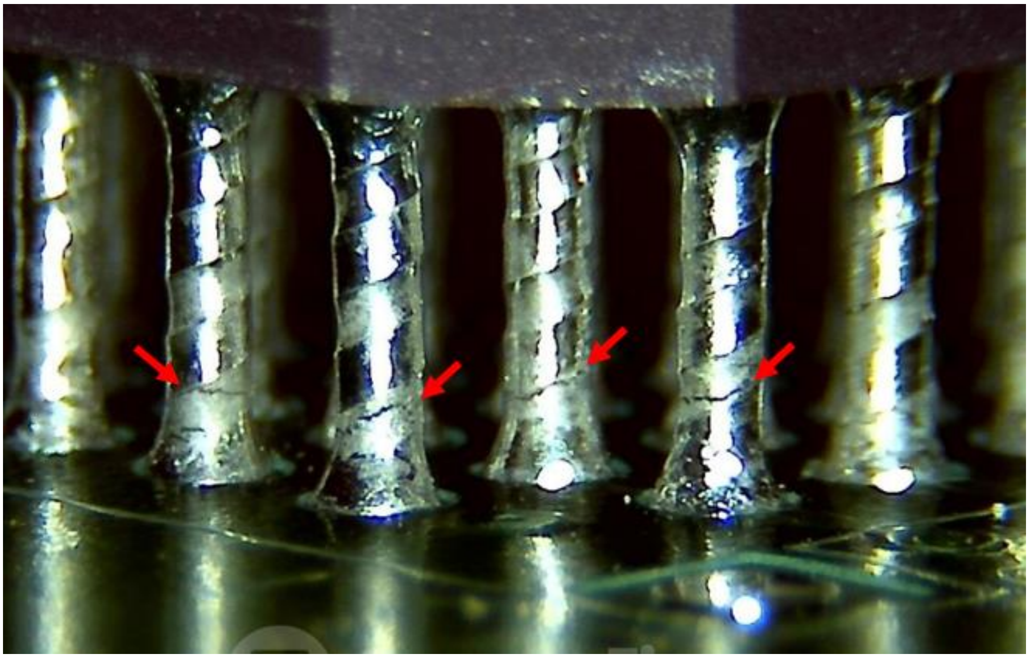

Fig. III-21 Representative optical micrograph of CCGA solder joints

Table III-9 Results of MoS and time to failure of CCGA package calculated using CST-QS-2 methodology

Type	**ε_{c} (μ-strain)**	**$\varepsilon_{p_{max}}$ (μ-strain)**	**MoS**	**Remarks**
CCGA	268	871	-0.72	TTF_{test}: 5.38 min ($< 2 \times 10^{7}$ cycles)

D. Methodology Validation (PBGA388 Package)

In the previous chapter, the effectiveness of the PCB strain-based methodology was validated by the fatigue life tests of PCB samples with BGA packages under random vibration. Their investigations also involved the feasibility of utilizing the FEM of the package simplified into the 0D lumped mass and rigid link elements to simulate the package and solder joints, respectively. However, it is necessary to validate the methodology with respect to the various PBGA package configurations, i.e., molded package shape to encapsulate the semiconductor die, and solder ball array (i.e., full array, peripheral), which were not investigated in the previous chapter. The investigations on these factors become especially important when the simplified package FEM form is used for the solder joint evaluation because the aforementioned package configuration features are not reflected in the FEM, which could, therefore, result in a severe error in the calculated MoS. In addition, there have been no sample cases to validate the methodology regarding the presence of mechanical fixations adjacent to the package in the previous chapter. Furthermore, the board eigenfrequency influence that affects the board strain rate has not been investigated and means that the feasibility of using the value of $\dot{\varepsilon}$ = 50,000 used for Eq. (III-1) in the previous chapter must be confirmed with respect to the various board eigenfrequencies. Therefore, in this study, we evaluated the effectiveness of the PCB strain-based methodology with respect to those factors.

1. Description of PBGA388 PCB Sample

To validate the effectiveness of PCB strain-based methodology for evaluating solder joint mechanical safety under a random vibration environment, PCB test samples with PBGA388 packages were fabricated, and an example of the sample in Case 1 is shown in Fig. III-22. A single PBGA388 package is mounted on an FR-4 PCB with dimensions of 125 mm × 125 mm × 1.6 mm. The total PCB sample mass is 51.1 g. Four holes for M3 screws were used for board fixation. Eutectic Sn63-Pb37 solder balls with space heritage were applied to mount the package. Table III-10 lists the PBGA388 package specifications. The key features of this package are that the area along the BT substrate edge is not covered with the molded package, and the solder ball peripheral array is formed beneath the package. These feature differences are the reasons for selecting this package for the methodology validation. For the experimental validation, five cases of PCB samples were fabricated in the configurations shown in Figs. III-23 and III-24. Here, Cases 1, 1-1, and 1-2 correspond to the situations where the packages are mounted on various board locations. In particular, the Case 1-2 sample package is located adjacent to a screw hole with a distance of only 5 mm, where the solder joint might be influenced by the strain response caused by the bolt constraint. Cases 2 and 3 correspond to the samples with higher eigenfrequencies as the board size is reduced compared with the Case 1 sample. The masses of Cases 2 and 3 PCBs are 29 g and 21 g, respectively.

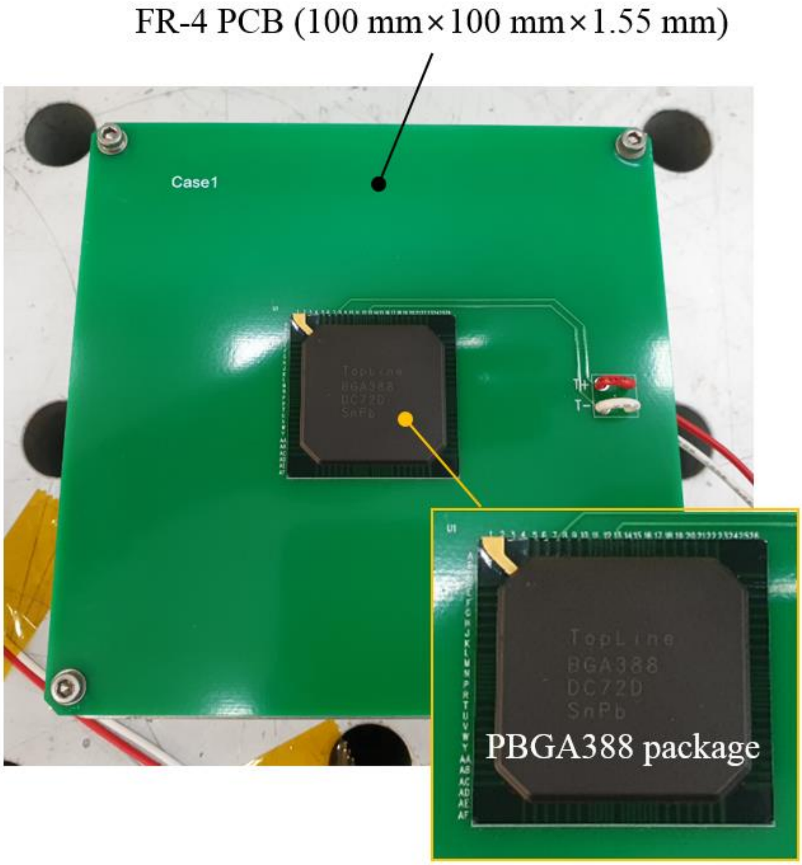

Fig. III-22 Case 1 PCB sample with PBGA388 package

Table III-10 Specifications of PBGA388 package

Item	Specification
Manufacturer	Topline Co. Ltd.
Configuration	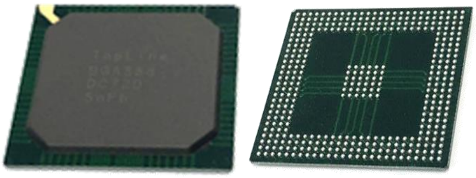
Solder ball	- Material: Sn-Pb37 - Dimension (mm): 0.45 × 0.7 (height × max. diameter) - Solder pitch (mm): 1.27 - No. of solder balls (EA): 388 - Array type: perimeter
Package dimension	- Dimension (mm): 35 × 35 × 2.3 (incl. solder balls) - Composition: BT substrate with mold - Mass (g): 5.0 (incl. solder balls)

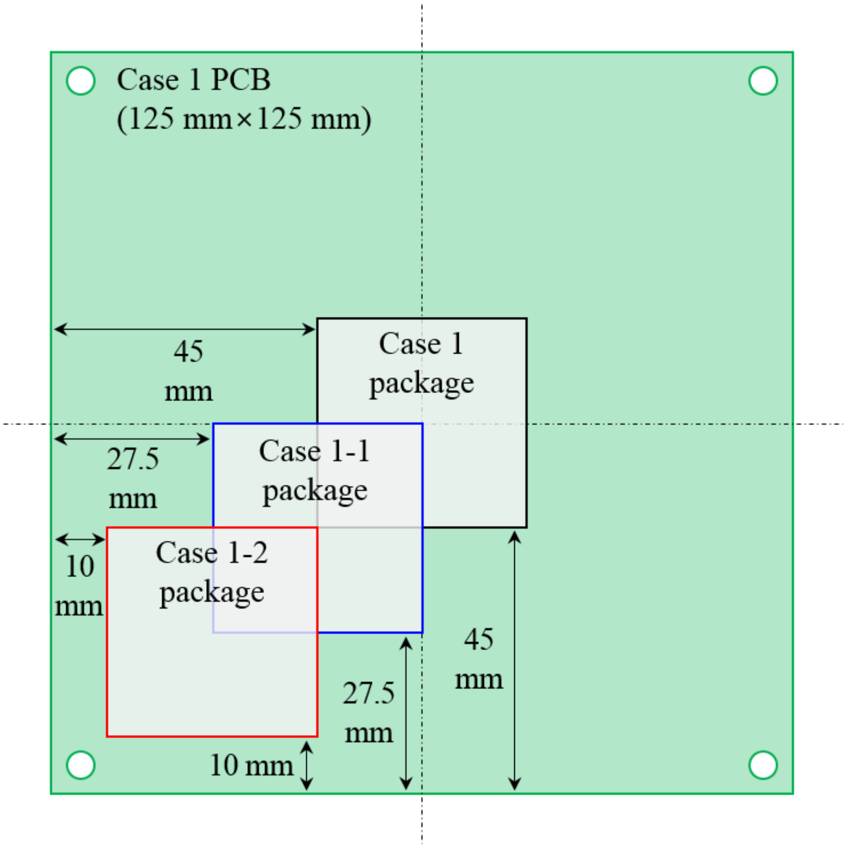

Fig. III-23 Configurations of PCB samples in each case (Cases 1, 1-1 and 1-2)

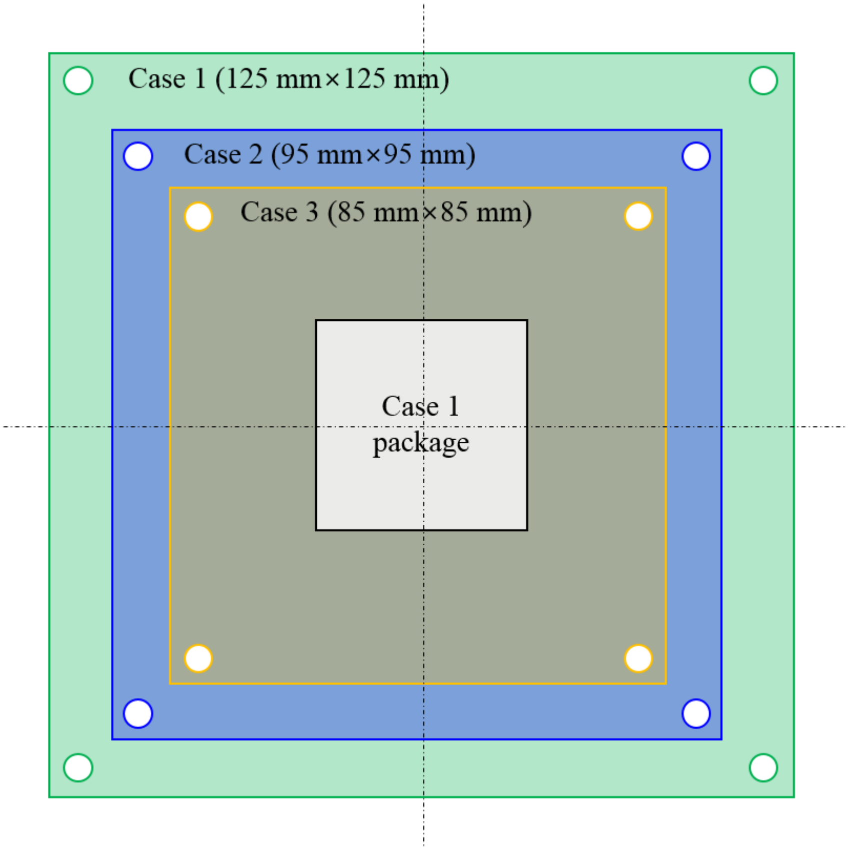

Fig. III-24 Configurations of PCB samples in each case (Cases 1, 2 and 3)

2. Fatigue Life Tests

To obtain the TTF_{test} of each sample packages for comparison with the evaluation results using the PCB strain-based methodology, the fatigue life test was performed in a random vibration environment. Figure III-25 shows the fatigue life test set-up for the PCB samples on the electrodynamic vibration shaker. In this study, only one sample was used for each case. During the test, the time to failure (TTF) of the packages was measured through an in-situ resistance monitoring based on a daisy-chain circuit implemented in each package. Figures III-26 shows the daisy-chain circuit configuration for a BGA package. The two-wire resistance measurement was performed on each sample by using the data acquisition equipment of DAQ6510 (Keithley Co. Ltd.), with an accuracy of 10^{-2} Ω and a sampling rate of 1.7 samples/s. The criterion for declaring the failure of a solder joint, which is crack initiation of solder joint, is determined when the equipment reads a 20% increased daisy-chain resistance value for five consecutive readings in accordance with the IPC-9701A standard [50]. The change in failure criterion from that used in the previous section is to more precisely assess TTF_{test} of packages by more sensitively detecting the micro-cracking of solder joint based on the lessons and learned from the previous test. Exposure to random vibration in the out-of-plane direction of PCBs was initiated for all the samples, and the sample that reached the failure criterion during the test was disassembled from the test set-up. Table III-11 shows the specifications of the random vibration input level, which is commonly used for spaceborne hardware qualification.

Figure III-27 shows the fatigue life test results, i.e., time histories of daisy-chain resistances for the PCB samples. The first failure signal from the resistance monitoring occurred from the Case 3 sample at 1.29 h of exposure to the random vibration environment specified in Table 2. The Case 1-1 sample also failed at a similar time. In addition, in Cases 1 and 2, the samples reached the failure criterion at 9.5 h and 10.4 h of progress, respectively. The resistance value of the Case 1-2 sample gradually increased during the test; however, it did not reach the failure criterion until the test completion at 12.4 h.

Figures III-28~III-31 shows the cross-sectional microphotographs of cracked BGA solder joints for the samples that reached the failure criterion, which were taken using scanning electron microscope (SEM) after completion of the fatigue life test. All observed samples showed the cracking of solder joints and these results confirmed the TTF determined through the resistance measurement shown in Fig. III-27. Most cracks were initiated and propagated along the interface boundary between the solder ball and package solder pad. Table III-12 summarizes the results of the fatigue life tests including SEM inspection for each PCB sample. The Case 1-1 and 3 samples failed much earlier than the Case 1 samples although their board displacement values are much lower than that of Case 1. All the packages at the center of the board failed earlier than those located relatively near the edge of the board. In addition, the exact TTF of the solder joint from the Case 1-2 sample could not be obtained due to the limited test duration although the data for the remaining four samples was obtained. These facts indicate that additional investigation is required for reliable evaluation on the PCB strain-based methodology. Therefore, in this study, we performed the fatigue life prediction on the solder joints of the tested samples.

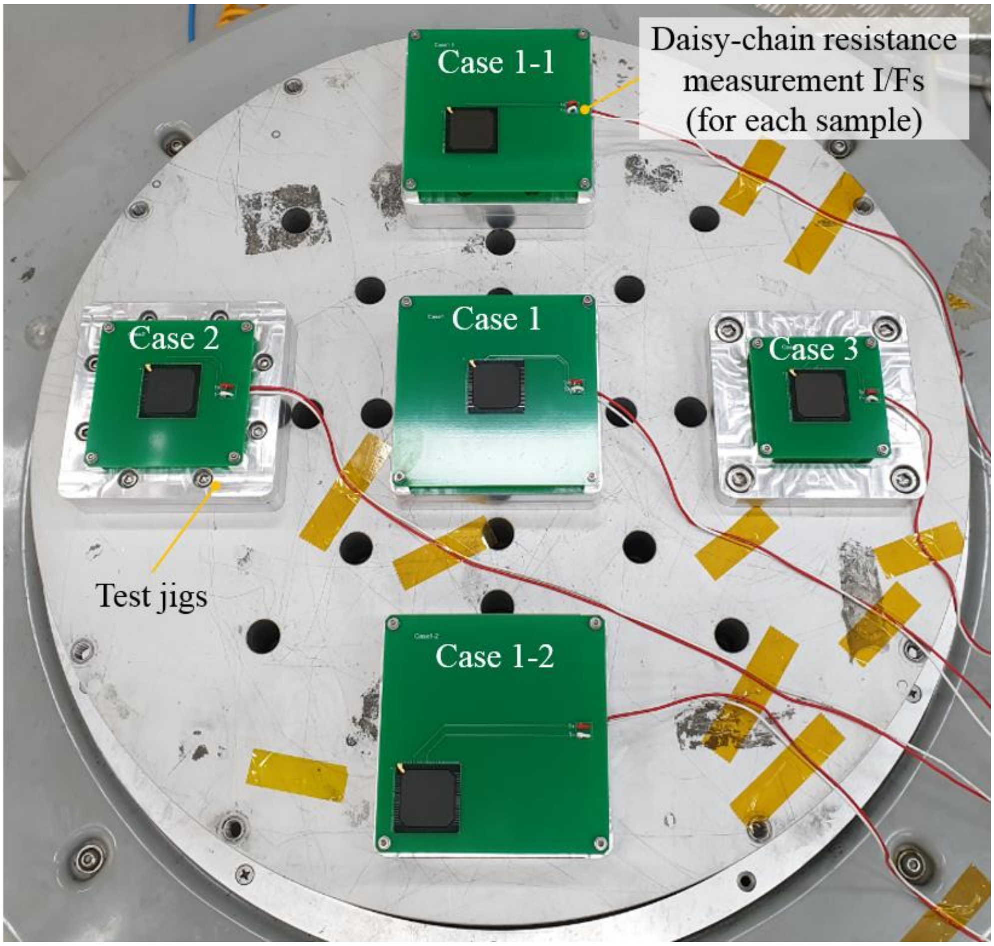

Fig. III-25 Fatigue life test set-up for PBGA388 PCB samples

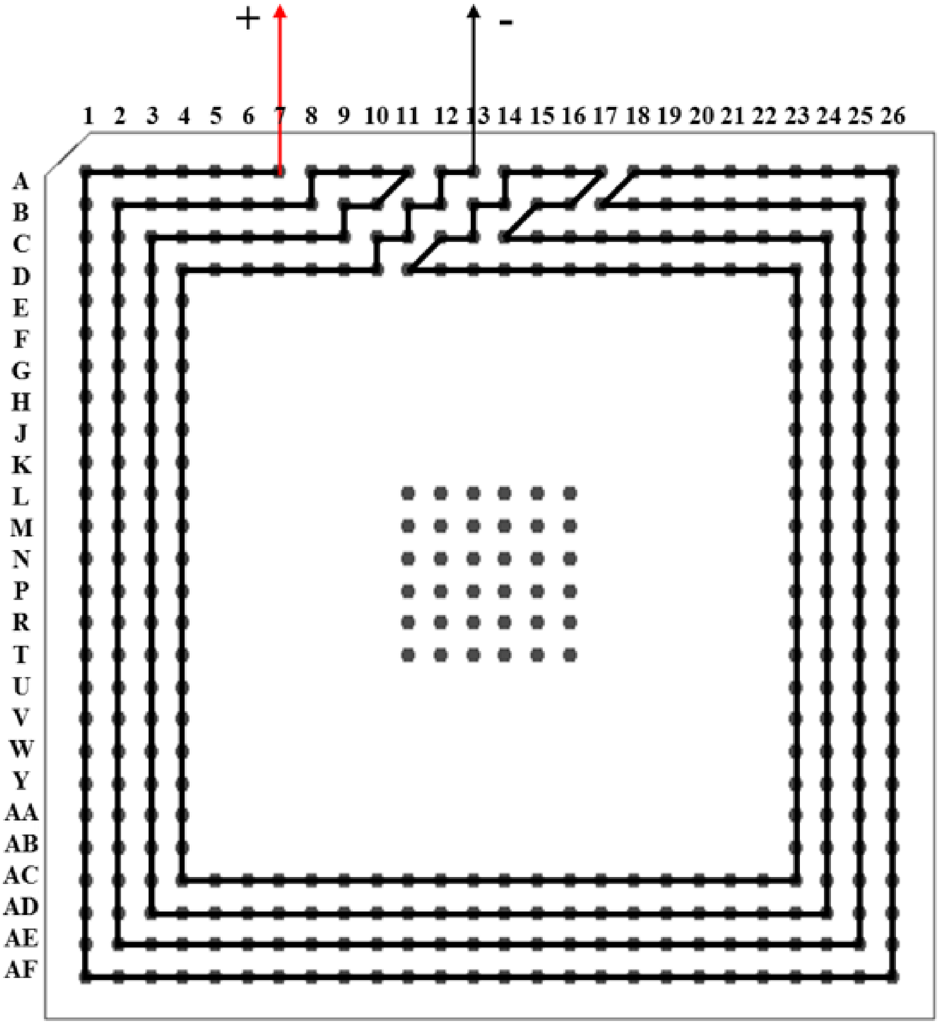

Fig. III-26 Configuration of daisy-chain circuit for PBGA388 package

Table III-11 Random vibration test specification (14.1 G_{rms})

Frequency (Hz)	**PSD acceleration (PSD, g^2/Hz)**
20	0.026
50	0.16
800	0.16
2,000	0.026
Overall	14.1 G_{rms}

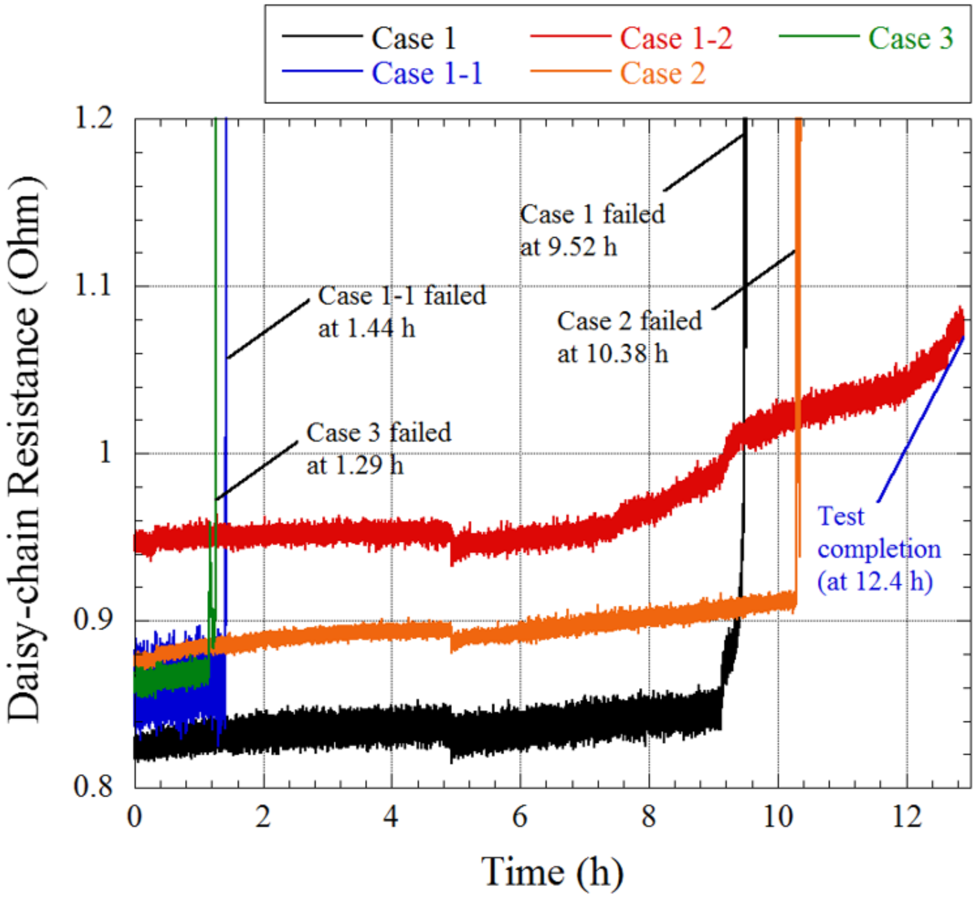

Fig. III-27 Time profiles of daisy-chain resistance on each PBGA388 PCB samples

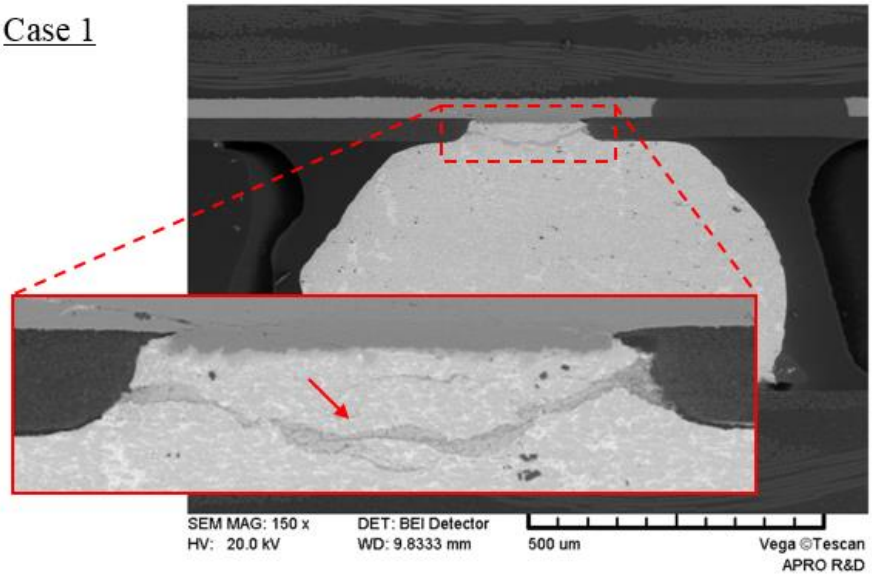

Fig. III-28 SEM microphotograph of cracked BGA solder joints of Case 1 sample

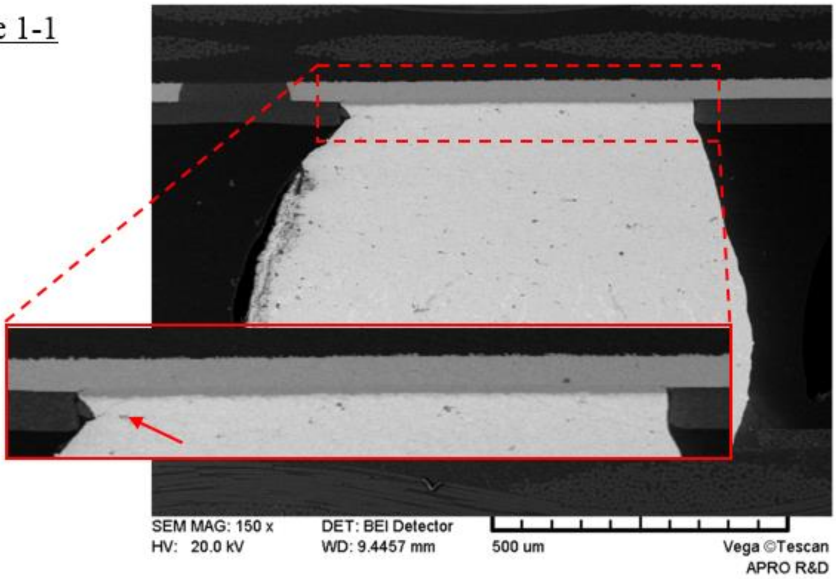

Fig. III-29 SEM microphotograph of cracked BGA solder joints of Case 1-1 sample

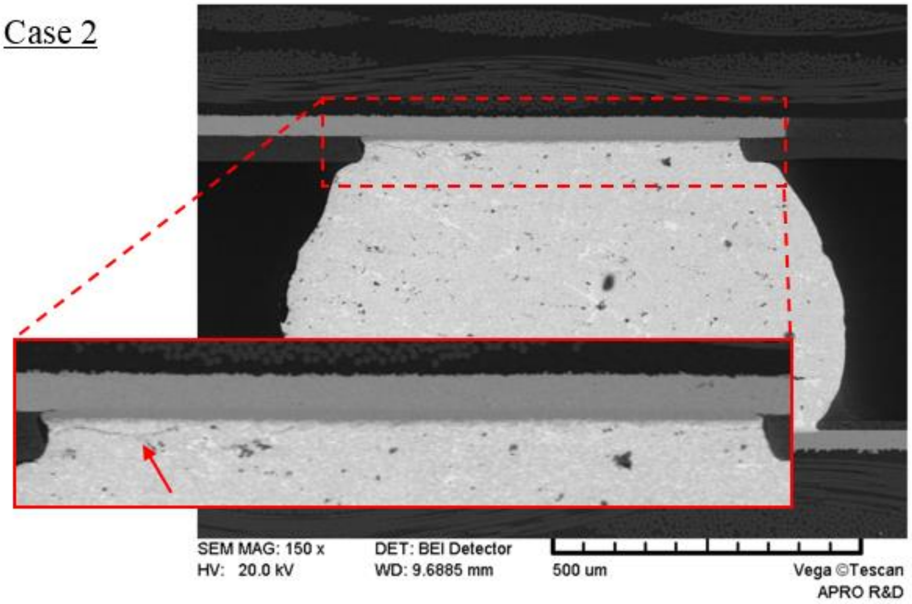

Fig. III-30 SEM microphotograph of cracked BGA solder joints of Case 2 sample

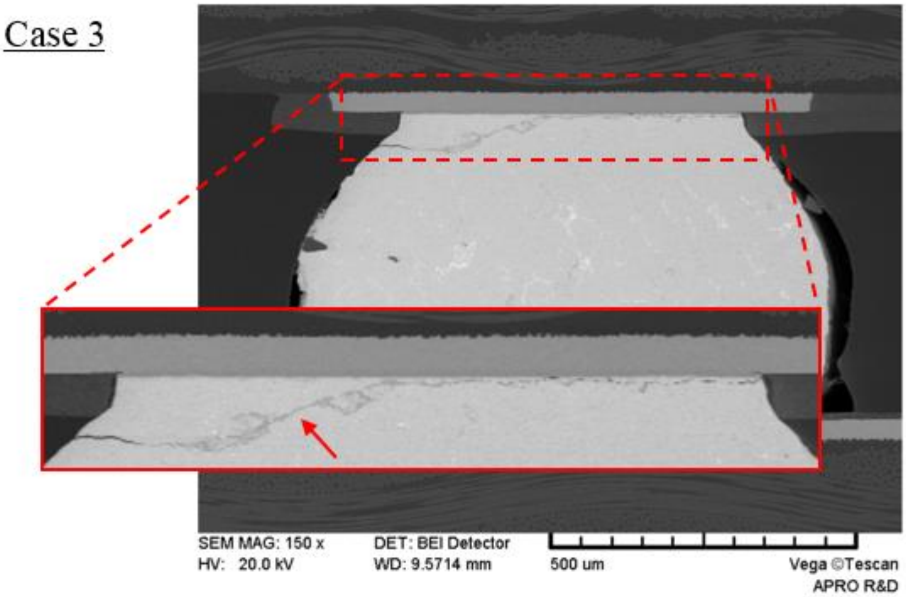

Fig. III-31 SEM microphotograph of cracked BGA solder joints of Case 3 sample

Table III-12 Summary of fatigue life test results

Case	Time to failure (TTF, h)	SEM inspection results
1	9.52	Solder ball cracked
1-1	1.44	Solder ball cracked
1-2	>12.4	Not observed
2	10.38	Solder ball cracked
3	1.29	Solder ball cracked

3. Mechanical Safety Evaluation

The primary objective of the fatigue life prediction is to determine whether the solder joints are expected to fail within the TTF ensured by the criterion of 2×10^7 cycles, which is specified for the methodologies investigated in this study. For the prediction, we used a life prediction approach, which is a Basquin's power law equation [51]. This approach predicts the fatigue life based on the stress acting on the solder joint under vibration excitation. Therefore, FEM-based structural analyses were performed to analyze the dynamic responses and resulting solder stress of the samples. The test input PSD profile specified in Table III-11 was applied for the analysis. Figure III-32(a) shows an example of the detailed FEM of the Case 1 sample, in which the actual package configurations, solder ball, and solder pad are modeled in detail. The FEM consists of 866,223 nodes, 31,184 CPENTA, 703,996 CHEXA elements, and four rigid body elements. As a boundary condition, six DoF constraints were applied on the four PCB screw hole interfaces. Table III-13 lists the material properties used for the analysis.

Figure III-33 shows the representative modal analysis results, i.e., modal shapes of Case 1 PCB sample at the first to third eigenfrequencies. The largest dynamic deflection is expected at the first eigenfrequency of 213.5 Hz where the global bending mode in the out-of-place direction of the board is observed. Table III-14 summarizes the first eigenfrequencies of all the PCB samples and these values were used for the fatigue life predictions.

Figures III-34 and III-35 show the representative RMS von-mises stress distributions of Cases 1 and 1-2 samples under 14.1 G_{rms} of random vibration. The major stress occurred at the interface layer between the solder ball and solder pad of the solder joint closest to the corner, where the largest relative displacement between the package and board occurred. This solder joint is, therefore, the most vulnerable to vibration excitation. Additionally, the stress concentration locations in the solder balls correspond with the crack propagations shown in Fig. 6. In the Case 1-2 sample, the major stress occurred at the corner solder ball located adjacent to the screw joint because the mechanical constraint achieved by the joint induces the local strain that increases the solder stress, as shown in Fig. III-35. As mentioned above, this is an important factor in the mechanical safety evaluation and, therefore, will be addressed in a later chapter of this paper. Table III-15 summarizes the von-mises stress of solder joints for each sample.

For the reliable prediction of fatigue life, a feasible solder stress value shall be computed from the FEM analysis. However, as described in the previous studies [10-11, 22, 24, 51], the solder stress or strain value is heavily dependent on the solid element mesh density and is a result of a stress–strain singularity at the interface layer between two different materials. To minimize the problem of mesh dependency, a volume-weighted average stress, σ_a, was used for prediction [51]. The σ_a can be derived by calculating the average effective stress over all the solid elements in the interface layer between the solder ball and the solder pad, using Eq. (III-6), as follows:

$$\sigma_{\mathrm{a}} = \frac{\Sigma(\sigma_{\mathrm{VM,e}} \times V_{\mathrm{e}})}{\Sigma V_{\mathrm{e}}} \qquad \text{(III-6)}$$

where $\sigma_{\mathrm{VM,e}}$ and V_{e} are the RMS von-mises stress and volume of the element, respectively. The Basquin's power law equation for predicting the total number of fatigue cycles, N_{f}, based on the σ_a can be expressed as follows:

$$\sigma_{\mathrm{a}} = \sigma'_{\mathrm{f}} \times (N_{\mathrm{f}})^b \qquad \text{(III-7)}$$

where σ_{a} is the von-mises stress derived from the analysis; σ'_{f} is the fatigue strength coefficient; and b is the fatigue exponent, which is typically derived from the slope of the stress-life cycle (S-N) curve. In this study, we used the material constants of σ'_f = 116.8 MPa and b = -0.116 developed for eutectic Sn63-Pb37 solder [52]. For prediction, we used a 1.95-sigma value of stress as σ_a, which is the equivalent of using 1-, 2-, and 3-sigma values considering a Gaussian distribution on the random vibration. The TTF_{pred} of the solder joint is predicted as follows:

$$TTF_\mathrm{pred} = \frac{N_\mathrm{f}}{f_\mathrm{n}} \tag{III-8}$$

where f_n is the first PCB eigenfrequency. In the prediction, factor of safety for TTF_pred, FoS_ttf, was set as 4.0, which is recommended on the fatigue as specified in the ECSS standard [53].

Figure III-36 shows the results of the fatigue life predictions for each PCB sample. For comparison, the TTF_pred obtained from the tests are also specified in the figure. The trend of the TTF_pred for the samples showed a difference from that observed from the test, in particular, for the Case 1-1 and 3 samples. We judge that this difference was primarily caused by the irregular quality in solder ball shapes for each sample, as observed from the SEM microphotographs shown in Fig. III-28~III-31; although, the Case 1 and 2 samples showed the TTF_pred with relatively reasonable accuracy compared with the former two samples. Additionally, the TTF_pred of the Case 1-2 sample was 16.04 h, which corresponds to the test results because the solder joint failures were not observed before the end of the 12.4 h duration. The important observation from the results of N_f for each sample, is that all the samples were expected to fail within the 2×10^7 random vibration cycles. These prediction results were used as comparison data to validate the mechanical design methodology.

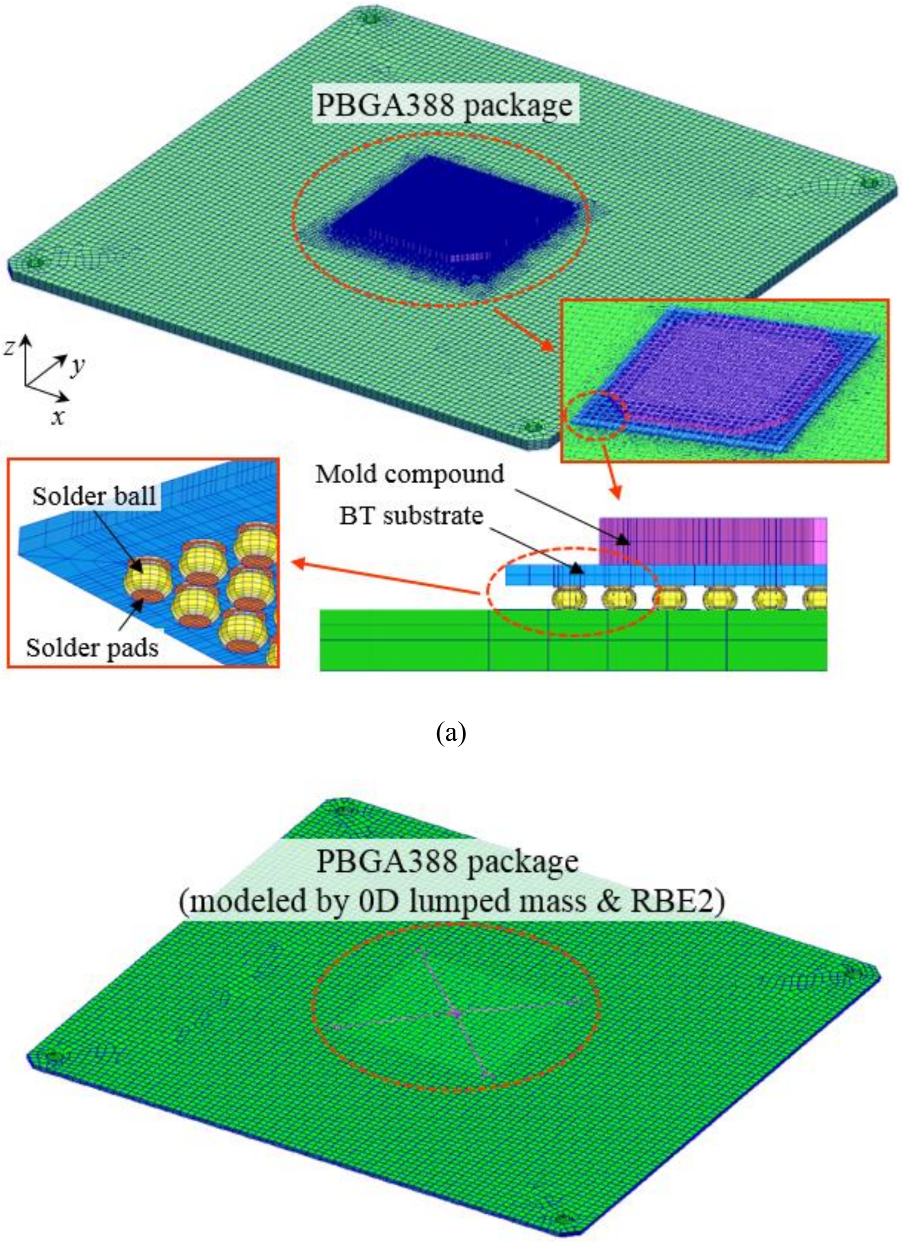

(a)

(b)

Fig. III-32 Configuration of (a) detailed and (b) simplified FEMs of Case 1 sample

Table III-13 Material properties for structural analysis

Material	**Elastic modulus (GPa)**	**Poisson's ratio (-)**	**Density (kg/m^3)**
PCB (FR-4)	18.73	0.136	2,000
Package substrate (BT)	22.00	0.280	2,000
Package mold	15.20	0.200	1,900
Solder ball (Sn63-Pb37)	29.40	0.340	8,490
Solder pad (copper)	113.00	0.340	8,900

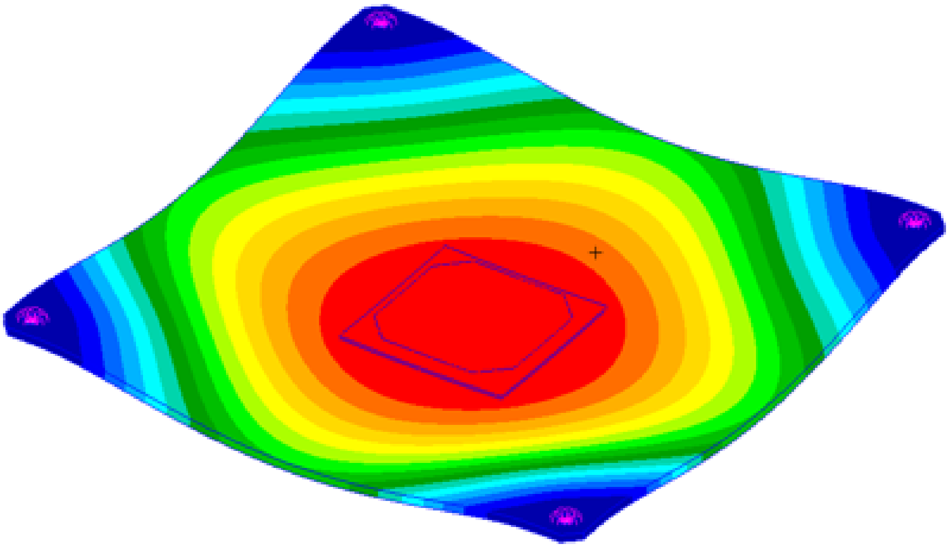

(a)

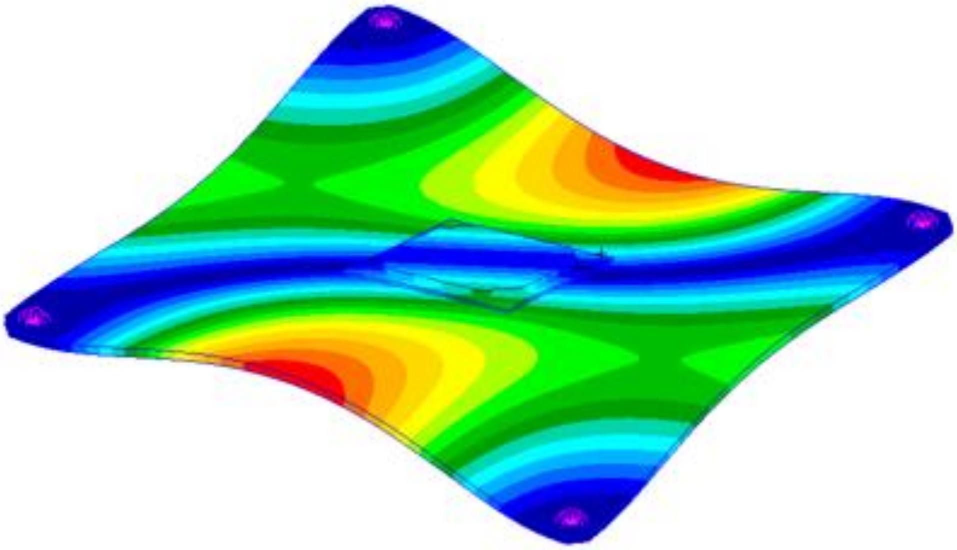

(b)

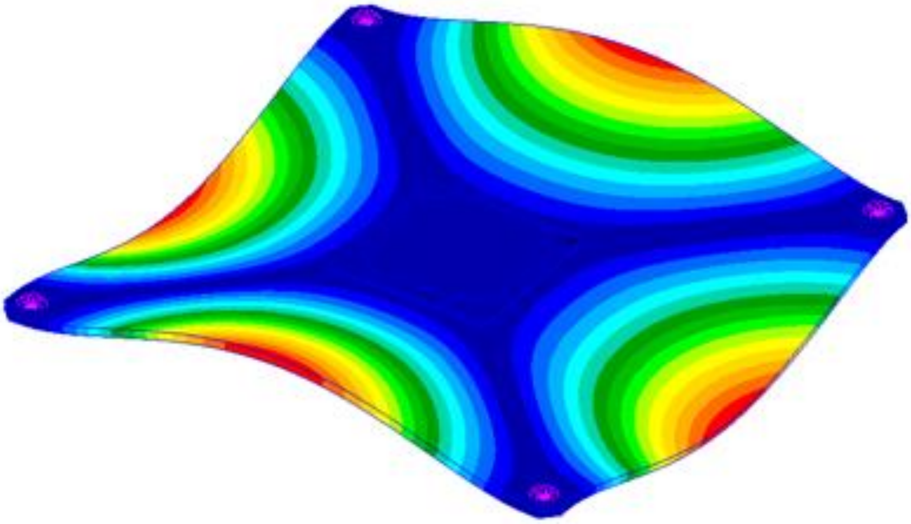

(c)

Fig. III-33 Mode shapes of Case 1 PCB ((a) 213.5 Hz, (b) 408.1 Hz, (c) 538.7 Hz)

Table III-14 First eigenfrequencies of PCB samples obtained from detailed and simplified FEMs

Case	First eigenfrequency (Hz)		Difference btw. FEMs (%)
	Detailed FEM	Simplified FEM	
1	213.5	197.8	7.4
1-1	214.2	199.9	6.7
1-2	214.3	211.1	1.5
2	419.3	377.9	9.9
3	666.3	584.9	12.2

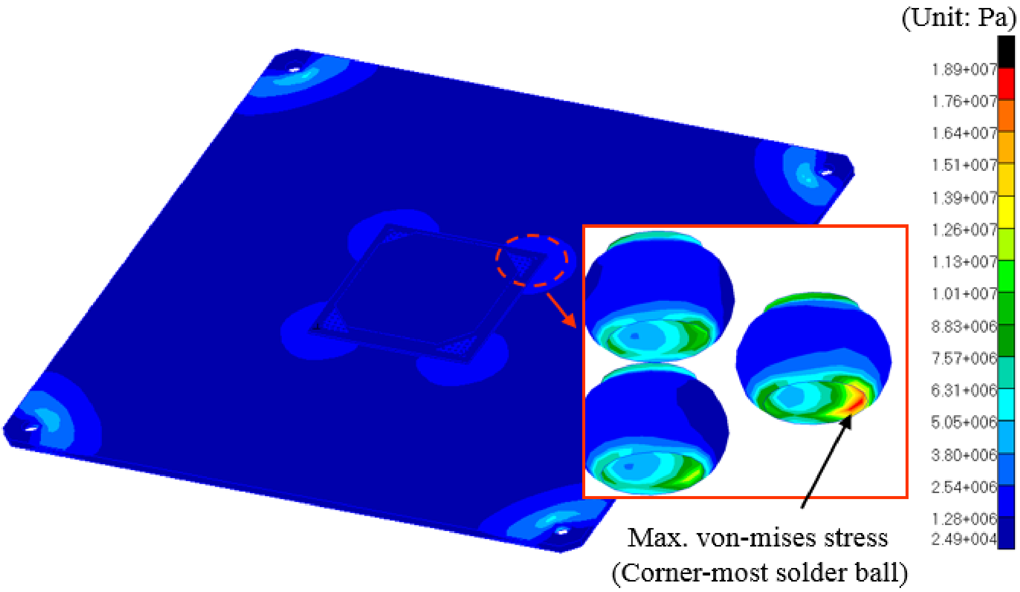

Fig. III-34 Von-mises stress distributions of Case 1 PCB sample

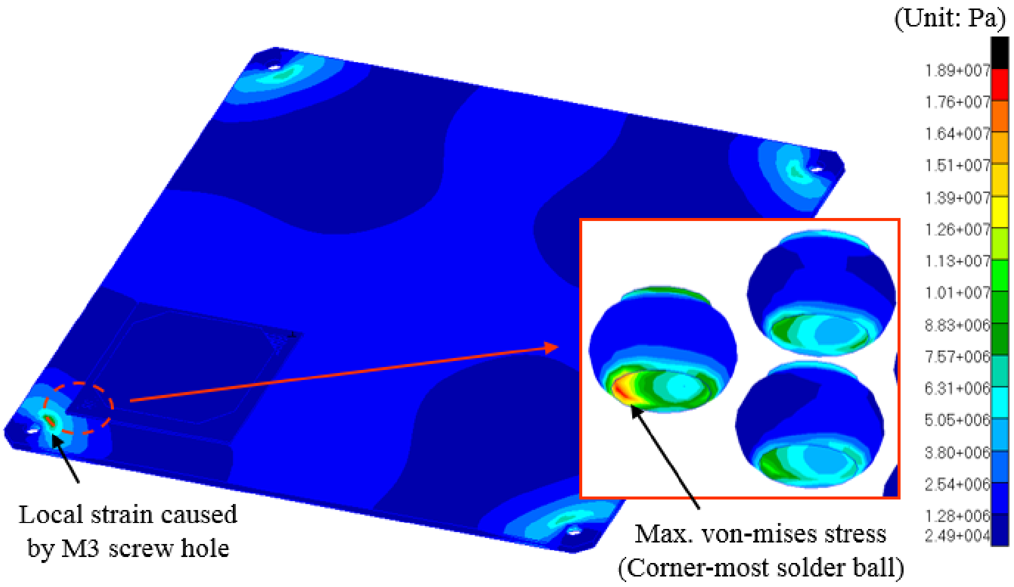

Fig. III-35 Von-mises stress distributions of Case 1-2 PCB sample

Table III-15 Analyzed volume-weighted average values of Von-mises stresses of solder balls for each PCB sample

Case	Volume-weighted average von-mises stress (MPa)
1	8.87
1-1	8.39
1-2	7.67
2	8.20
3	8.00

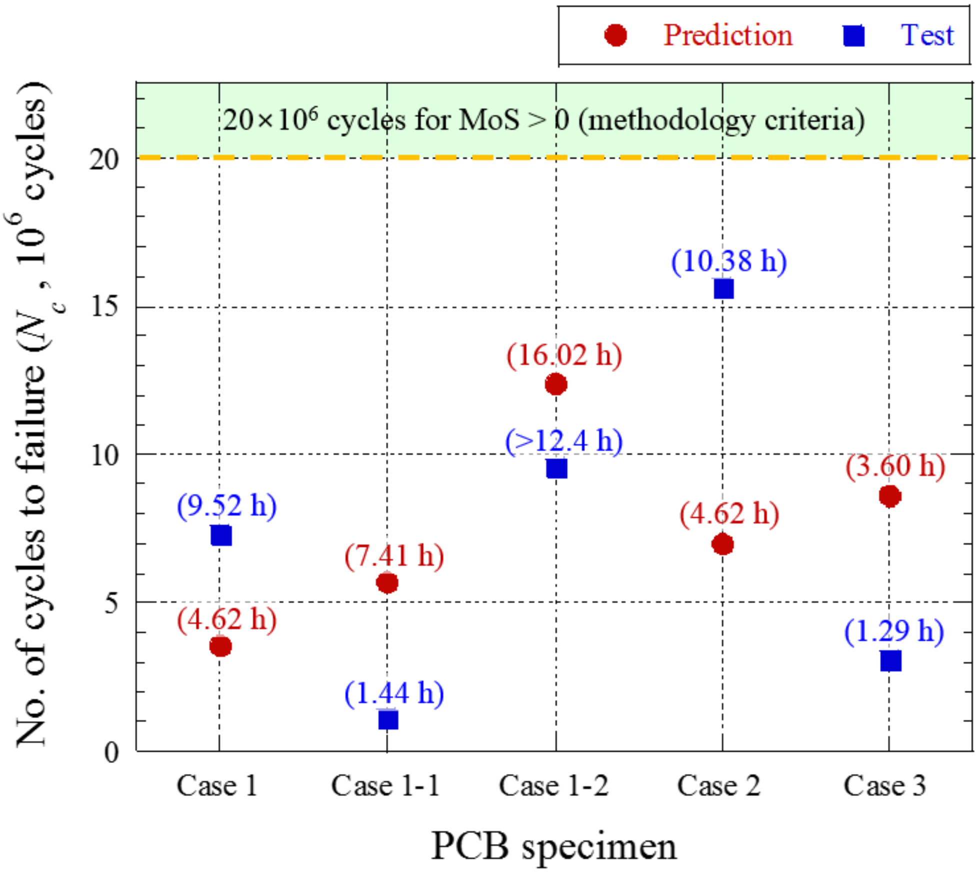

* ( ) : Time to failure (TTF_{test} & TTF_{pred})

Fig. III-36 Summary of fatigue life prediction results on solder joints of PCB samples

To validate the effectiveness of the PCB strain-based methodology, the evaluation scheme shown in Fig. III-37 was established on the methodologies based on PCB strain-based methodology and Steinberg's theory described in Chapters II and III. This was derived in accordance with the fatigue failure theory factors and the FEM configuration. The effectiveness of these methodologies was evaluated by comparison between the estimated MoS values and the TTF derived from the experimental and numerical approach shown in Fig. III-36. In this study, FoS_{m}=1.25 was used for the MoS estimation, which approximately corresponds to FoS_{ttf}=4.0 with regard to the fatigue life of the Sn63-Pb37 solder material.

For the mechanical safety evaluation of the PCB samples, random vibration analysis was performed on the detailed FEM, as shown in Fig. III-32(b). The MoS was calculated from the analyzed displacement and strain responses of the samples by using Eqs. (II-1)–(II-3) and (III-1)–(III-4). Here, we defined the methodologies based on the PCB strain-based methodology and Steinberg's theories as M.CST-1 and M.STT-1, respectively. The MoS values derived from these methodologies are summarized in Table III-16. The MoS values of all the samples estimated from the M.CST-1 methodology showed the negative margin with regard to the criterion of 2×10^7 cycles and these results also correspond to the N_{f} of samples obtained by experimental and numerical approaches shown in previous sections. In particular, it was clearly shown that the MoS value estimated by the M.CST-1 methodology well represented the Case 1-2 sample being affected by the local strain resulting from the adjacent screw joint. Furthermore, the MoS was well estimated for the PCBs with various eigenfrequencies, as observed from the results of Cases 1, 2, and 3. Conversely, M.STT-1 methodology showed inaccurate results because only the Case 1 sample showed the negative margin of MoS on the sample when estimated by this methodology. These results indicate that the M.CST-1 methodology based on critical strain theory is much more effective in the mechanical solder joint safety evaluation for the BGA package located at various PCB locations, as compared with the M.STT-1 methodology.

To minimize the time-consuming and effort-intensive FEM construction process, we proposed the use of a simplified form of FEM. This modeling approach simplifies the package into the 0D lumped mass element and the rigid link element connection between the mass element and the PCB, which simulate the package body and the solder joints, respectively. The representative simplified FEM configuration of the Case 1 PCB sample is shown in Fig. III-32(b). The modal analysis results summarized in Table III-14 indicate that the first eigenfrequency of the PCB samples had differences of up to 12.2%. However, this level of difference is not a problem with respect to using the simplified FEM because the frequency values are slightly lower than those of the detailed FEM, which gives slightly more conservative evaluation results in terms of the dynamic board response. For the evaluation, the methodologies based on the PCB strain-based methodology and Steinberg's theory, which use the simplified FEM, were referred to as M.CST-2 and M.STT-2, respectively.

Table III-17 summarizes the results of MoS calculations based on the M.CST-2 and M.STT-2 methodologies. The MoS value trends derived from both methodologies are approximately the same as the results presented in Fig. III-36. In contrast to the M.STT-2 methodology, the MoS of M.CST-2 represents the actual fatigue life of solder joints well, even though it was estimated by the PCB strain derived from the simplified FEM. These results indicate that the M.CST-2 methodology estimates the MoS more accurately than the M.STT-2 methodology and confirm the feasibility of the use of a simplified FEM as shown in this study. This approach provides the evaluation results within a significantly shorter time compared with the detailed FEM as investigated in the previous section.

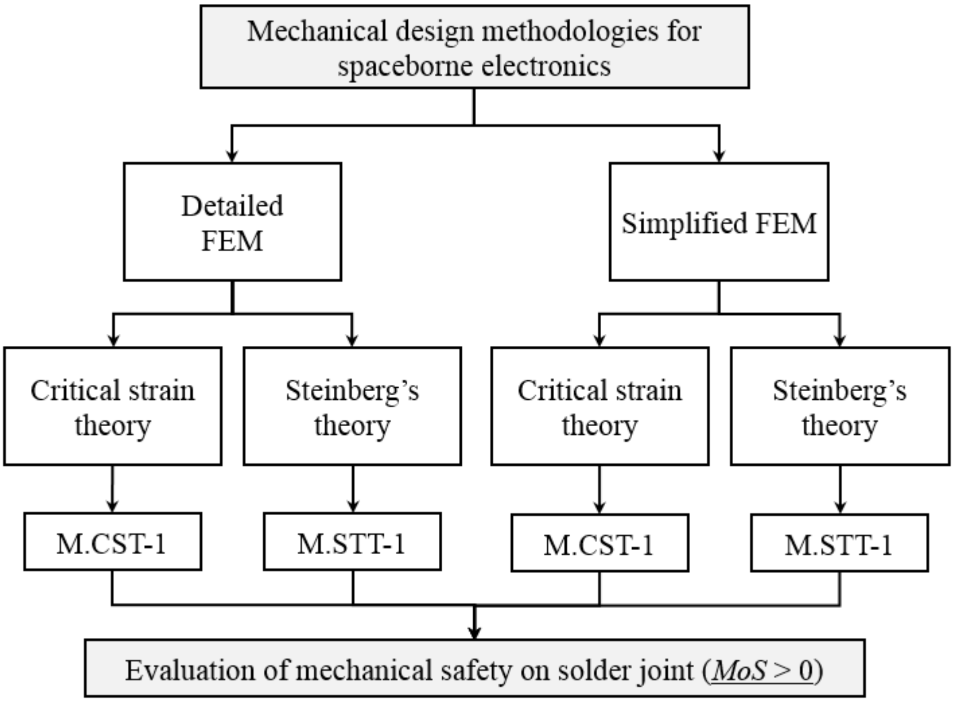

Fig. III-37 Evaluation scheme for structural design methodologies (w.r.t PBGA388 packages)

Table III-16 Comparison of MoS estimated by M.CST-1 and M.STT-1 methodologies

Case	M.CST-1			M.STT-1			Experimental & numerical results (Fig. III-36)
	ε_c (μ-strain)	ε_{max} (μ-strain)	MoS	Z_{allow} (mm)	Z_{max} (mm)	MoS	
1	293.9	1039.5	-0.75	0.218	0.295	-0.33	$< 2 \times 10^7$ cycles failed
1-1	293.9	1003.5	-0.74	0.267	0.239	0.01	$< 2 \times 10^7$ cycles failed
1-2	293.9	747.0	-0.65	0.760	0.112	5.14	$< 2 \times 10^7$ cycles failed
2	293.9	807.0	-0.67	0.166	0.052	1.88	$< 2 \times 10^7$ cycles failed
3	293.9	756.0	-0.65	0.148	0.016	7.56	$< 2 \times 10^7$ cycles failed

*FoS_m=1.25 (Equivalent to FoS_{ttf}=4.0 for TTF_{pred})

Table III-17 Comparison of MoS estimated by M.CST-2 and M.STT-2 methodologies

Case	M.CST-2			M.STT-2			Experimental & numerical results (Fig. III-36)
	ε_{c} (μ-strain)	ε_{max} (μ-strain)	MoS	Z_{allow} (mm)	Z_{max} (mm)	MoS	
1	293.9	946.8	-0.72	0.201	0.267	-0.26	$< 2 \times 10^7$ cycles failed
1-1	293.9	752.6	-0.65	0.226	0.213	0.13	$< 2 \times 10^7$ cycles failed
1-2	293.9	353.4	-0.25	0.604	0.096	6.14	$< 2 \times 10^7$ cycles failed
2	293.9	816.3	-0.68	0.148	0.069	1.16	$< 2 \times 10^7$ cycles failed
3	293.9	736.8	-0.64	0.131	0.030	3.45	$< 2 \times 10^7$ cycles failed

*FoS_{m}=1.25 (Equivalent to FoS_{ttf}=4.0 for TTF_{pred})

IV. PCB Strain-based Structural Design Methodology for Rapid Evaluation of Spaceborne Electronics

In the previous section, to validate the effectiveness of the PCB strain-based methodology, fatigue life tests of a sample PCB with the PBGA324 and TSSOP48 packages were performed, and the TTF_{test} of the tested packages were compared with the calculated MoS. For the application of their methodology, they investigated the effectiveness of both detailed and simplified FEM modeling techniques of the electronic packages. In case of the simplified FEM, the package was modeled using a 0D lumped mass and rigid link element to simulate the package body and solder joints, respectively. This modeling technique saves considerable time and effort compared with the detailed FEM, and is therefore useful when many number of tradeoff studies are required to verify the structural design of electronics in its initial design stage. The validation results confirmed that this methodology provides a relatively reliable prediction of the mechanical safety of a solder joint compared to Steinberg's theory. In addition, this study also revealed the possibility of using the simplified FEM as a rapid solution for the evaluation.

However, the design criterion of 2×10^7 cycles, used in both Steinberg's theory and the PCB strain-based methodology, provides too much margin on the TTF of the solder joint. In several previous studies [32-33, 35, 38] on the structural design of spaceborne electronics, PCBs have been designed to allow them to have a first resonant frequency of PCB (f_{n}) typically between 100 and 800 Hz. For example, if an electronic package is assumed to be mounted on the PCB with f_{n} of 800 Hz and the calculated MoS indicates a positive margin (> 0), the fatigue life of the solder joint would be higher than 6.94 h in accordance with the 2×10^7 cycles criterion. However, this value is extremely large in comparison with the total duration of on-ground vibration tests and the actual launch, which typically ranges from a few minutes to tens of minutes.

In addition, further investigation is required for different types of packages mounted on boards with various boundary conditions. In particular, the influence of the strain effect induced by the adjacent mechanical fixation, that is, package, connector, or screws, should be addressed. Moreover, the fixed value of $\dot{\varepsilon}$ = 50,000 in Eq. (III-2) might not be feasible because the board strain rate is actually dependent on f_{n} and $\varepsilon_{\mathrm{p_{max}}}$. This means that the estimation method for $\dot{\varepsilon}$ is required for reliable evaluation of solder joint safety.

Consequently, to overcome the limitations of conventional methodologies, it is essential to develop a design methodology to prevent excessive margins on the fatigue life by establishing a new design criterion that is suitable for spaceborne electronics. This criterion should be derived based on the actual duration of exposure to the random vibration during the vibration tests as well as the actual launch. A detailed investigation of the simplified FEM modeling technique with a strain-based theory to estimate $\varepsilon_{\mathrm{p_{max}}}$ and $\dot{\varepsilon}$ for various board boundary conditions is also required to achieve a rapid and reliable solution for the structural design of electronics. These are the primary objectives of the proposal of the Oh-Park methodology in this study.

A. Description of Design Methodology

To solve aforementioned issues in evaluating the mechanical safety of a solder joint under a launch random vibration environment, we proposed the Oh-Park methodology that evaluates the structural design of spaceborne electronics. The proposed methodology evaluates solder joint safety based on the MoS calculation with respect to the PCB strain based on the PCB strain-based methodology described in Chapter III. However, a key difference associated with the novelty of this methodology in comparison with previous ones is that the design factor DF, which is inverse number of FoS_{m} in Eq. (III-4) is derived by estimating TTF_{req} for a given vibration test and the launch processes of electronics. The mechanical safety evaluation is performed in accordance with the process shown in Fig. IV-1, and the details of each step are described below. In this study, following assumptions and conditions were reflected to establish the design methodology.

- The design methodology proposed in this study only evaluates the mechanical safety of solder joint under random vibration. The specific failure mechanism on the solder joint considered in this study is the initiation of fatigue crack on solder or lead frame of electronic package. This becomes the failure criterion in the test and analysis.

- The design methodology is established based on stress-life cycle (S-N) relationship ($N \times S^b$=Constant). In the proposed design methodology, the S-N curve region, where the stress value is above the yield strength of material, is ignored under assumption that the solder stress is occurred in elastic region (constant slope region in S-N curve). In addition, endurance limit is not considered since the recent studies

[54-55] suggest that it does not exist for metallic materials. This means that the fatigue failure can be eventually occurred by even the smallest magnitude of stress as long as the sufficient number of fatigue cycles is applied to the solder joint. This enables to let the proposed methodology only consider the constant slope of the S-N curve, which is described as fatigue exponent b.

- The fatigue behavior of the solder joint is assumed to be occurred in elastic region of solder or lead material. Therefore, the approximate fatigue life, which is predicted TTF, is directly related to the fundamental resonant frequency (f_n) of PCB where the major board deflection is occurred. The fatigue cycles accumulated at higher frequency modes are not accounted to estimate the TTF. This assumption makes it possible to use the following relation [8].

$$N = f_\mathrm{n} \times T \quad \text{or} \quad T = \frac{N}{f_n} \tag{IV-1}$$

The main objective of this study is not to accurately predict the fatigue life, but to calculate the MoS of solder joint. In this perspective, above relation gives sufficiently reasonable evaluation results on the solder joint.

- Based on the assumption described above, the stress S is directly related to the acceleration G and to the displacement Z as follows [8].

$$T \times G^b = \text{Constant} \tag{IV-2}$$

$$N \times Z^b = \text{Constant} \tag{IV-3}$$

$$N \times G^b = \text{Constant} \tag{IV-4}$$

- PCB strain are assumed to be proportional to stress and strain of solder joint in accordance with the critical strain theory [47].

- The proposed design methodology estimates MoS value based on the total number of cycles accumulated in random vibration derived from the relation shown in Eq. IV-1. Here, the number of cycle N can be underestimated as the modal participation of PCB mode at f_{n} is less dominant as compared to the other modes. In this study, the uncertainty resulted from the above simplified cycle estimation approach is considered to be compensated by factor of safety of 4.0 on the required time to failure for survival in the test and launch process. This factor of safety value is based on the ECSS-E-ST-32C standard [53]. In addition, the fatigue damage accumulated in the vibration tests for all the axes of electronics is assumed to be same as that accumulated in the out-of-plane random excitation of PCB. This assumption adds more conservatism as well. Therefore, these assumptions make it possible to include resonable extent of margin on the MoS of solder joint. Though, the total number of accumulated cycles are far smaller than the original Steinberg's criterion of 2×10^{7} cycles.

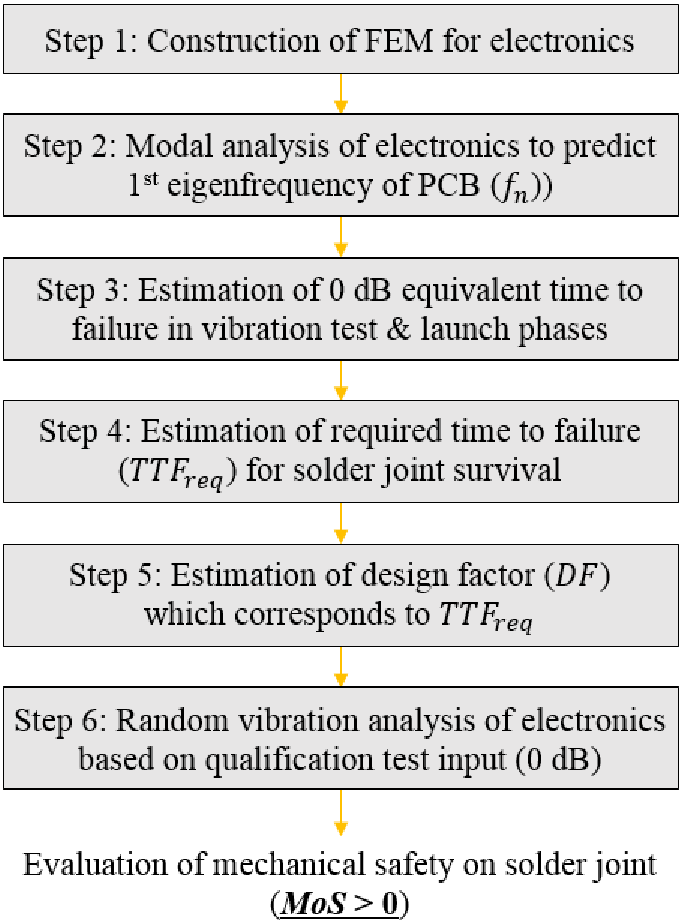

Fig. IV-1 Evaluation approach on structural design of spaceborne electronics using Oh-Park methodology

1. FEM Construction & Modal Analysis (Step 1-2)

As the first step of the evaluation, the FEM of electronics is constructed and f_n is determined by modal analysis. This is because the dynamic PCB strain and the resulting fatigue life of solder joints are directly related to f_n where the largest board deflection occurs. The f_n shall be defined for each package because the deflection can primarily be caused by either the global and local modes of the board in accordance with its boundary conditions (location of fixations, application of stiffeners, and asymmetric and irregular board shape). This rule is appropriate considering the possible occurrence of a complicated mode shape owing to the dynamic coupling between the PCB and the housing structure in some cases. The FEM modeling technique for PCBs with electronic packages will be addressed in a later section of this paper.

2. Estimation of TTF_{req} for Survival in Vibration Test and Launch Process (Step 3-4)

Next, TTF_{req} is estimated based on the summation of 0 dB equivalent time on the solder joint under a random vibration environment in the test and launch phases. Figure IV-2 shows the vibration test scenario and the launch processes effecting electronics. This was established under the assumption that only a single development model was fabricated not only to qualify the design but also to be used as flight hardware to reduce the development time and cost.

In this scenario, electronics are exposed to the qualification level of random vibration excitation at the component level and then undergo an acceptance test again at the satellite system (S/S) level. Finally, it was exposed to launch random vibration, which was assumed to be equivalent to the acceptance level of random vibration for 4 min in three axis simultaneously. Here, a single set of qualification tests includes four steps of random vibration tests, where the input level is gradually increased from -12 to 0 dB with a +3 dB interval, and they are performed for each axis. The acceptance test is performed following the same steps as the qualification test except for the tests with 0 dB level. To estimate TTF_{req} in the above scenario, the equivalent exposure time of each test level with respect to full qualification level of test input (0dB), $T_{\mathrm{x\ dB}}$, is first estimated as follows:

$$T_{\mathrm{x\ dB}} = (t_{\mathrm{test}}\ \ or\ \ t_{\mathrm{lnch}}) \times (G_{\mathrm{ratio}})^{b} \times n \tag{IV-5}$$

where t_{test} and t_{lnch} are the durations of an individual vibration test and actual launch random vibration, respectively. b is the fatigue exponent of the solder material, which is 6.4 for the Sn63-Pb37 solder [18]. G_{ratio} is the ratio of RMS input test level to the 0 dB input, which is described as follows.

$$G_{\mathrm{ratio}} = 10^{\left(\frac{x}{20}\right)} \tag{IV-6}$$

The n is the number of vibration tests for each test level. In this study, $n = 3$ was used under the assumption that the damage in PCB out-of-plane excitation is accumulated in all excitation axes of the electronics. This assumption made it easier to estimate the equivalent time and generate an extent of conservatism on solder joint safety.

Total 0 dB equivalent exposure time during a single set of vibration test is estimated by the summation of $T_{\mathrm{x\,dB}}$ values at each test level calculated using Eqs. (IV-5) and (IV-6). Considering the qualification test at component level as an example, total 0 dB equivalent exposure time, $\sum T_{\mathrm{C-Q}}$, can be estimated as follows.

$$\sum T_{\mathrm{C-Q}} = T_{-12\mathrm{dB}} + T_{-6\mathrm{dB}} + T_{-9\mathrm{dB}} + T_{-3\mathrm{dB}} + T_{0\mathrm{dB}} \tag{IV-7}$$

Lastly, the TTF_{req} for the test and launch process is estimated as follows.

$$TTF_{\mathrm{req}} = \left(\sum T_{\mathrm{C-Q}} + \sum T_{\mathrm{S/S-A}} + \sum T_{\mathrm{L}}\right) \times FoS_{\mathrm{ttf}} \tag{IV-8}$$

where $\sum T_{\mathrm{S/S-A}}$ is the total 0 dB equivalent exposure time in the acceptance test at S/S level. $\sum T_{\mathrm{L}}$ represents 0 dB equivalent exposure time for random vibration in the launch phase, which is equivalent to when the full acceptance level (-3 dB) input is applied to electronics for 4 min, following the assumption described above. TTF_{req} is estimated by summation of the time values for each test and launch process with regard to the fatigue life accumulated in a single full level qualification test (0 dB). This is because the structural analysis is typically performed by applying a 0 dB input for the design validation. FoS_{ttf} is a factor of safety with regard to the time to failure, which shall be a sufficiently high value because the fatigue has a large amount of scatter. In this study, the FoS_{ttf} = 4.0 recommended for metallic materials was applied in Eq. (IV-8) following the ECSS standard [53].

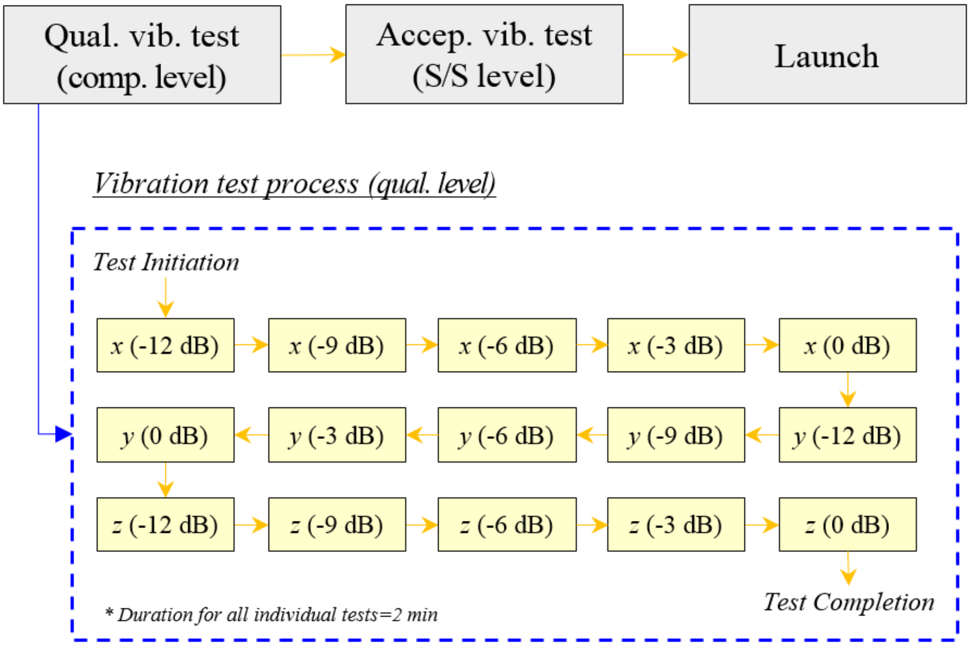

Fig. IV-2 Assumed scenario of test and launch processes for spaceborne electronics

3. DF Estimation & MoS Calculation with respect to PCB Strain (Step 5-6)

To calculate the MoS, DF for ϵ_{c} is estimated from the values of TTF_{req} and f_{n} as below.

$$DF = \left(\frac{N_{\mathrm{org}}}{N_{\mathrm{req}}}\right)^{1/b} = \left(\frac{2\times10^{7}}{TTF_{\mathrm{req}}\times60\times f_{\mathrm{n}}}\right)^{1/b} \tag{IV-9}$$

where N_{org} is the original criterion (2×10^7 cycles) used in the previous methodologies. The N_{req} ($=TTF_{\mathrm{req}} \times 60 \times f_{\mathrm{n}}$) is the total number of fatigue life cycles required for survival in test and launch processes.

The final step of the evaluation is to perform a random vibration analysis of electronics based on the 0 dB input for calculating the MoS with respect to the PCB strain on each package using Eqs. (III-1)–(III-4). However, the $\dot{\varepsilon}$ in Eq. (III-1) is analytically estimated by taking the derivative of $\varepsilon_{\mathrm{p_{max}}}$ as follows:

$$\dot{\varepsilon} = 2\pi \times \varepsilon_{p_{max}} \times f_n \tag{IV-10}$$

The MoS for the solder joint is calculated based on the estimated DF as below.

$$MoS = \frac{DF \times \epsilon_{\mathrm{c}}}{\varepsilon_{\mathrm{p_{max}}}} - 1 > 0 \tag{IV-11}$$

The above Eq. (IV-11) is calculated based on the estimated DF using Eq. (IV-9), and this is the key feature of the proposed Oh-Park methodology that prevents an excessive fatigue margin on the solder joint and has not been proposed in previous studies.

B. Fatigue Life Tests

1. Description of PBGA388 PCB Sample (Sample Set #1)

Prior to the validation of the effectiveness of the proposed Oh-Park methodology, a 388-pin plastic BGA (PBGA388) package with Sn63-Pb37 eutectic solder balls was selected and applied to fabricate the sample PCB assemblies for the fatigue life test under random vibration. Table IV-1 lists the specifications of this package. Figure IV-3 shows a representative configuration of the sample PCB assembly in Case 1. The PCB was made of FR-4 laminate with an area of 125 mm × 125 mm and a thickness of 1.55 mm. The mass of the PCB assembly was 51.1 g. The PCB is mechanically fixed using four M3 screw joints. The daisy-chain circuit shown in Fig. IV-4 was implemented in the PBGA388 package and the PCB to detect the occurrence of cracking on the solder joint by monitoring the circuit variation resistance in the fatigue life test. For the validation of the proposed methodology for various boundary conditions of the PCB, five cases of PCB samples were fabricated as shown in Figs. III-24 and III-25. Here, Cases 1, 2, and 3 correspond to the samples with higher eigenfrequencies as the board size becomes smaller than that of the Case 1 PCB. Cases 1-1 and 1-2 correspond to the samples where the packages are mounted on a position closer to the edge of the board as compared with the Case 1 PCB. Among these, the package of Case 1-2 is located adjacent to the screw joint at a distance of 5 mm. Therefore, the cornermost solder joint of the package can be influenced by the board strain caused by the screw joint.

Table IV-1 Specifications of PBGA388 package

Item	Specification
Manufacturer	Topline Co. Ltd.
Configuration	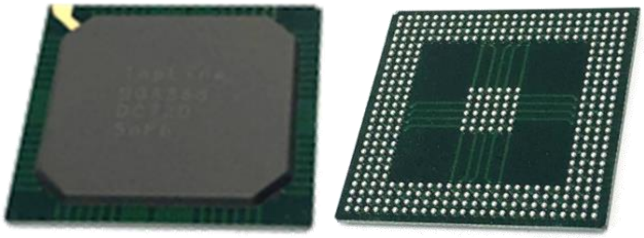
Solder ball	- Material: Sn63-Pb37 eutectic solder - Dimension (mm): 0.45 × 0.7 (height × maximum ball diameter) - Solder pitch (mm): 1.27 - No. of solder balls (EA): 388 (26 solder balls in one side) - Array type: perimeter
Package	- Type: Daisy-chained (dummy package) - Dimension (mm): 35 × 35 × 2.3 (incl. solder balls) - Composition: BT substrate with mold encapsulation - Mass (g): 5.0 (incl. solder balls)

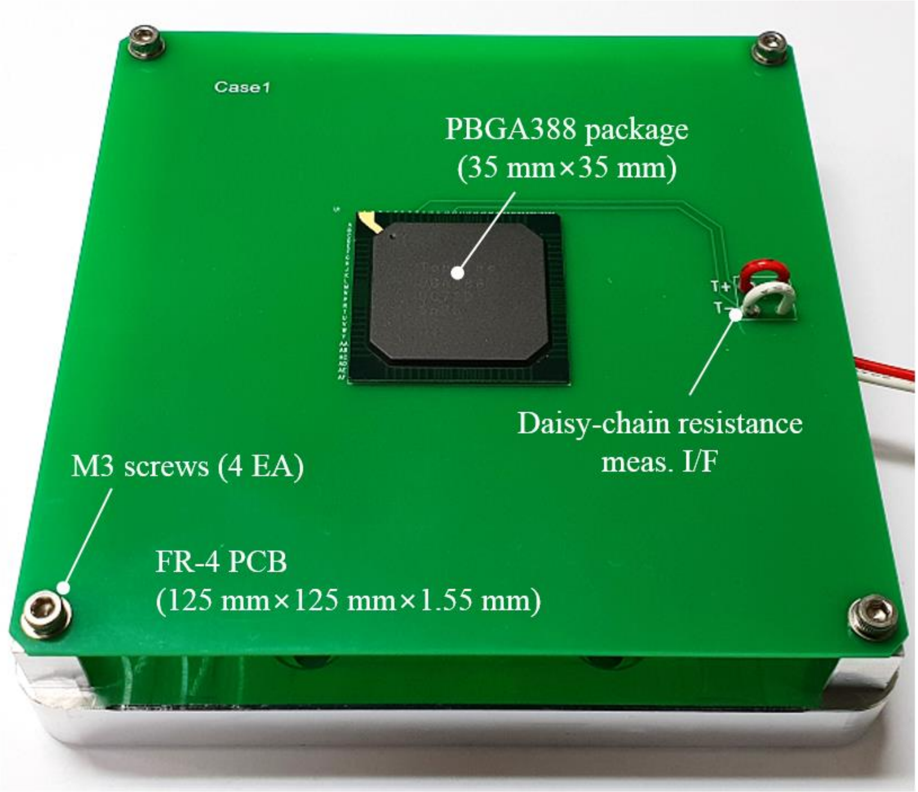

Fig. IV-3 Representative configuration of sample PCB assembly in Case 1

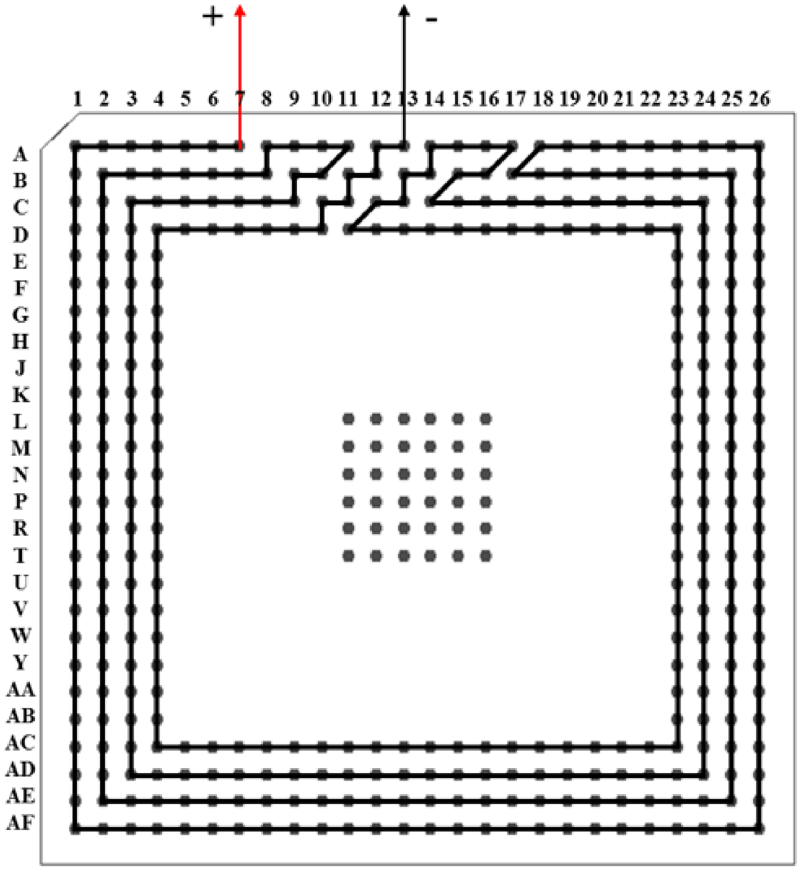

Fig. IV-4 Configuration of daisy-chain circuit for PBGA388 package

2. Results of Fatigue Life Tests

The fatigue life test set-up for a set of PCB samples mounted on the vibration shaker is shown in Fig. IV-5. In this study, three sets of board samples were fabricated and tested to ensure the reliability of the test results. To assess TTF_{test} of each package, in-situ monitoring of the daisy-chain resistance was performed. Two-wire resistance measurements were performed for each sample using the data acquisition (DAQ) device of DAQ6510 (Keithley Co. Ltd., USA). The measurement accuracy of the DAQ was less than 10^{-2} Ω, and the sampling rate was set as 1.7 samples/s. The failure criterion on the solder joint was defined as when the DAQ detects a resistance value 20% higher than the initial value, five times consecutively, in accordance with the IPC-9701A standard [50]. The random vibration test input of 20 G_{rms} specified in Table IV-2 was continuously applied for the excitation of board samples until the failure criterion was achieved.

Figure IV-6 shows the time histories of the daisy-chain resistance values for the first set of PCB samples. The initial failure of the solder joint was detected in the Case 1 sample at 42 min of random excitation. The Case 2 sample subsequently failed at 57 min, and Case 1-1 also failed at approximately the same time. The Case 1-2 and Case 3 samples failed at 148 and 240 min of test progress, respectively. Table IV-3 shows the measured TTF values of the tested packages, TTF_{test}, for all the sets of PCB samples. The TTF of PCB samples in the same case was similar between each other although some of the samples showed slight differences. These test results were used to validate the Oh-Park methodology.

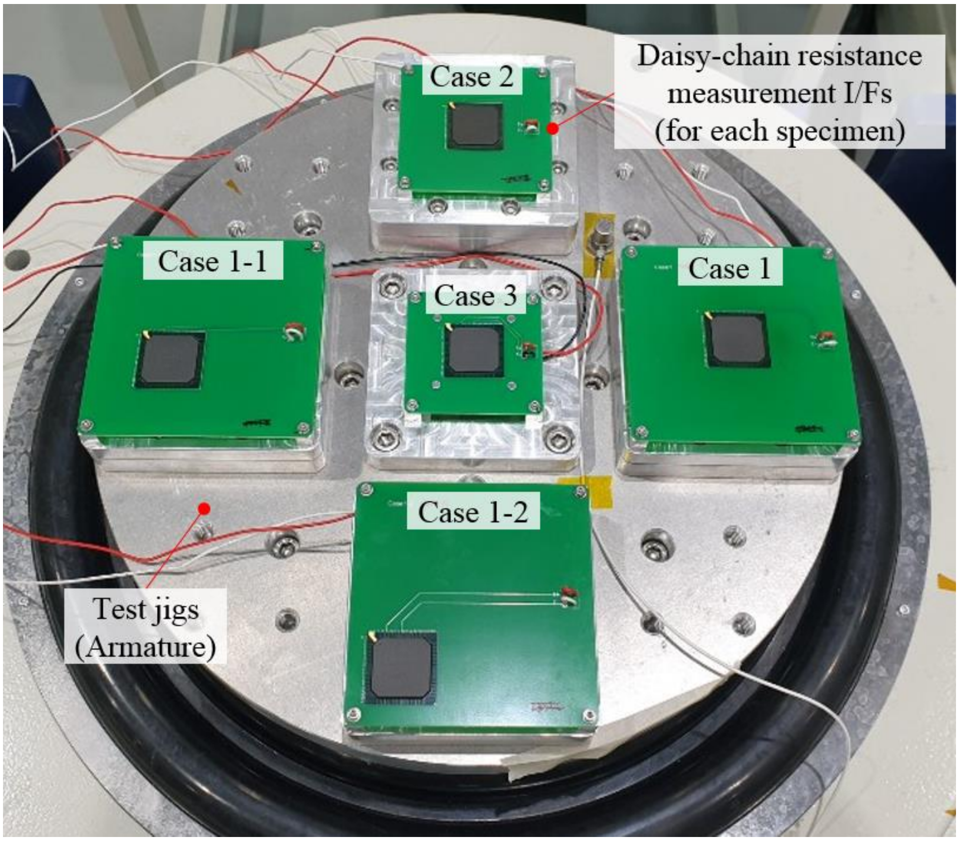

Fig. IV-5 Fatigue life test set-up for a set of PCB samples

Table IV-2 Specifications of input random vibration

Frequency (Hz)	PSD acceleration (g^2/Hz)
20	0.091
60	0.273
1,000	0.273
2,000	0.069
Overall (full level (0 dB))	20 G_{rms}

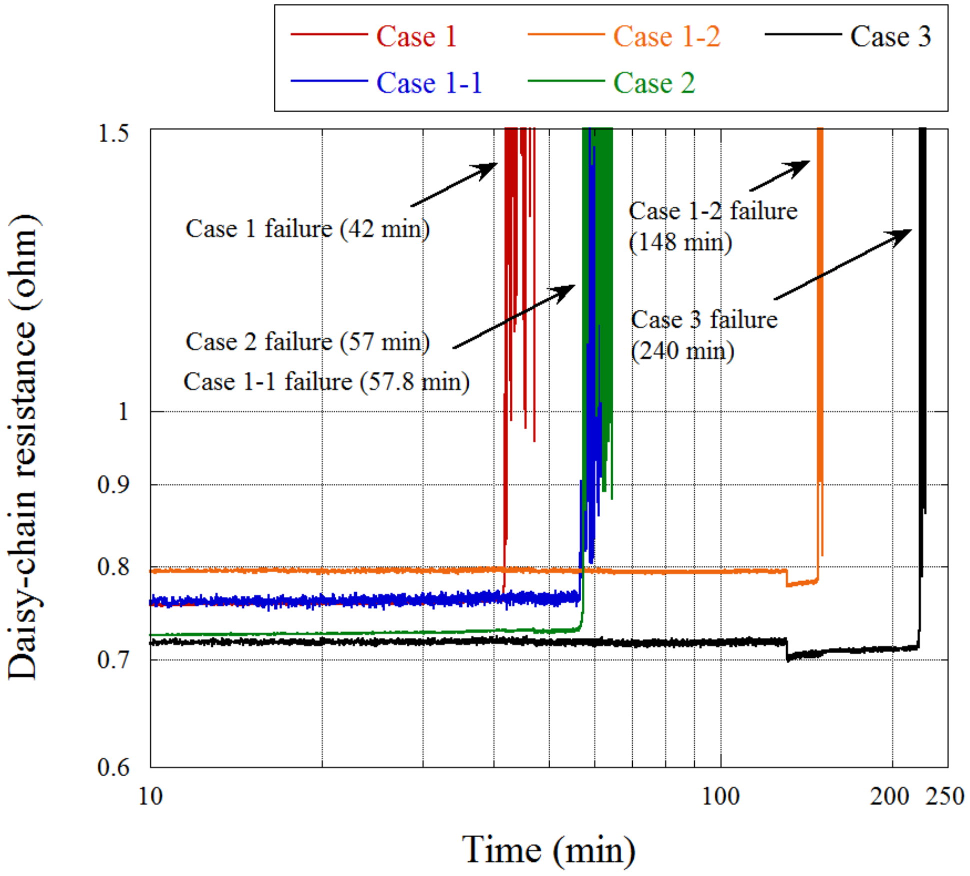

Fig. IV-6 Time profile of measured daisy-chain resistance for each sample during random vibration excitation

Table IV-3 TTF_{test} of PCB samples measured from fatigue life test

Case	Set 1 samples	Set 2 samples	Set 3 samples
1	42	54	34.5
1-1	57.8	47	223
1-2	148	114.3	222.5
2	57	60	63
3	240	70	600

C. Methodology Validation

To validate the effectiveness of the proposed Oh-Park methodology, the validation scheme shown in Fig. IV-7 was established in accordance with the various simplified FEM modeling techniques. The evaluation was also performed using Steinberg's theory for comparison with the proposed methodology. In addition, the validation involves a comparison between the MoS calculated based on FoS_{m} value with respect to the original criterion of 2 × 10^7 cycles and DF value based on TTF_{req}. The mechanical safety of the tested sample PCBs was evaluated in accordance with the approach described in Fig. IV-1. We also predicted the TTF using both methodologies to determine whether the calculated MoS accurately represents the actual TTF of the tested packages.

The predicted TTF, TTF_{pred}, based on the PCB displacement, is calculated using the power law-based equation described as follows:

$$TTF_{\mathrm{pred}} = N_{\mathrm{org}} \times \left(\frac{\delta_{\mathrm{allow}}}{\delta_{\mathrm{max}}}\right)^{b} \times \left(\frac{1}{f_{\mathrm{n}} \times 60}\right) \qquad \text{(IV-12)}$$

where N_{org} is 2 × 10^7 cycles for random vibration. Based on the PCB strain, TTF_{pred} is calculated as follows:

$$TTF_{\mathrm{pred}} = N_{\mathrm{org}} \times \left(\frac{\varepsilon_{\mathrm{c}}}{\varepsilon_{\mathrm{p_{max}}}}\right)^{b} \times \left(\frac{1}{f_{\mathrm{n}} \times 60}\right) \qquad \text{(IV-13)}$$

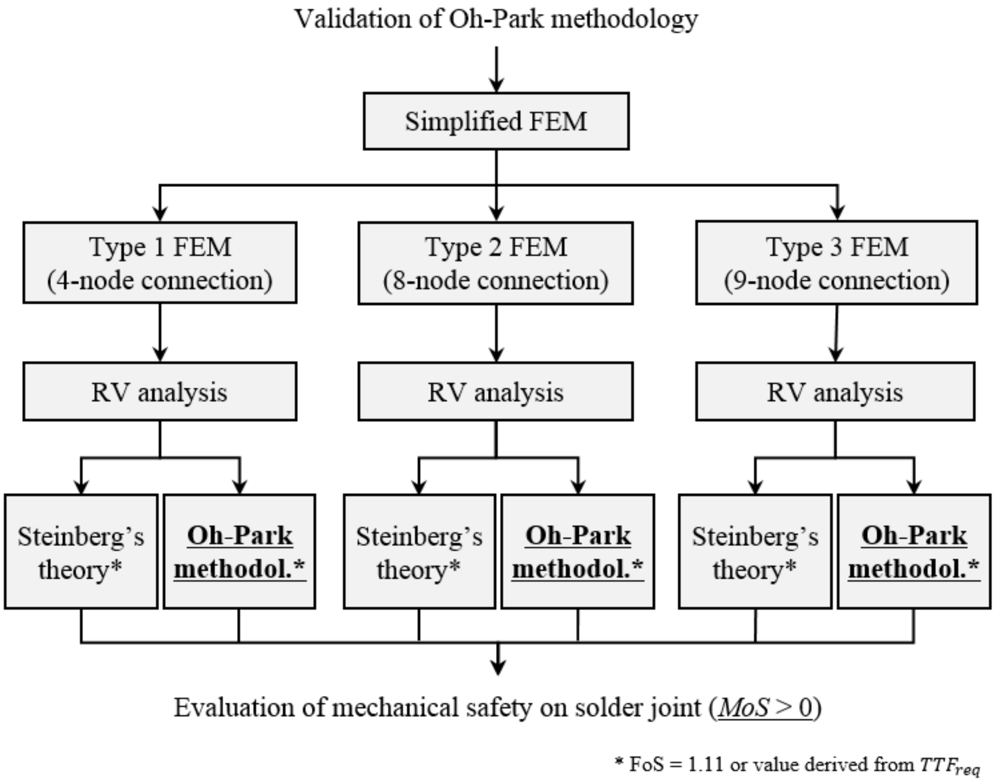

Fig. IV-7 Validation scheme for Oh-Park methodology

1. FEM Modeling Technique of PCB

In this study, a guideline on the simplified FEM modeling technique for the PCB and electronic package was established for the reliable evaluation of solder joint safety. The guideline includes the estimation method for $\varepsilon_{\mathrm{p}_{\mathrm{max}}}$. Fig. IV-8 shows a representative example of a simplified FEM of a sample PCB in Case 1 modeled by the proposed technique. The modeling guideline was established by a trial and error method based on numerous structural analyses. The FEM of the package is based on the lumped mass and rigid link elements, as presented in the chapter III because it is the simplest form of modeling to save time and effort in constructing the model among the existing modeling techniques of the electronic package. The rigid link elements used for simulating the package and bolted junctions have the constraints in only three translational DoFs. As the boundary condition, six DoF constraints are applied to the independent nodes of the rigid link elements of bolted junctions. To find the most feasible modeling technique for evaluating solder joint safety, three different modeling configurations for the BGA-type package, with various numbers of nodes on the PCB connected with the lumped mass by a rigid link element, as shown in Fig. IV-9, were proposed and investigated. Types 1, 2, and 3 correspond when the rigid link elements are connected to the numbers of 4, 8, and 9 nodes on the PCB, respectively.

The shell elements of QUAD4 and TRI3 are used for modeling the PCB as they provide more precise board strain results compared with the solid elements, which could overestimate the stiffness due to the inability to provide the rotational DOFs. Here, the package mounting area, which is equivalent to the package body size, is uniformly modeled by QUAD4 elements. Because the board strain is overestimated when the element is constrained by a rigid link, a technique to determine the appropriate size of the shell element is essential to mitigate the overestimation problem. In practice, it is known that the solder joint becomes vulnerable to fatigue failure under mechanical loading as the density of the solder ball array decreases because it typically leads to a reduction in the size of the solder ball [15]. Based on this, we found that reasonable strain estimation is possible for the BGA package when the element size is equivalent to the value of the package body length divided by the number of solder balls on one side of the package. For the PBGA388 package, with a length of 35 mm and a number of 26 solder balls on one side, the element size was approximately 1.35 mm, and this value was used in the FEM modeling shown in Fig. IV-8. This modeling technique is advantageous as it enables a reflection of the effect of the density of the solder ball array even if its actual configuration is not implemented in the FEM. For the rest of the area on the board, a mesh size that can obtain uniform mesh quality is recommended. In this study, a 1.5 mm mesh size was used for the FEM. After the random vibration analysis, $\varepsilon_{\mathrm{p}_{\mathrm{max}}}$ is derived from the RMS nodal strains extrapolated from the element centroid. Here, $\varepsilon_{\mathrm{p}_{\mathrm{max}}}$ is the averaged value of strains at four nodes belonging to the cornermost QUAD4 element in the package mounting area, as shown in Fig. IV-10.

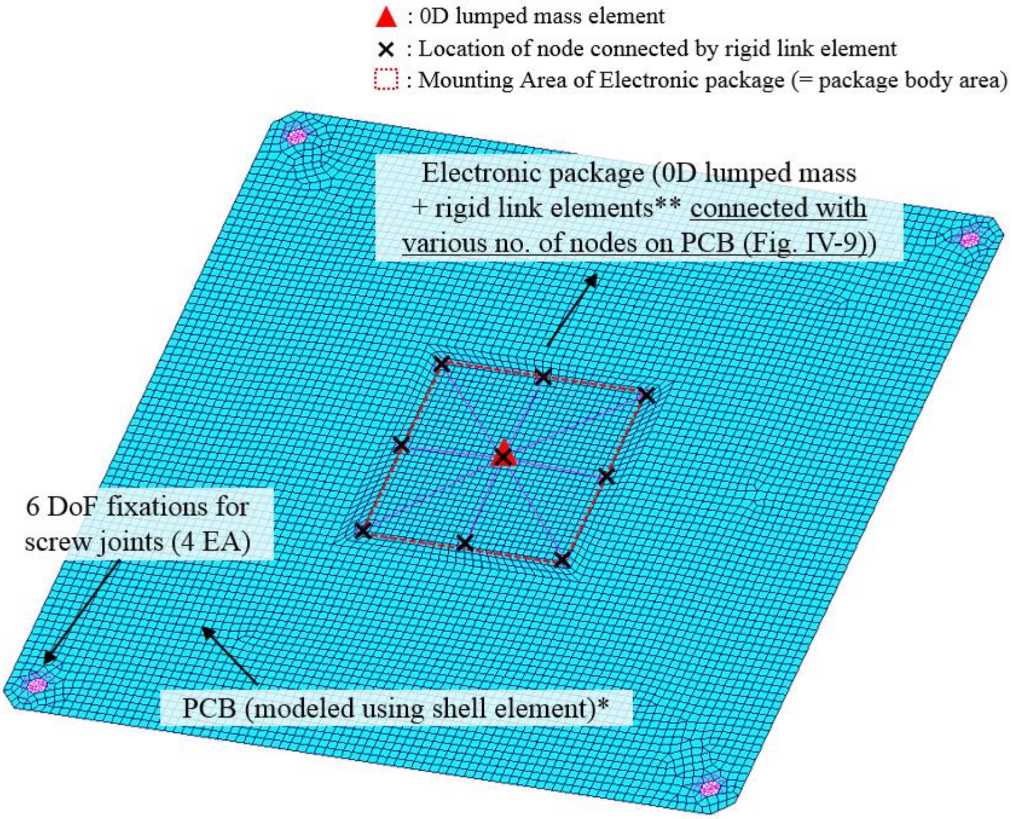

* Mesh size of PCB (mm)
- Package mounting area: Package length/No. of solder joints on one side
- Rest of the PCB area: Sufficient value for uniform mesh quality (1.5mm was used in this study)

** Rigid link element (used for package, fixation points)
- 3 trans. DoF constraints (6 DoFs constraints applied at independent node of each rigid link element)

Fig. IV-8 Example of FEM of PCB assembly with Case 1 modeling technique for electronic package

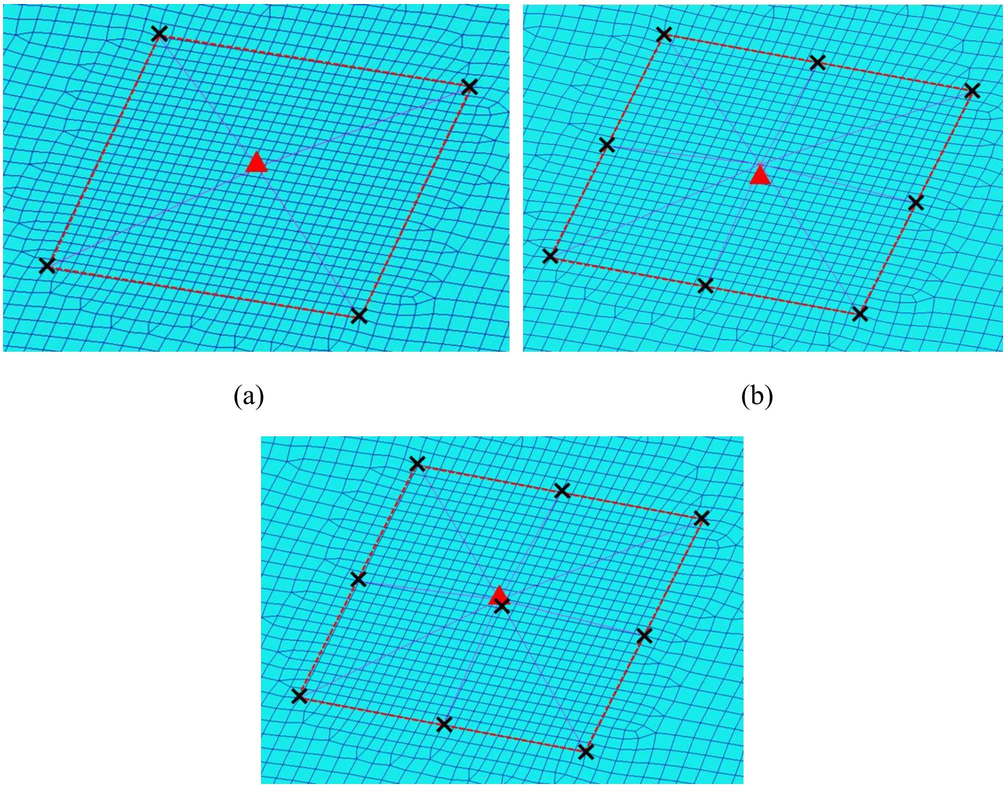

(a)

(b)

(c)

Fig. IV-9 Various simplified modeling techniques for electronic package ((a) Type 1 (4 nodes connection), (b) Type 2 (8 nodes connection), (c) Type 3 (9 nodes connection))

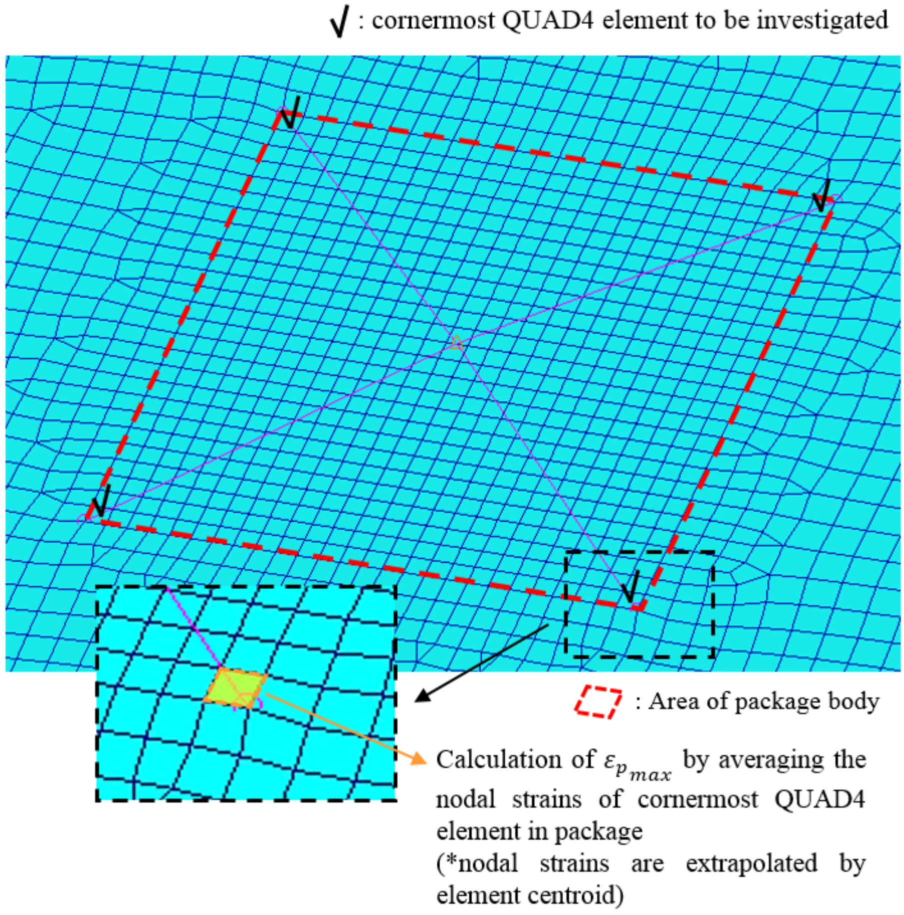

Calculation of $\varepsilon_{p_{max}}$ by averaging the nodal strains of cornermost QUAD4 element in package
(*nodal strains are extrapolated by element centroid)

Fig. IV-10 Calculation method to derive $\varepsilon_{\mathrm{p_{max}}}$ from simplified FEM

2. Mechanical Safety Evaluation

Prior to the structural analysis of sample PCBs, the conformity between measured and analyzed dynamic responses of sample PCBs was investigated based on the bare PCBs in Case 1, 2 and 3 without packages. The FEMs of these bare PCBs were constructed and random vibration analysis was performed. Cases 1-1 and 1-2 were not analyzed because the board configurations are same as that of Case 1 and only difference is the mounting location of PCB. Figs. IV-11~IV-13 are measured and analyzed PSD acceleration responses of bare PCBs and these comparison results are summarized in Table IV-4. The modal damping values of 0.02, 0.0355 and 0.047 was applied in the analyses of Case 1, 2 and 3. The damping ratio is a function of stiffness, damping coefficient and mass of the system. Increased modal damping values of Cases 2 and 3 are caused by smaller masses of the PCB compared with the Case 1. Same phenomenon was also reported in previous researches on the vibration response characteristics of metal beam and PCB [56-57]. The analyzed G_{rms} responses and f_{n} values of all the bare PCBs correspond with the measured ones with only maximum difference of 2.7 % and 3.4 %, respectively. Although the bare PCBs in Cases 1 and 3 showed some differences in response at 2nd or 3rd peaks, it does not a problem for analysis since the 1st peak response is dominant in terms of the mechanical safety of solder joint. Therefore, we concluded that the FEM of PCB provides reliable analysis results.

After construction of the FEMs with various modeling techniques shown in Fig. IV-9, modal analysis was performed for each case. The representative results of the first three major mode shapes of the Case 1 PCB constructed by the Type 3 modeling are shown in Fig. IV-11. The analyzed values of f_{n} for each sample PCB are summarized in Table IV-4. Table IV-5 summarizes the estimation results of TTF_{req} for survival in the scenario shown in Fig. IV-2.

The results indicated that TTF_{req} = 35.2 min became the design criterion for electronics. Fig. IV-12 shows the variation of the estimated DF as a function of f_{n} when TTF_{req} = 35.2 min. It can be seen that DF becomes larger than 1.0 as the f_{n} increases. In contrast, the previous studies [4, 13] used FoS_{m} = 1.11–1.4 regardless of the f_{n}, which is equivalent to DF=0.71–0.91. These results indicate that the DF estimated by TTF_{req} in accordance with the proposed methodology would be effective to prevent the unnecessary margin for fatigue life of solder joint.

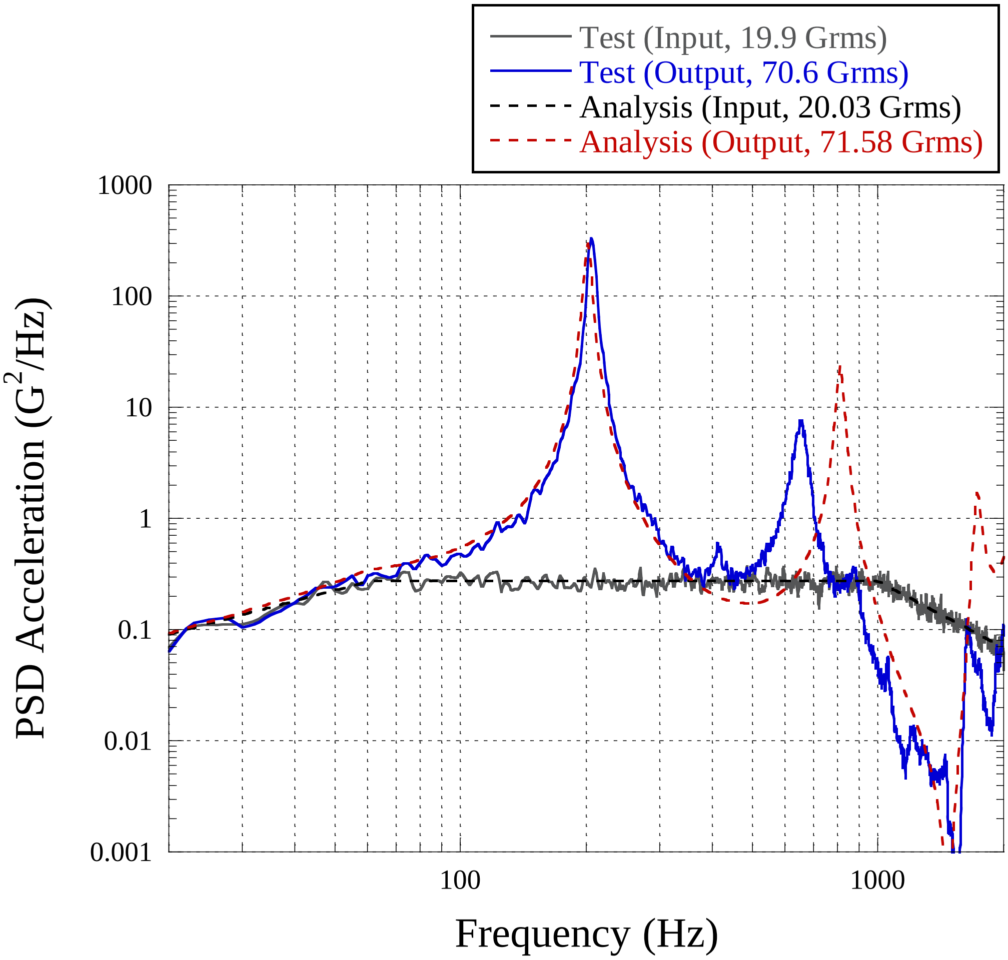

Fig. IV-11 Measured and analyzed PSD acceleration responses of bare PCB in Case 1 (w/o package)

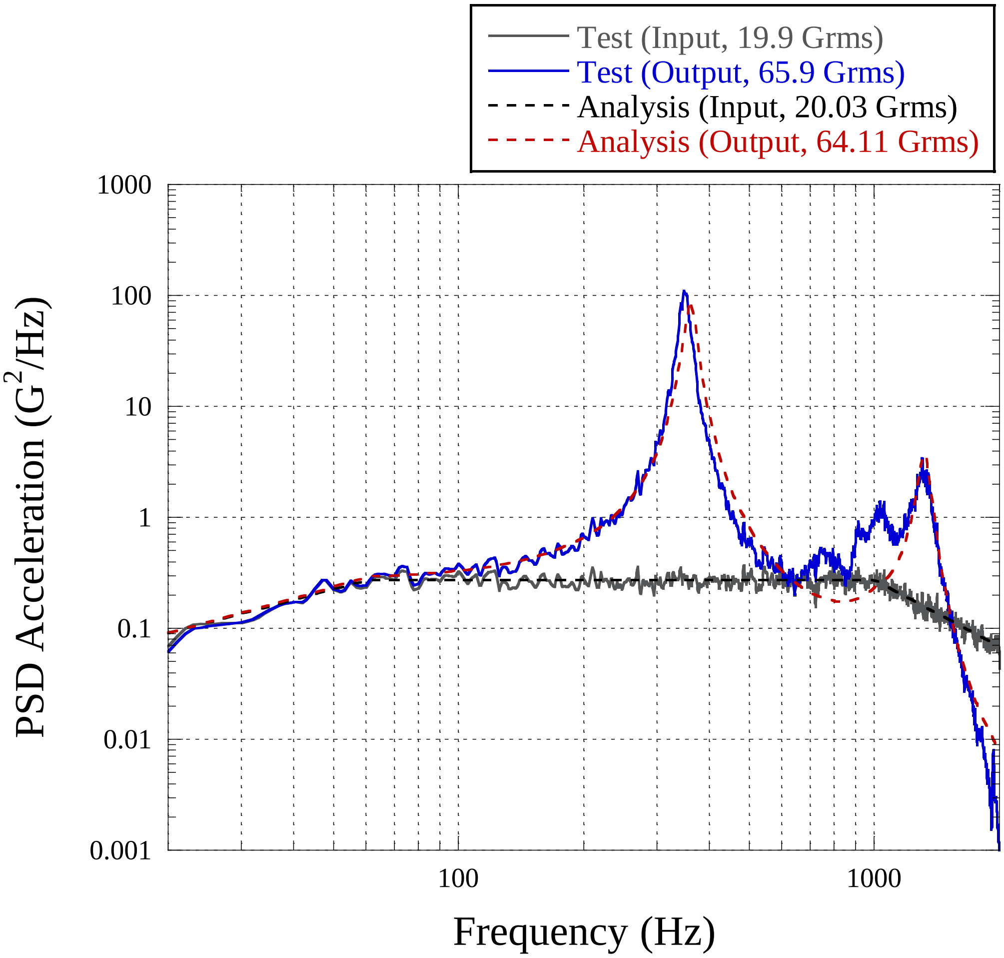

Fig. IV-12 Measured and analyzed PSD acceleration responses of bare PCB in Case 2 (w/o package)

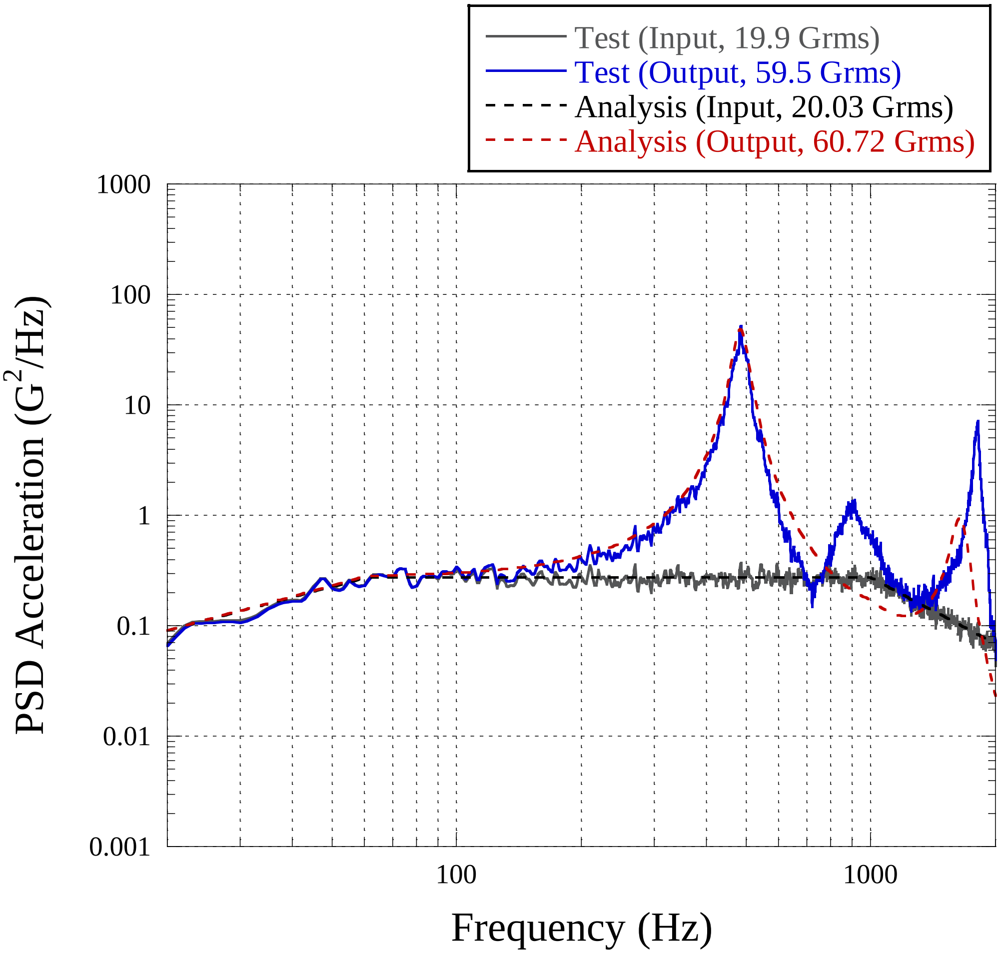

Fig. IV-13 Measured and analyzed PSD acceleration responses of bare PCB in Case 3 (w/o package)

Table IV-4 Summary of measured and analyzed responses of bare PCBs

Case	**Measured G_{rms} Response**	**Analyzed G_{rms} Response**	**Difference (%)**
1	70.6	71.58	1.4
2	65.9	64.11	2.7
3	59.5	60.72	2.0
Case	**Measured f_n (Hz)**	**Analyzed f_n (Hz)**	**Difference (%)**
1	205	201	1.9
2	348	360	3.4
3	485	484	0.2

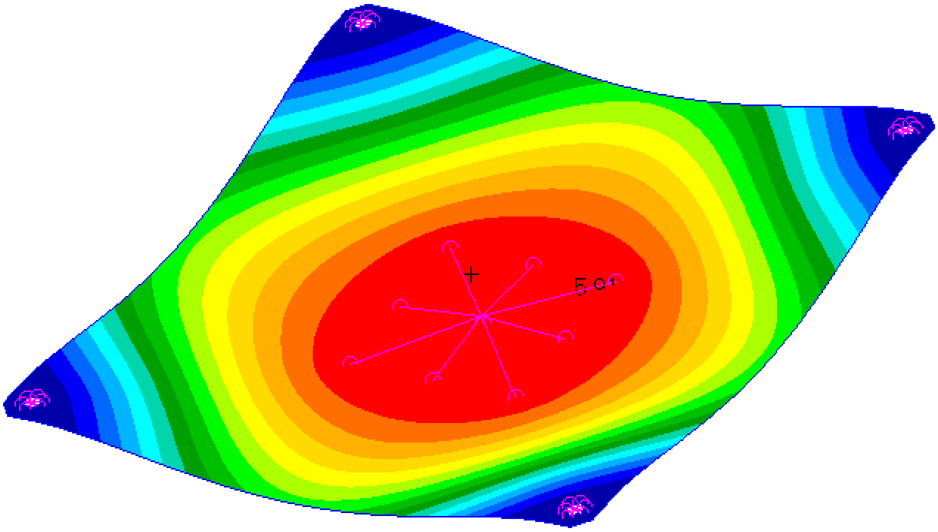

(a)

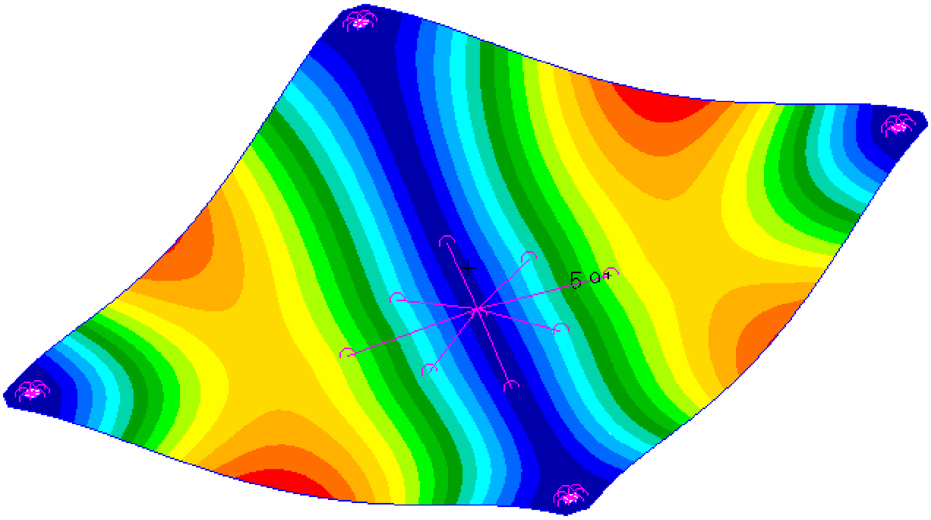

(b)

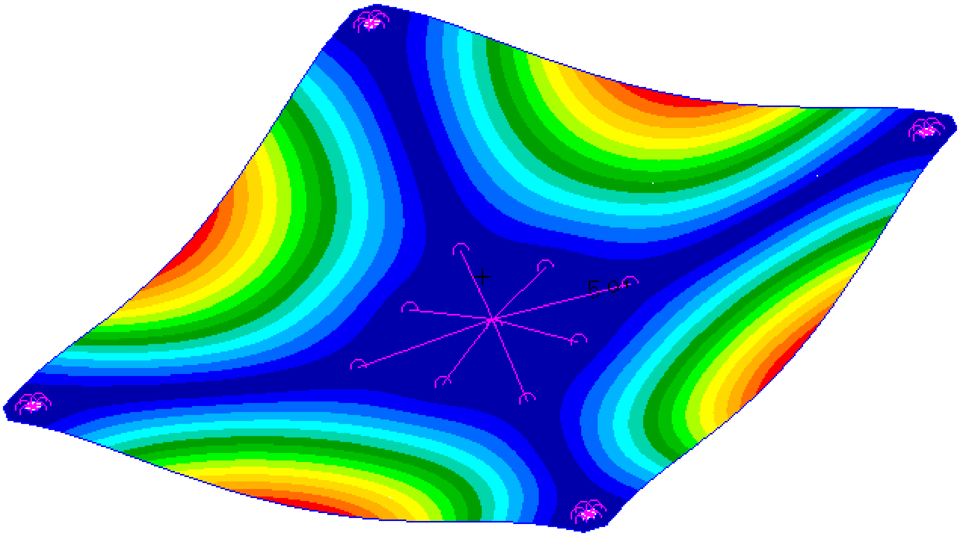

(c)

Fig. IV-14 Mode shapes of sample PCB in Case 1 with Type 3 package modeling ((a) 1st mode: 198.2 Hz, (b) 2nd mode: 386.8 Hz, (c) 3rd mode: 520.5 Hz)

Table IV-5 Analyzed values of f_{n} for each sample PCB assembly

Case	Type 1 FEM (4 nodes connection)	Type 2 FEM (8 nodes connection)	Type 3 FEM (9 nodes connection)
1	186.0	196.7	198.2
1-1	188.4	196.1	197.0
1-2	193.0	194.5	196.0
2	351.1	389.3	393.4
3	537.2	627.2	635.9

Table IV-6 Estimation results of TTF_{req} for survival of solder joint in test and launch processes

Step	Factor	Value	Unit	Remarks
No. of tests per each test level	n	3	-	-
Fatigue exponent for solder joint	b	6.4	-	for solder or lead frame material
Duration for a single test (min)	t_{test}	2.00	min	-
Duration for launch random vibration (min)	t_{lnch}	4.00	min	-
Eqv. time for vibration tests at each test level (min)	$T_{\text{-12dB}}$	0.00029	min	-
	$T_{\text{-9dB}}$	0.0026	min	-
	$T_{\text{-6dB}}$	0.024	min	-
	$T_{\text{-3dB}}$	0.219	min	-
	T_{0dB}	2.00	min	-
Eqv. time for qualification test (comp. level)	$\Sigma T_{\text{C-Q}}$	6.74	min	for 3-axis tests
Eqv. time for qualification test (S/S level)	$\Sigma T_{\text{S/S-A}}$	0.74	min	
Eqv. time for launch (S/S level)	ΣT_{L}	1.32	min	Eqv. to AT ($\Sigma T_{\text{-3dB}}$), 3 axis excitation
Factor of safety w.r.t. required fatigue life (min)	FoS_{ttf}	4	-	Referred ECSS-E-ST-32C
Required fatigue life for solder joint (min)	TTF_{req}	35.2	min	-

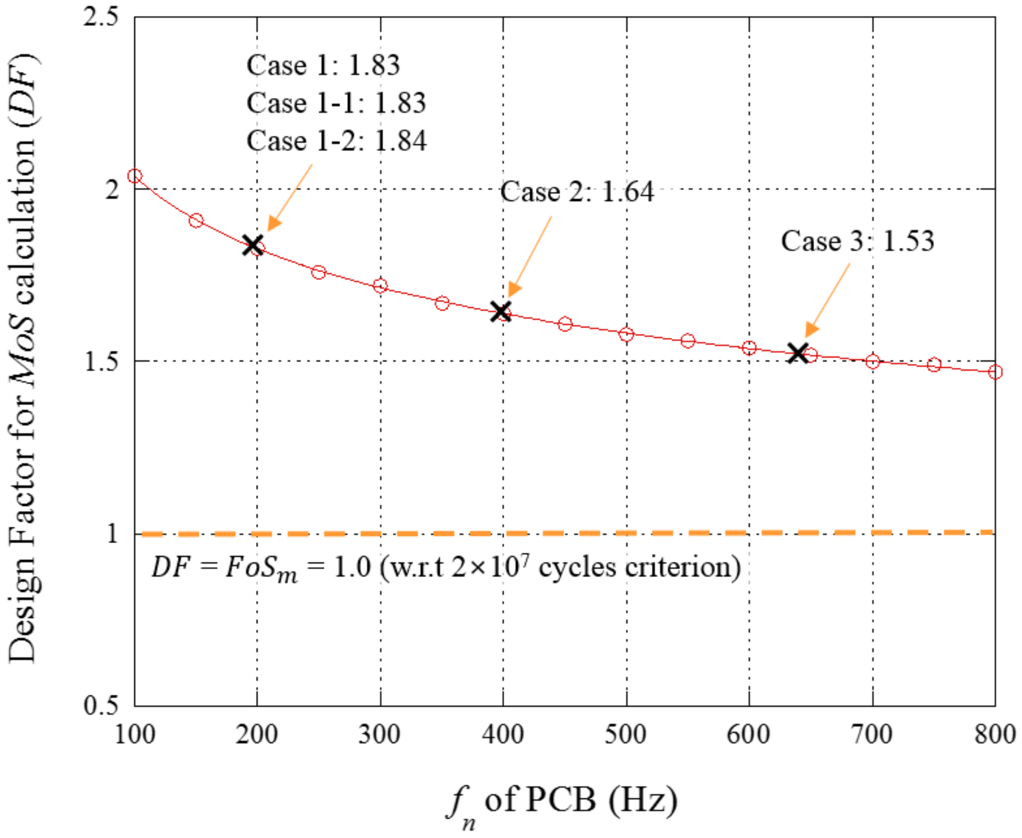

Fig. IV-15 Estimated DF for estimated TTF_{req} as a function of f_{n}

Table IV-7 summarizes the MoS calculated for each package using the proposed Oh-Park methodology and Steinberg's theory when the Type 1 modeling is applied. The results derived from FoS_{m} = 1.11, used in the previous chapter, are also summarized in Table IV-7 for comparison with the proposed methodology. Fig. IV-16 shows the TTF_{pred} calculated using Eqs. (IV-12) and (IV-13) to validate the effectiveness of the methodologies. In this study, the TTF_{pred} is considered to be accurate if it is within the range of four times longer and shorter values of the minimum value of TTF_{test} considering the scatter factor of 4.0 specified in the ECSS standard [53]. The overall results obtained from both methodologies indicate that the application of DF derived from TTF_{req} effectively mitigates the problem of excessive margins in the MoS calculation. However, the opposite trend was observed between the results of these methodologies. The MoS values calculated by Steinberg's theory, based on the TTF_{req}, seem to accurately represent mechanical safety because only the Case 1 package failed at 34.5 min in the test, which is earlier then the TTF_{req} = 35.2 min, revealed the negative margin. However, TTF_{pred} for the Cases 1-2, 2, and 3 packages are much longer than TTF_{test} and this overestimation results from the theoretical limitations of Steinberg's theory. The Oh-Park methodology, however, provides conservative results for MoS and TTF_{pred} because the values of $\varepsilon_{\mathrm{p_{max}}}$ were excessive in most cases. This phenomenon was caused by the strain concentration at the rigid link element connected to only four nodes of the PCB, which has a largely different configuration as compared to the actual PBGA388 package with a 2D solder ball matrix. Therefore, we investigated the Types 2 and 3 modeling with 8 and 9 nodes constrained by rigid links, respectively, to more effectively simulate the actual package configuration.

Table IV-8 summarizes the results of the MoS calculations based on the Type 2 FEM, and the TTF_{pred} values obtained using Eqs. (IV-12) and (IV-13) are shown in Fig. IV-17. It is evident that the MoS calculated by the Oh-Park methodology accurately represents the mechanical safety with respect to TTF_{req} = 35.2 min as compared with the results obtained using the Type 1 FEM presented in Table IV-6. This is because the phenomenon of strain concentration seen in the Type 1 FEM was mitigated by adding additional rigid constraint points for the package. Meanwhile, the MoS calculated by Steinberg's theory also seems to well represent the mechanical safety; however, the graph shown in Fig. IV-14 indicates that the TTF_{pred} values derived from Steinberg's theory are still outside the acceptable error ranges specified above, except for the Case 1-1 package. This means that the problem with Steinberg's theory seen in Table IV-7 and Fig. IV-16 could not be solved by changing the package modeling configuration, whereas the Oh-Park methodology provides considerably reliable results.

Table IV-9 and Fig. IV-18 show the results of the MoS and TTF_{pred} values calculated by the design methodologies based on the Type 3 FEM. The MoS values obtained by the Oh-Park methodology are similar to the results of the Type 2 model presented in Table IV-8. However, the TTF_{pred} values for all the sample packages were within the specified error range, which is more accurate than those of the Type 2 model. Although a maximum difference of up to three times was observed between the TTF_{pred} and the minimum value of TTF_{test} according to the sample cases, this degree of over- or under-estimation, is judged to be acceptable in the evaluation because FoS_{ttf} = 4.0 is considered in TTF_{req}. In contrast, as observed in the former analysis results using the Types 1 and 2 FEMs, Steinberg's theory continuously provides inaccurate results for the TTF_{pred}, which is critical in reliable MoS calculation. These results indicate that the problems associated with Steinberg's theory cannot be solved regardless of the modeling technique used. These results validated the effectiveness of the Oh-Park methodology for evaluating solder joint safety in comparison with previous methodologies. In addition, we also concluded that the Type 3 FEM with 9 nodes of PCB connected with a rigid link element is the most feasible solution for reliable and rapid design evaluation of electronics based on the proposed methodology among the Type 1–3 modeling techniques.

Table IV-7 Comparison between methodologies based on *MoS* of sample PBGA388 package calculated using Type 1 FEM

Case		**$\dot{\varepsilon}$ (μ-strain/s)**	**ε_{c} (μ-strain)**	**$\varepsilon_{p_{max}}$ (μ-strain)**	**DF (TTF_{req} =35.2 min)**	**MoS (TTF_{req} =35.2 min)**	**MoS (FoS_{m} =1.11)**
Oh-Park methodol.	1	666,933	91.6	570.7	0.542	-0.70	-0.86
	1-1	628,179	96.2	530.7	0.543	-0.67	-0.84
	1-2	217,938	178.9	179.7	0.545	0.83	-0.10
	2	879,625	70.0	398.7	0.599	-0.71	-0.84
	3	987,798	60.9	292.7	0.640	-0.67	-0.81
Case		**r**	**Z_{allow} (mm)**	**Z_{max} (mm)**	**DF (TTF_{req} =35.2 min)**	**MoS (TTF_{req} =35.2 min)**	**MoS (FoS_{m} =1.11)**
Steinberg's theory	1	1.000	0.201	0.363	0.542	0.02	-0.50
	1-1	0.887	0.226	0.291	0.543	0.43	-0.30
	1-2	0.332	0.604	0.135	0.545	7.21	3.03
	2	1.000	0.148	0.072	0.599	2.44	0.86
	3	1.000	0.131	0.024	0.640	7.52	3.91

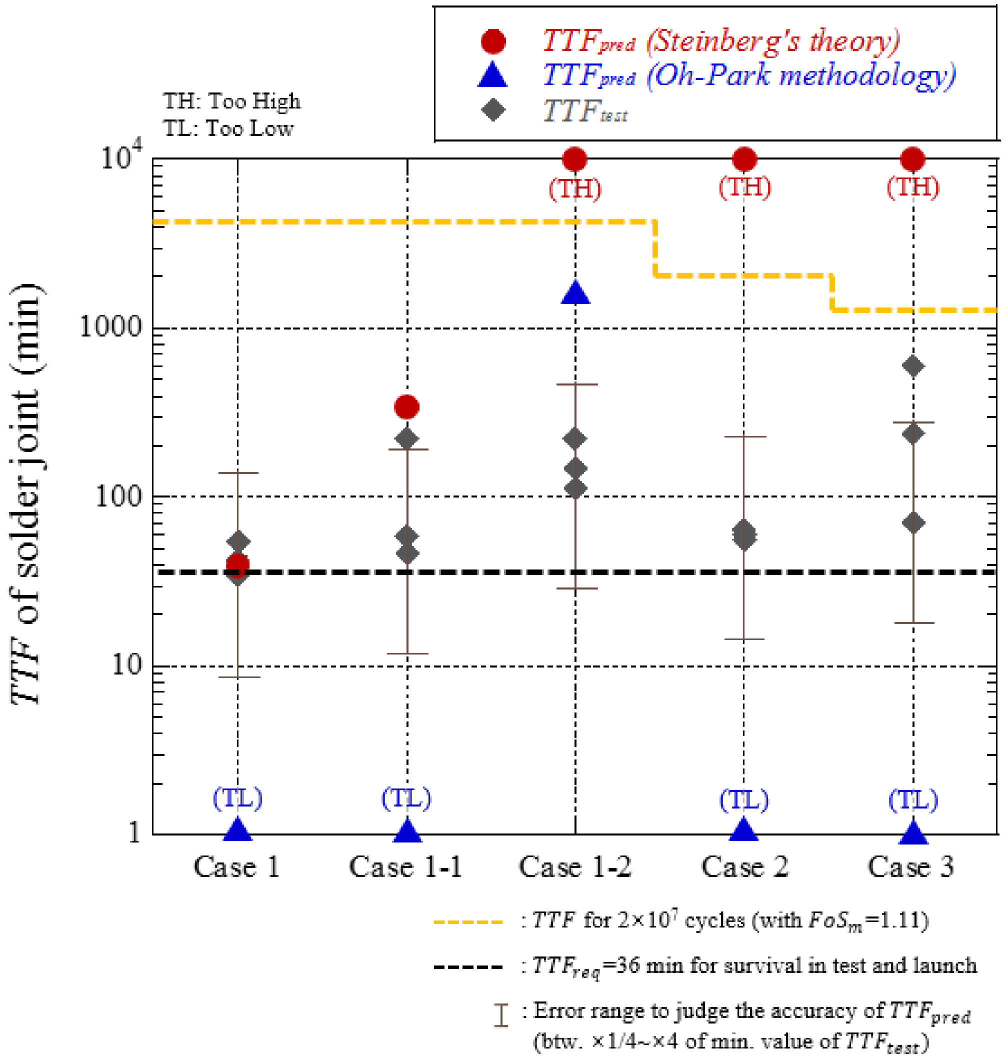

Fig. IV-16 Comparison between TTF_{test} and TTF_{pred} calculated by methodologies with Type 1 FEM

Table IV-8 Comparison between methodologies based on MoS of sample PBGA388 package calculated using Type 2 FEM

Case		$\dot{\varepsilon}$ **(μ-strain/s)**	ε_c **(μ-strain)**	$\varepsilon_{p_{max}}$ **(μ-strain)**	DF **(**TTF_{req} **=35.2 min)**	MoS **(**TTF_{req} **=35.2 min)**	MoS **(**FoS_m **=1.11)**
Oh-Park methodol.	1	358,000	140.2	289.7	0.547	-0.12	-0.56
	1-1	312,581	150.8	253.7	0.547	0.09	-0.46
	1-2	246,408	169.3	201.6	0.546	0.54	-0.24
	2	502,239	113.7	205.3	0.609	-0.09	-0.50
	3	602,408	99.5	152.9	0.656	-0.01	-0.41
Case		r	Z_{allow} **(mm)**	Z_{max} **(mm)**	DF **(**TTF_{req} **=35.2 min)**	MoS **(**TTF_{req} **=35.2 min)**	MoS **(**FoS_m **=1.11)**
Steinberg's theory	1	1.000	0.201	0.279	0.547	0.31	-0.35
	1-1	0.887	0.226	0.228	0.547	0.81	-0.11
	1-2	0.332	0.604	0.120	0.546	8.22	3.53
	2	1.000	0.148	0.069	0.609	2.53	0.94
	3	1.000	0.131	0.012	0.656	15.62	8.82

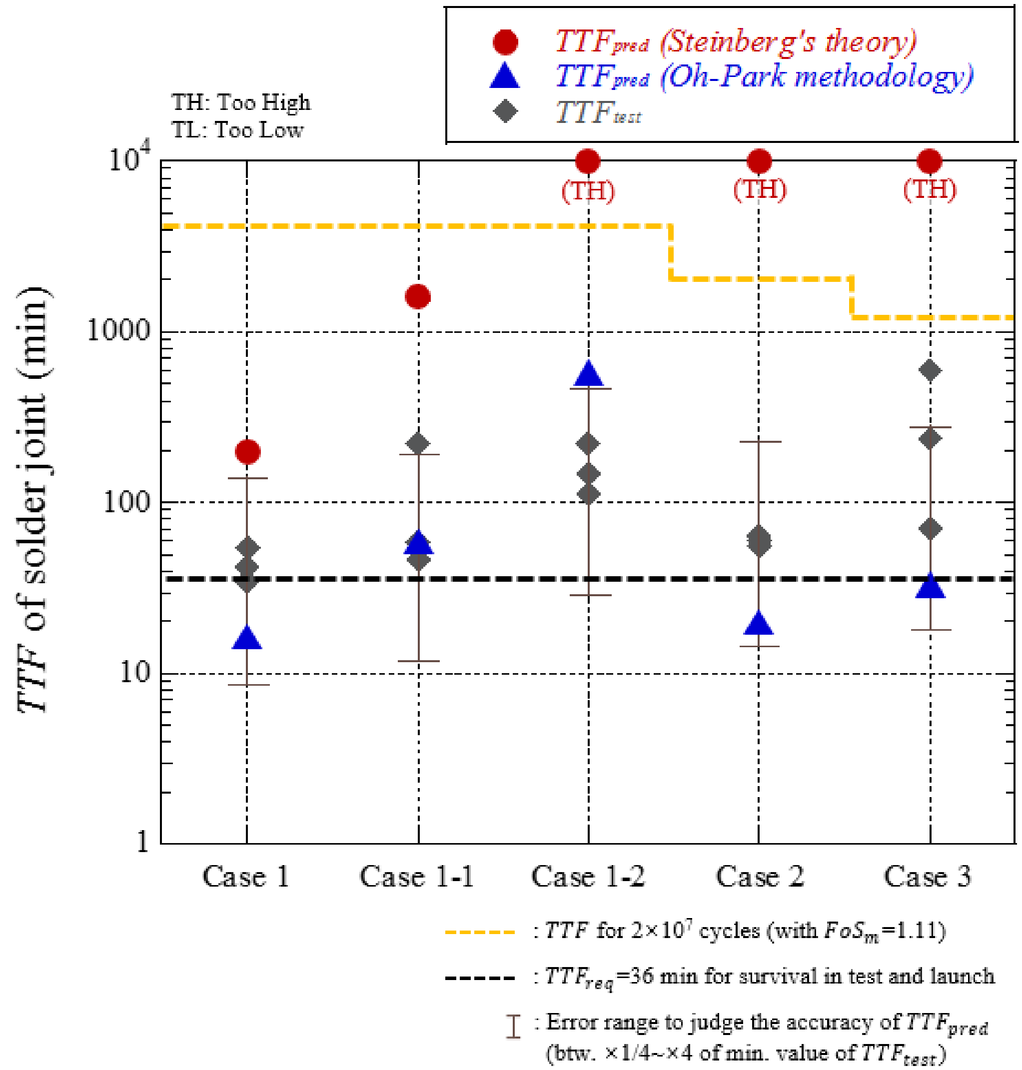

Fig. IV-17 Comparison between TTF_{test} and TTF_{pred} calculated by methodologies with Type 2 FEM

Table IV-9 Comparison between methodologies based on *MoS* of sample PBGA388 package calculated using Type 3 FEM

Case		$\dot{\varepsilon}$ **(μ-strain/s)**	ε_c **(μ-strain)**	$\varepsilon_{p_{max}}$ **(μ-strain)**	DF **(TTF_{req} =35.2 min)**	MoS **(TTF_{req} =35.2 min)**	MoS **(FoS_m =1.11)**
Oh-Park methodol.	1	358,000	145.2	269.4	0.547	-0.02	-0.51
	1-1	312,581	152.3	247.4	0.547	0.13	-0.45
	1-2	246,408	162.3	217.9	0.546	0.23	-0.33
	2	502,239	118.6	191.0	0.609	0.02	-0.44
	3	602,408	103.1	144.0	0.656	0.09	-0.36
Case		r	Z_{allow} **(mm)**	Z_{max} **(mm)**	DF **(TTF_{req} =35.2 min)**	MoS **(TTF_{req} =35.2 min)**	MoS **(FoS_m =1.11)**
Steinberg's theory	1	1.000	0.201	0.270	0.547	0.36	-0.33
	1-1	0.887	0.226	0.216	0.547	0.91	-0.06
	1-2	0.332	0.604	0.114	0.546	8.70	3.77
	2	1.000	0.148	0.042	0.609	4.79	2.18
	3	1.000	0.131	0.012	0.656	15.60	8.82

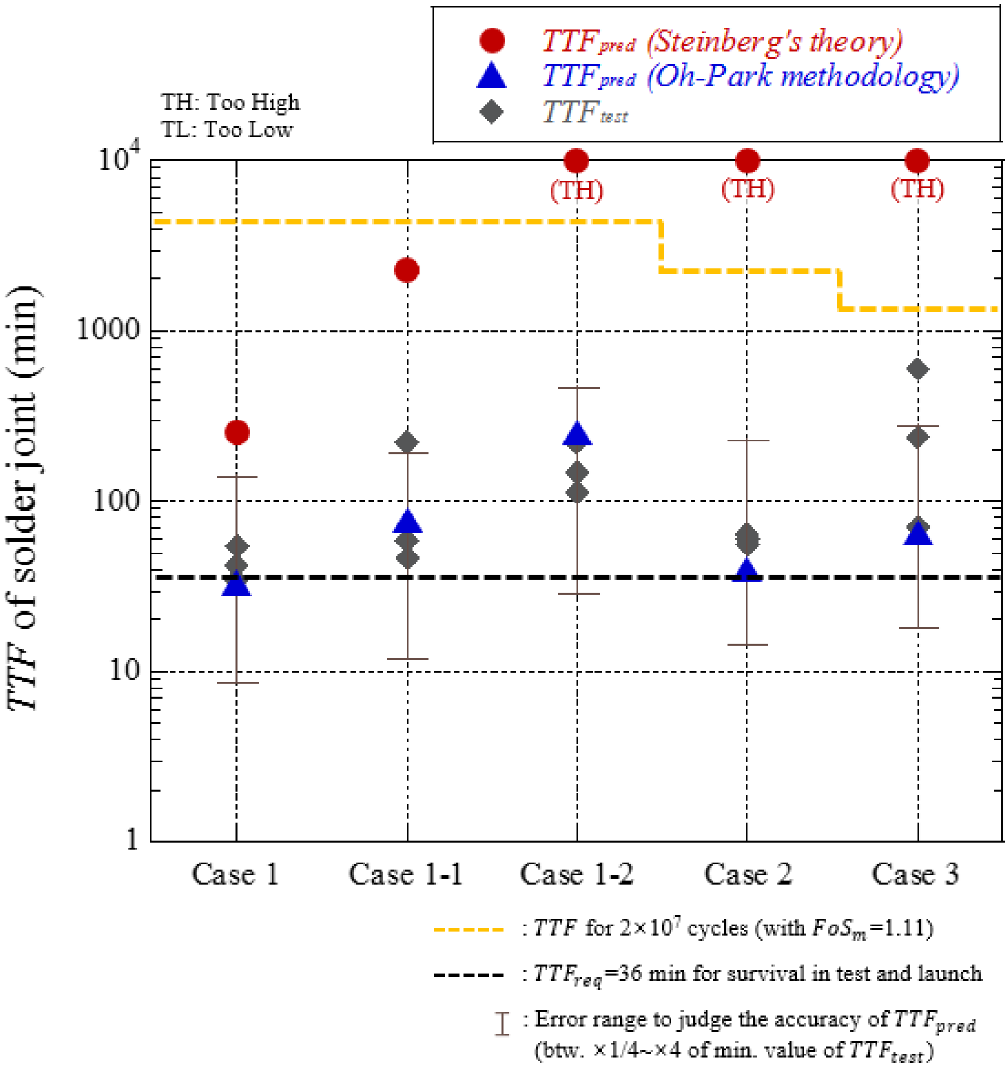

Fig. IV-18 Comparison between TTF_{test} **and** TTF_{pred} **calculated by methodologies with Type 3 FEM**

D. Methodology Validation on Various Packages

1. Sample Set #2: CCGA624 Package

In the present study, we also evaluated the 624-pin ceramic CGA (CCGA624) package, presented in the previous chapter based on the Oh-Park methodology with the Type 3 FEM modeling technique. A daisy-chained CCGA624 package with a size of 32.5 mm × 32.5 mm × 4.9 mm was mounted on the center of the PCB with dimensions of 100 mm × 100 mm × 2 mm. The total mass of the PCB assembly is 51.1 g, including the package with a mass of 13.3 g. An array of Sn20-Pb80 solder columns was integrated on the PCB using a Sn63-Pb37 material. The sample PCB was exposed to 28 G_{rms} of random vibration excitation until the daisy-chain resistance indicated failure of the solder joint. A TTF_{test} = 5.38 min was observed from the test results. The FEM was constructed using the approach shown in Figs. IV-8 and IV-9. The analyzed f_{n} was 382.6 Hz.

Table IV-10 summarizes MoS and TTF values calculated by the design methodologies. The test results in the Section III-C showed that the fatigue fracture was occurred at the solder column. This means that the evaluation shall be performed by applying the value of b for Sn20-Pb80 material, however, it has not yet been developed thus far. Therefore, in the analysis, we applied b=3.44 that was originally developed for Sn10-Pb90 column material [11] as a substitute. The MoS calculated by the Oh-Park methodology using DF showed a negative margin and it accurately represents the mechanical safety as TTF_{pred} was smaller than the TTF_{req} = 35.2 min. In addition, TTF_{pred} has only 1.72 times difference with TTF_{test}. In contrast, using Steinberg's theory still provided inaccurate results. These results indicate that the proposed Oh-Park methodology is also effective for providing reliable evaluation results on the CCGA package.

Table IV-10 Comparison between methodologies based on MoS of sample CCGA624 package

Design methodol.	MoS					TTF		
	$\dot{\varepsilon}$ (μ-strain/s)	ε_c (μ-strain)	$\varepsilon_{p_{max}}$ (μ-strain)	DF (TTF_{req} =35.2 min)	MoS (TTF_{req} =35.2 min)	TTF_{pred} (min)	TTF_{test} (min)	**Diff. btw.** TTF **(times)**
Oh-Park methodol.	838,668	67.8	348.9	0.395	-0.51	3.12	5.38	1.72

Design methodol.	MoS					TTF		
	r	Z_{allow} (mm)	Z_{max} (mm)	DF (TTF_{req} =35.2 min)	MoS (TTF_{req} =35.2 min)	TTF_{pred} (min)	TTF_{test} (min)	**Diff. btw.** TTF **(times)**
Steinberg's theory	1.0	0.141	0.09	0.395	2.98	4,124	5.38	766.5

2. Sample Set #3: QFP208 Package

In addition to the BGA and CGA type packages, the effectiveness of the proposed design methodology was also evaluated with regards to the QFP type package as well. This package is also one of the common types applied for the electronics being developed recently. In this study, a daisy-chained 208-pin QFP (QFP208) package was selected for the methodology evaluation. Figure IV-19 shows the illustration of the PCB sample with QFP208 package and the specifications of the package are listed in Table IV-11. The package with a size of 28 mm × 28 mm × 4 mm was mounted on the PCB sample with dimensions of 243 mm × 160 mm × 2.4 mm, and the total mass of PCB assembly is 196 g. The copper lead frames of the package were soldered on the PCB using Sn63-Pb37 material. Figure IV-20 shows set-up for random vibration fatigue tests. The sample PCB was exposed to 14 G_{rms} of random vibration excitation until the daisy-chain resistance indicated failure of the solder joint. A TTF_{test} = 277 min was observed from the daisy-chain resistance measurement results shown in Fig. IV-21.

In this study, we proposed the simplified modeling technique for QFP type package and it is illustrated in the Fig. IV-22. The overall modeling methodology is same as that shown in Figs. IV-8 and IV-9, but the difference in contrast to the modeling of BGA package is that the number of 16 points at the edge of the package body area are connected by rigid link element. The structural analysis was performed after making the FEM. Figure IV-23 shows representative mode shapes of the QFP208 PCB. The analyzed board f_{n} was 119 Hz. Table IV-12 summarizes MoS and TTF values calculated by the design methodologies. The MoS calculated by the Oh-Park methodology using DF showed a positive margin and it accurately represents the mechanical safety because TTF_{pred} was 120 min than the TTF_{req} = 35.2 min. In addition, TTF_{pred}=120 min has only the difference of 2.31 times with TTF_{test}. Meanwhile, the Steinberg’s theory showed the similar results as that of the Oh-Park methodology. The reason for the accurate results of the Steinberg’s theory is that the mode shape is close to the ideal half-sine wave such that the Z_{allow} is calculated with minimal error. The conclusion of the analysis is that the proposed Oh-Park methodology might be also effective for providing reliable evaluation results on the QFP package.

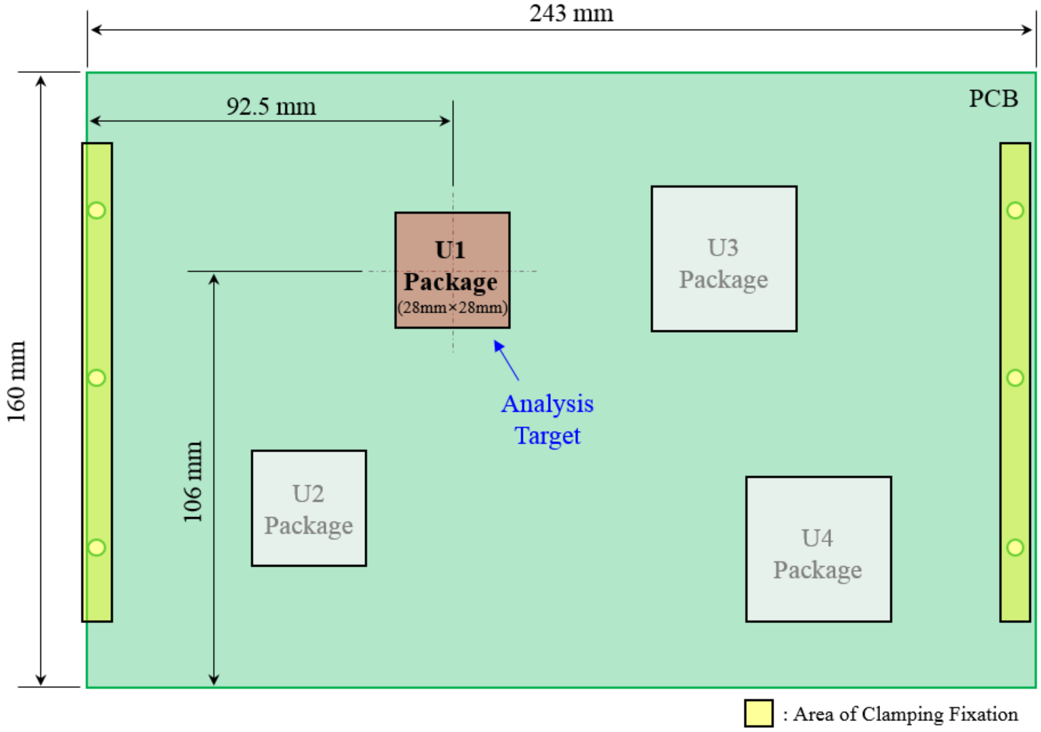

Fig. IV-19 Illustration of PCB sample with QFP208 package

Table IV-11 Specifications of QFP208 package

Package No.	Configuration	Properties
U1		- Package Type: QFP - Pin Count: 208 - Mount Type: Surface Mount - Size (mm): 28×28×4 - Mass (g): 5.4 - Solder Material: Sn63-Pb37

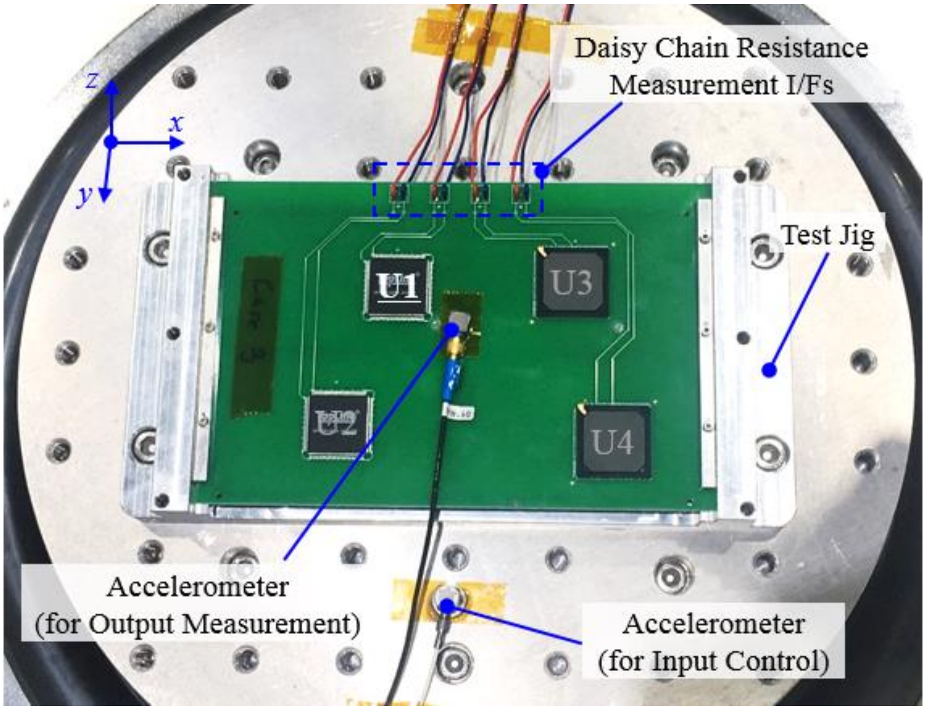

Fig. IV-20 Random vibration test set-up for QFP208 PCB sample (sample set #3)

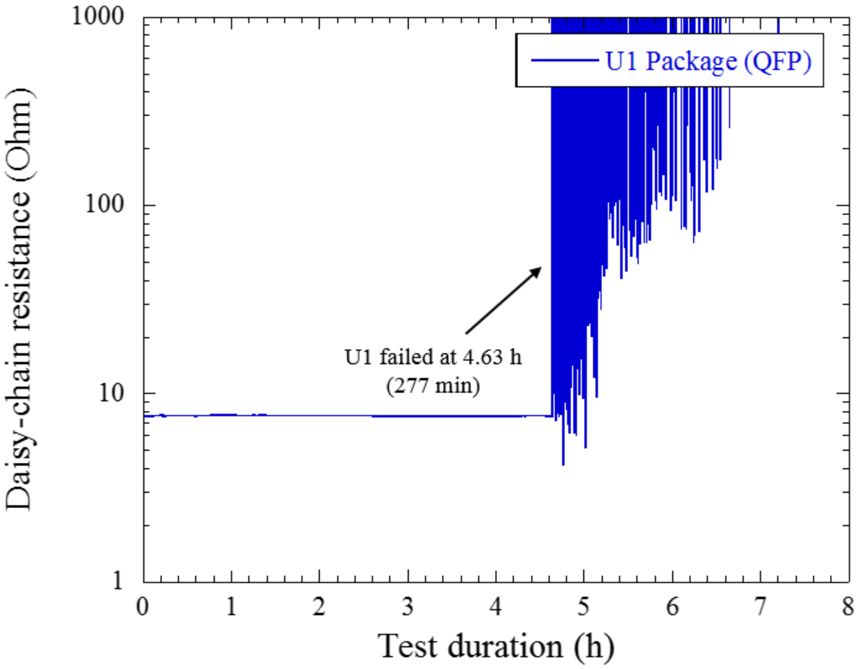

Fig. IV-21 Time profile of daisy-chain resistance for QFP208 package (sample set #3)

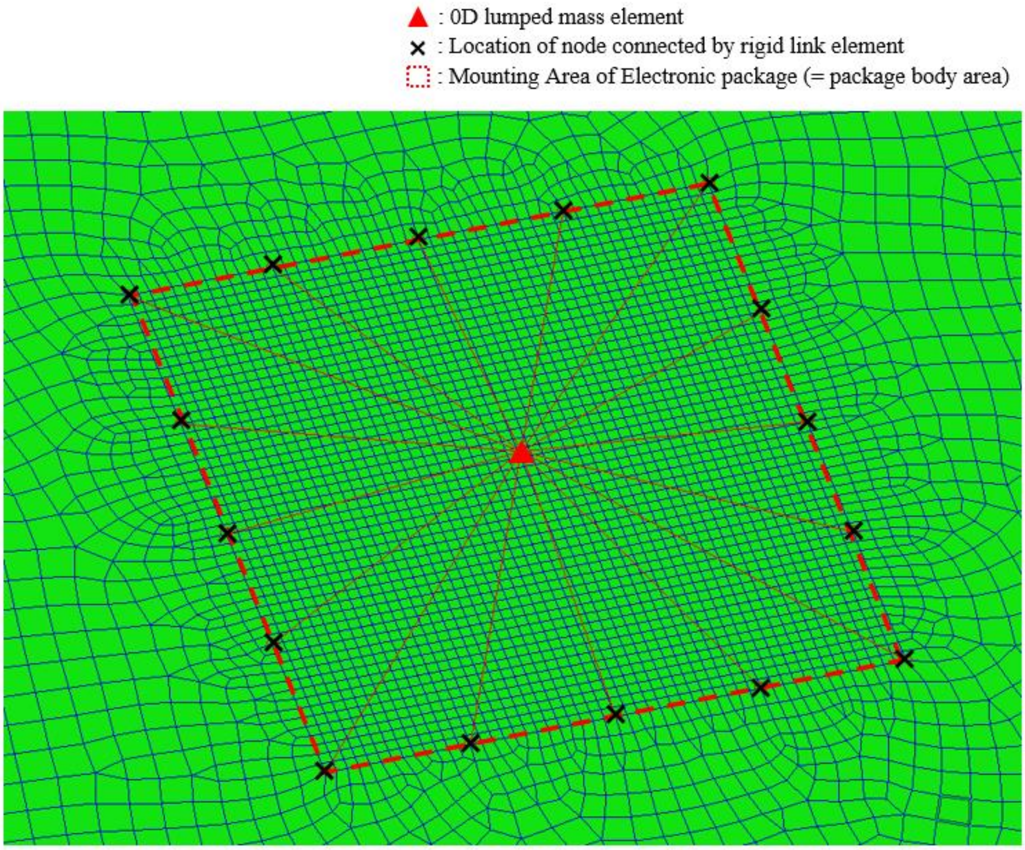

Fig. IV-22 Simplified FEM modeling technique for QFP package

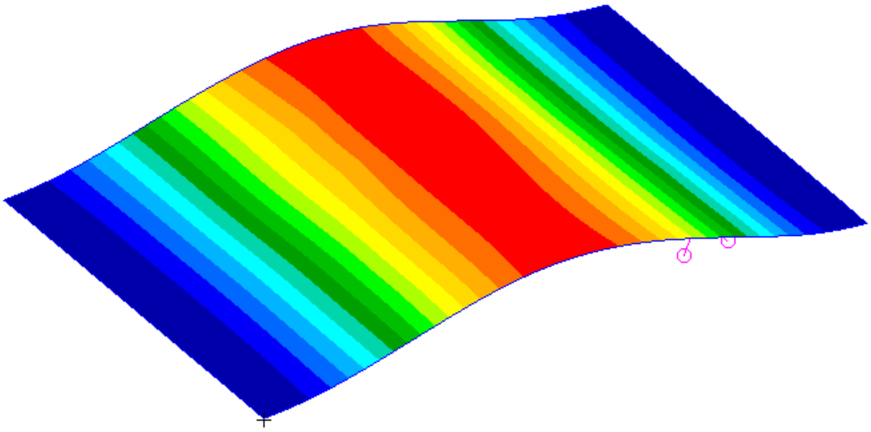

(a)

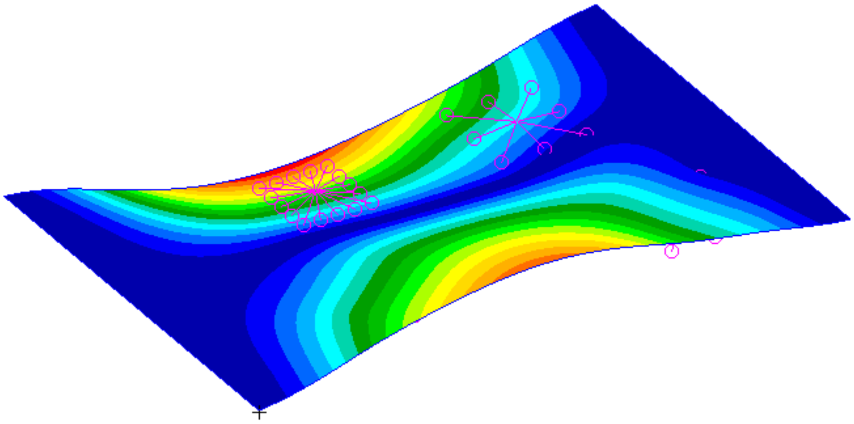

(b)

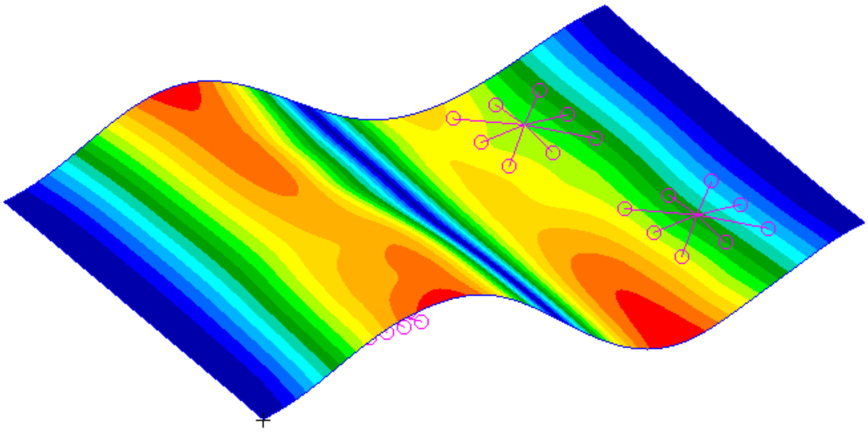

(c)

Fig. IV-23 Representative mode shapes of QFP208 PCB ((a) 119.0 Hz, (b) 216.1 Hz, (c) 374.1 Hz)

Table IV-12 Comparison between methodologies based on MoS of sample QFP208 package (sample set #3)

Design methodol.	MoS					TTF		
	$\dot{\varepsilon}$ (μ-strain/s)	ε_c (μ-strain)	$\varepsilon_{p_{max}}$ (μ-strain)	DF (TTF_{req} =35.2 min)	MoS (TTF_{req} =35.2 min)	TTF_{pred} (min)	TTF_{test} (min)	**Diff. btw. TTF (times)**
Oh-Park methodol.	254,621	208.1	340.5	0.506	0.21	120	277	2.31

Design methodol.	MoS					TTF		
	$\dot{\varepsilon}$ (μ-strain/s)	ε_c (μ-strain)	$\varepsilon_{p_{max}}$ (μ-strain)	DF (TTF_{req} =35.2 min)	MoS (TTF_{req} =35.2 min)	TTF_{pred} (min)	TTF_{test} (min)	**Diff. btw. TTF (times)**
Steinberg's theory	0.812	0.524	0.801	0.506	0.29	184.2	277	1.50

3. Sample Set #4: PBGA388 Package

The evaluation on the PBGA388 package was additionally performed with respect to the PCB with different boundary condition with that shown in Fig. III-24 and III-25. Figure IV-24 shows the illustration of the PCB sample used for the methodology evaluation. The PCB has same dimensions in area as those shown in Fig. IV-22. However, the difference is that the PCB thickness was reduced from 2.4 mm to 1.2 mm and the stiffener made up of aluminum 6061 with 0.8 mm thickness was integrated on the bottom side of the PCB. The sample PCB was exposed to 20 G_{rms} of random vibration excitation until the daisy-chain resistance indicated failure of the solder joint. A TTF_{test} = 277 min was observed from the daisy-chain resistance measurement results shown in Fig. IV-25. The FEM was constructed using the approach shown in Figs. IV-8 and IV-9. The analyzed f_n was 104 Hz.

Table IV-13 summarizes MoS and TTF values calculated by the design methodologies. The MoS calculated by the Oh-Park methodology using FoS_m showed a positive margin and it accurately represents the mechanical safety because TTF_{pred} was 158 min than the TTF_{req} = 35.2 min. In addition, TTF_{pred} has only the difference of 1.8 times with the TTF_{test}. However, the Steinberg's theory showed inaccurate results as the calculated MoS was -0.50 and TTF_{pred} was 13.4 min. These results indicated the effectiveness of the proposed Oh-Park methodology for different boundary condition of PCB.

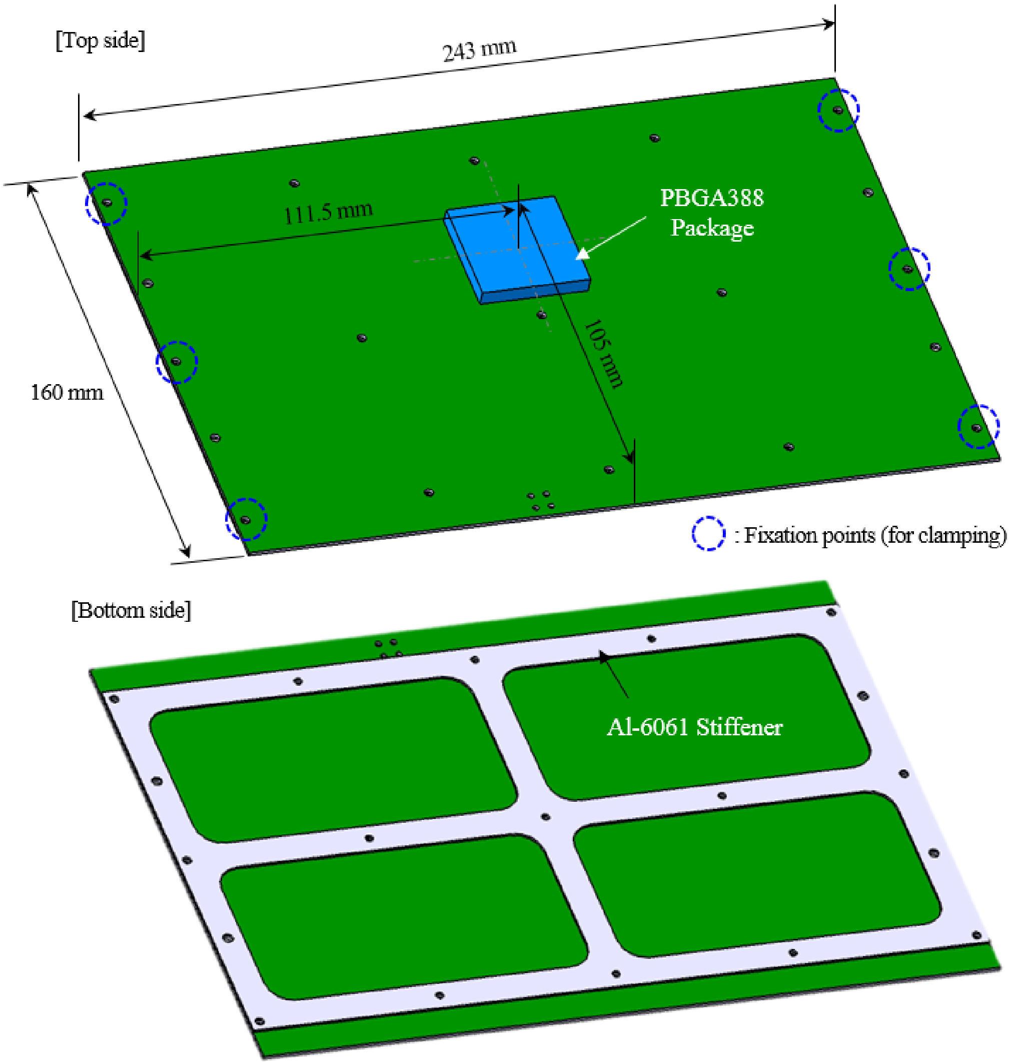

Thickness: 1.2 mm (PCB), 0.8 mm (Al stiffener)

Fig. IV-24 Illustration of PCB sample with PBGA388 package

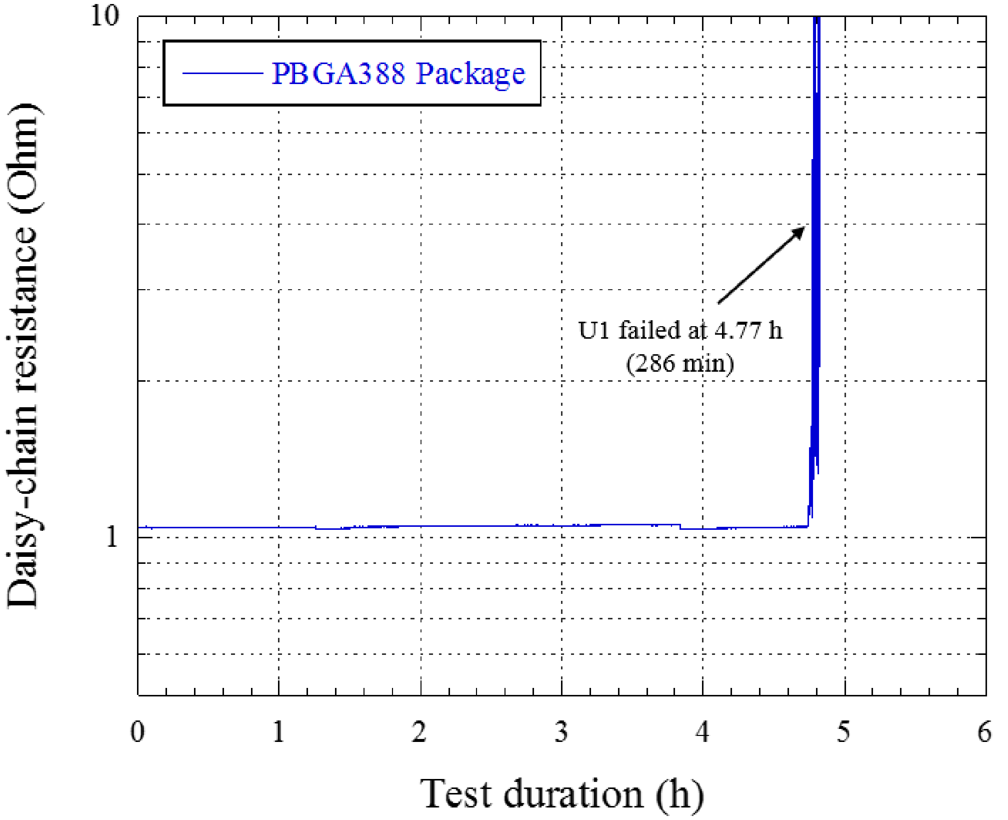

Fig. IV-25 Time profile of daisy-chain resistance for PBGA388 package (sample set #4)

Table IV-13 Comparison between methodologies based on MoS of sample PBGA388 Package (sample set #4)

Design methodol.	**MoS**					**TTF**		
	$\dot{\varepsilon}$ (μ-strain/s)	**ε_c (μ-strain)**	**$\varepsilon_{p_{\max}}$ (μ-strain)**	**DF (TTF_{req} =35.2 min)**	**MoS (TTF_{req} =35.2 min)**	**TTF_{pred} (min)**	**TTF_{test} (min)**	**Diff. btw. TTF (times)**
Oh-Park methodol.	214,292	204.8	327.9	0.495	0.26	158	282	1.8
Design methodol.	**MoS**					**TTF**		
	r	**Z_{allow} (mm)**	**$Z_{\max}$ (mm)**	**DF (TTF_{req} =35.2 min)**	**MoS (TTF_{req} =35.2 min)**	**TTF_{pred} (min)**	**TTF_{test} (min)**	**Diff. btw. TTF (times)**
Steinberg’s theory	0.875	0.626	1.473	0.495	-0.14	13.4	282	21

E. Considerations in Practical Structural Design of Spaceborne Electronics

For the structural design methodology proposed in this study to be used in the practical structural design of spaceborne electronics, the mechanical safety evaluation process is better to be minimized in the viewpoint of a rapid design and evaluation.

1) Possibility of minimizing mechanical safety evaluation process

The evaluation approach described in Fig. IV-1, obviously, requires an increased number of calculation steps to reach the final evaluation results as compared to those of Steinberg's theory that only needs steps 1, 2 and 6. However, steps 3 and 4 to derive the TTF_{req} might be sufficient to be performed once in an entire space program because test and launch processes for all the electronics are determined in accordance with the development model philosophy established in early design process of spacecraft. Meanwhile, the value of DF in step 5 is originally intended to be calculated for each package because f_{n} would be different for each package. However, the highest value of DF among the values for all the packages in the electronics can be derived and applied to all the packages. This would also simplify the calculation process.

In case of the FEM modeling technique for electronic package shown in Fig. IV-8, simulating the package by mesh sizing of the package mounting area on the PCB and connecting different number of rigid links according to the package type is necessary for estimating reliable MoS based on PCB strain. This requires more effort as compared to that of the Steinberg's theory. However, the package type and the number of solder joints on one side of package can be easily found in the package datasheet or specification. No other mechanical information is needed to model the package. Therefore, we can say that it would still be useful for rapid model construction and analysis of electronics, even in the initial structural design phase when the electronics design is not mature.

2) Absence of S-N data of solder or lead material

One potential problem in applying the proposed design methodology is that some solder or lead material developed in recent does not have S-N curve data, which means the absence of fatigue exponent b. This is the limitation in evaluating solder joint safety because additional material fatigue tests are required to obtain that data, which is out of scope of this study. Currently, there is no other option but to apply the value of other similar solder or lead material. Nevertheless, if there is concern with vulnerability to fatigue failure, additional fatigue tests of sample package might be one feasible solution.

3) Assumption in estimation of the number of fatigue cycles

In the proposed design methodology, the number of fatigue cycles N was derived by $f_n \times TTF_{\mathrm{req}}$. This simplified calculation approach was possible under assumption that the N is directly related to f_n. Since the f_n is the fundamental resonant frequency, the participation of the other modes at lower or higher frequency range is not included in estimating the value of N accumulated under given random vibration loading. In case of the single PCB mounted on the rigid base, the f_n is obtained at first major peak response, which is highly dominant in the modal participation point of view. To qualitatively prove this fact, the number of positive zero crossings, ${N_0}^+$, were estimated and compared with the f_n. The definition of ${N_0}^+$ is the average number of times where the displacement trace crosses the zero axis with a positive slope [8]. This value can be estimated from multiple number of responses at various PCB modes as the equation described below.

$$N_0{}^+ = \frac{1}{2\pi}\left(\frac{\frac{\frac{\pi}{2}\cdot P_1\cdot f_1\cdot Q_1}{(2\pi f_1)^2}+\frac{\frac{\pi}{2}\cdot P_2\cdot f_2\cdot Q_2}{(2\pi f_2)^2}+\cdots}{\frac{\frac{\pi}{2}\cdot P_1\cdot f_1\cdot Q_1}{(2\pi f_1)^4}+\frac{\frac{\pi}{2}\cdot P_2\cdot f_2\cdot Q_2}{(2\pi f_2)^4}+\cdots}\right)^{1/2} \tag{IV-14}$$

where, f, P and Q denote eigenfrequency, power spectral density at f and amplification factor at f, respectively.

As a representative example of comparison between $N_0{}^+$ and f_n, the bare PCBs in Case 1, 2 and 3 described above were selected and their test results were used for the estimation. The f and Q values were derived from three major modes for each PCB from the low level sine sweep results. P were derived from the random vibration specification in Table III-2. Table IV-14 (a), (b) and (c) summarizes the results of comparisons between $N_0{}^+$ and f_n for Cases 1, 2 and 3, respectively. The results indicate that all the sample bare PCBs showed $N_0{}^+$ values having differences of less than 6.3 % with f_n. This means that the estimated TTF or N values would have a similar extent of difference. This amount of error does not produce any problem in evaluating mechanical safety of a single PCB by the proposed design methodology because the FoS_{ttf}=4.0 is considered in the TTF_req. However, the modal participation at f_n could be less dominant when the PCB integrated with the housing structure of the electronics as the dynamic coupling between housing and PCB creates various complex modes. However, the error still could be covered by the above FoS_{ttf} value. If necessary, the estimation of $N_0{}^+$ might be one way to investigate on the use of f_n for TTF_req estimation.

4) Estimation of TTF_{req} in various space programs

In the proposed design methodology, TTF_{req}=35.2 min was derived with regards to the development scenario shown in Fig. IV-2. One thing to note is that it is not the fixed value applied for every space program. The scenario shown in Fig. IV-2 was established under assumption that a single electronics (FM) is developed and exposed to vibration during qualification test, acceptance test and launch. If the scenario changes, TTF_{req} shall be calculated based on the changed test and launch processes. In this study, several other examples of TTF_{req} estimation in accordance with three assumed development scenarios were provided. Followings are the development scenarios investigated in this study.

Scenario 1 EQM, QM and FM of electronics are developed and tested separately (One of the typical process in satellite development program) (Fig. IV-26)
- The EQM or QM is not used for flight

Scenario 2 One electronics is developed and undergoes PFM level test and launch (Fig. IV-27)
- Typical duration of random vibration test at PFM level: 1 min (*Qualification level: 2 min)

Scenario 3 Reusable launch vehicle, 20 times of repetitive launch after component acceptance test (Fig. IV-28)
- Vibration during re-entry of launch vehicle was not considered.

Table IV-15 summarizes the estimation results of TTF_{req} with respect to scenario 1. Here, we calculated TTF_{req} for the qualification test of EQM or QM and acceptance test and launch of FM. The TTF_{req}=25.4 min was estimated for the QM with FoS_{ttf} = 4.0 and it was approximately 2.7 times larger value than that of FM even if it undergoes component, payload and satellite system level acceptance tests as well as launch. Therefore, if the structural design is analytically validated for TTF_{req}=25.4 min, the FM would not be failed during acceptance tests and launch.

Table IV-16 summarizes the estimation results of TTF_{req} with respect to scenario 2. Here, we calculated TTF_{req} for the PFM level tests and launch of FM. The TTF_{req}=45.5 min was estimated for the FM with FoS_{ttf} = 4.0. This development approach would reduce the development cost and schedule as compared to the scenario 1 shown in Table IV-15. However, a care must be taken to the increased value of TTF_{req} in the structural design of electronics.

Table IV-17 shows the estimation results of TTF_{req} with respect to scenario 3. Here, we calculated TTF_{req} for the QM and FM of electronics for launch vehicle. In this scenario, the component-level qualification test is separately performed for QM of electronics. FM is fabricated and tested at acceptance level, and then it goes to 20 times of repetitive launch without refurbishment once integrated with the launch vehicle. The TTF_{req}=106.7 min was estimated for the FM with FoS_{ttf} = 4.0. This is 4.2 times larger value than that of QM. These results indicate that the multiple number of repetitive launches produce much larger fatigue damage on the solder joint of electronics as compared to that of qualification-level vibration test. This factor shall be considered for ensuring the structural safety of electronics.

Table IV-14 Comparison between N_0^+ and f_n of bare PCBs

(a) Case 1 PCB

Mode	**Eigenfreq.**	**Amp. Factor**	**PSD Level**
	f (Hz)	**Q (-)**	**P (G^2/Hz)**
1	202	20.9	0.273
2	655	9.3	0.273
3	1644	3.21	0.11
Difference btw. N_0^+ and f_n (%)			**6.30**

(b) Case 2 PCB

Mode	**Eigenfreq.**	**Amp. Factor**	**PSD Level**
	f (Hz)	**Q (-)**	**P (G^2/Hz)**
1	360	26.8	0.273
2	681	3.38	0.273
3	1255	5.2	0.177
Difference btw. N_0^+ and f_n (%)			**3.90**

(c) Case 3 PCB

Mode	**Eigenfreq.**	**Amp. Factor**	**PSD Level**
	f (Hz)	**Q (-)**	**P (G^2/Hz)**
1	498	13.5	0.273
2	898	2	0.273
3	1771	5.84	0.09
Difference btw. N_0^+ and f_n (%)			**4.46**

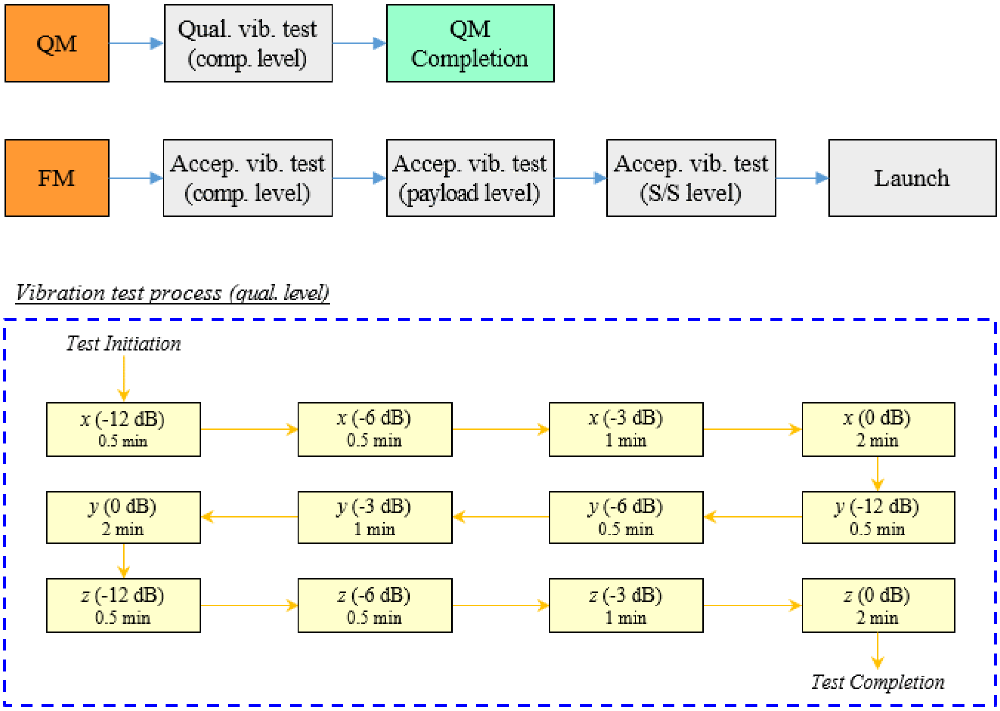

Fig. IV-26 Assumed electronics development scenario 1 (Typical QM-FM approach)

Table IV-15 Estimation results of TTF_{req} for assumed development scenario 1

Step		Factor	Value	Remarks
No. of tests per each test level		N	3	tests per each level in 3 axes
Fatigue exponent for solder joint		b	6.4	for solder or lead frame material
Eqv. time for vibration tests at each test level (min)		T_{-12dB}	0.00007	-12
		T_{-9dB}	0.0007	-9
		T_{-6dB}	0.006	-6
		T_{-3dB}	0.110	-3
		T_{0dB}	2.00	0
Duration for a single test (min)		t_1	0.50	for low level tests (-12, -9, -6 dB)
		t_2	1.00	for accept. test (-3 dB)
		t_Q	2.00	for qual. test (0 dB)
Duration for launch random vibration (min)		t_L	4.00	for launch
QM	Eqv. time for qual. test (comp. level) (min)	ΣT_{C-Q}	6.35	
FM	Eqv. time for accept. test (comp. level) (min)	ΣT_{C-A}	0.35	
	Eqv. time for accept. test (payload level) (min)	$\Sigma T_{P/L-A}$	0.35	
	Eqv. time for accept. test (S/S level) (min)	$\Sigma T_{S/S-A}$	0.35	
	Eqv. time for launch (min)	ΣT_L	1.32	Eqv. to accep. test, 3 axis excitation, 4 min duration
Summary	Factor of safety w.r.t. Required *TTF* (min)	FoS_{ttf}	4	ECSS-E-ST-32C
	Required *TTF* for solder joint (min)	TTF_{req}	25.4	for QM
		TTF_{req}	9.5	for FM

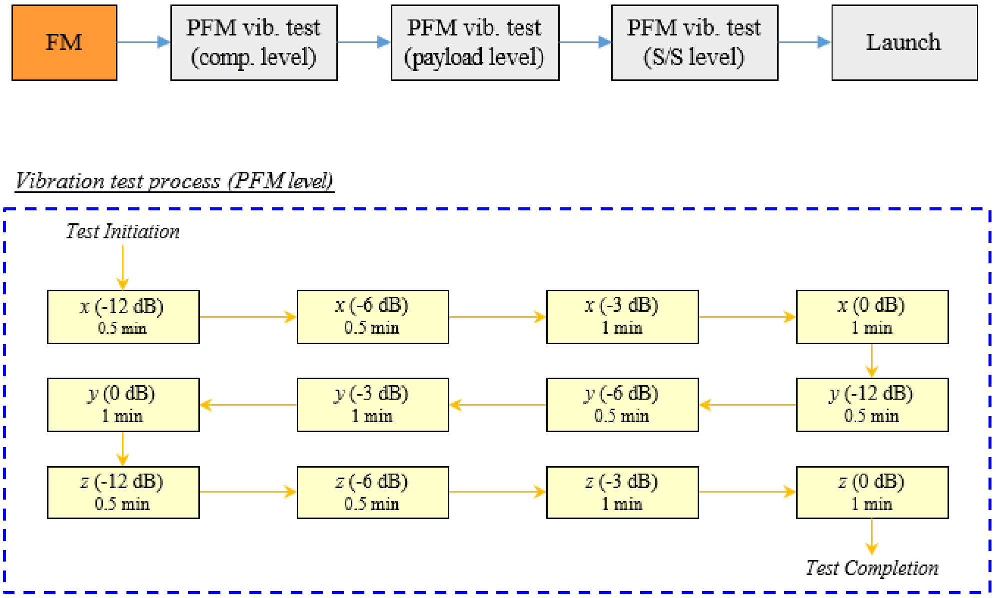

Fig. IV-27 Assumed electronics development scenario 2 (PFM approach)

Table IV-16 Estimation results of TTF_{req} for assumed development scenario 2

Step		Factor	Value	Remarks
No. of tests per each test level		N	3	tests per each level in 3 axes
Fatigue exponent for solder joint		b	6.4	for solder or lead frame material
Eqv. time for vibration tests at each test level (min)		T_{-12dB}	0.00007	-12
		T_{-9dB}	0.0007	-9
		T_{-6dB}	0.006	-6
		T_{-3dB}	0.110	-3
		T_{0dB}	1.00	0
Duration for a single test (min)		t_1	0.50	for low level tests (-12, -9, -6 dB)
		t_2	1.00	for -3 dB test
		t_Q	1.00	for PFM test (0 dB)
Duration for launch random vibration (min)		t_L	4.00	for launch
FM	Eqv. time for qual. test (comp. level) (min)	$\Sigma T_{C\text{-}A}$	3.35	
	Eqv. time for accept. test (comp. level) (min)	$\Sigma T_{P/L\text{-}A}$	3.35	
	Eqv. time for accept. test (payload level) (min)	$\Sigma T_{S/S\text{-}A}$	3.35	
	Eqv. time for accept. test (S/S level) (min)	ΣT_L	1.32	Eqv. to accep. test, 3 axis excitation, 4 min duration
Summary	Eqv. time for launch (min)	FoS_{ttf}	4	ECSS-E-ST-32C
	Required *TTF* for solder joint (min)	TTF_{req}	45.5	for FM

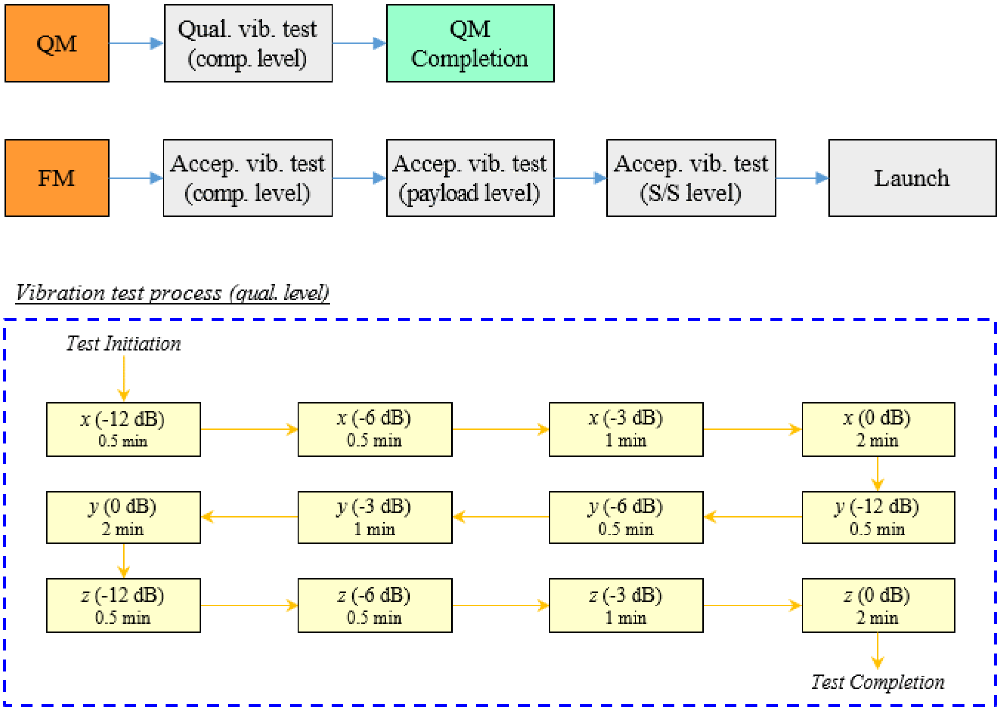

Fig. IV-28 Assumed electronics development scenario 3 (for reusable launch vehicle)

Table IV-17 Estimation results of TTF_{req} for assumed development scenario 3

Step		Factor	Value	Remarks
No. of tests per each test level		N	3	tests per each level in 3 axes
Fatigue exponent for solder joint		b	6.4	for solder or lead frame material
Eqv. time for vibration tests at each test level (min)		T_{-12dB}	0.00007	
		T_{-9dB}	0.0007	
		T_{-6dB}	0.006	
		T_{-3dB}	0.110	
		T_{0dB}	2.00	
Duration for a single test (min)		t_1	0.50	for low level tests (-12, -9, -6 dB)
		t_2	1.00	for accept. test (-3 dB)
		t_Q	2.00	for qual. test (0 dB)
Duration for launch random vibration (min)		t_L	4.00	for launch
QM	Eqv. time for qual. test (comp. level) (min)	$\Sigma T_{C\text{-}Q}$	6.35	
FM	Eqv. time for accept. test (comp. level) (min)	$\Sigma T_{C\text{-}A}$	0.35	
	Eqv. time for accept. test (payload level) (min)	ΣT_L	26.32	Eqv. to accep. test, 3 axis excitation, 4 min duration per launch, 20 times repetitive launch (vibration during re-entry was not accounted for estimation)
Summary	Eqv. time for accept. test (S/S level) (min)	FoS_{ttf}	4	ECSS-E-ST-32C
	Eqv. time for launch (min)	TTF_{req}	25.4	for QM
		TTF_{req}	106.7	for FM test + launch (20 times)

V. Conclusion

In this study, to find a more practical structural design methodology for evaluating mechanical safety on the solder joint in the initial structural design phase of spaceborne electronics under launch random vibration environment, a novel structural design methodology based on MoS calculation with respect to the PCB strain, which makes up for the drawbacks of the Steinberg's fatigue failure theory, was proposed. As a first step for implementing the design methodology, the effectiveness of the use of a PCB strain-based methodology for evaluating solder joint safety was evaluated by comparing the calculated MoS with the results of the fatigue test of the PCB sample with the PBGA packages and TSSOPs under a random vibration environment. In the evaluation, the possibility of using a simplified form of FEM for electronic package was also investigated via the comparison with the detailed FEM. The comparison indicated that the MoS calculated based on the PCB strain was much more effective in evaluating the mechanical safety on the solder joint compared with the conventional Steinberg's theory. In addition, the methodology based on the quasi-static analysis of the simplified FEM using 0D lumped mass and rigid link element was found to be applicable for structural design of electronics as a methodology based on the random vibration analysis of a detailed FEM. The effectiveness of this methodology was also validated for the CCGA package by comparing the calculated MoS with an additional sample test under random vibration.

Based on the PCB strain-based methodology established as described above, a structural design methodology that evaluates the solder joint safety according to the accumulated exposure time to vibration during on-ground tests and actual launch was proposed and investigated with the aim of solving the problem of structural overdesign of electronics caused by the conventional Steinberg's design criterion. The proposed methodology, named as "Oh-Park methodology", evaluated solder joint safety by MoS calculation using FoS_m estimated by total 0 dB equivalent time during the vibration tests and launch. This mitigates problems associated with previous methodologies, i.e., the provision of an excessive margin on the fatigue life of the solder joint. In this study, for the application of the proposed methodology, simplified FEM modeling techniques of the electronic package based on the lumped mass and rigid link elements were developed as a reliable and rapid solution to the structural design of electronics. The novelties and important points of the Oh-Park methodology proposed in this study are summarized in detail as follows.

1) PCB strain-based structural design methodology

The Oh-park methodology evaluates the mechanical safety of solder joint based on the MoS calculation based on PCB strain as described above. The approach of using the PCB strain for calculating MoS of solder joint is key point that provides the novelty of this methodology and has not yet been proposed after appearance of Steinberg's theory in 1970. The proposed MoS calculation methodology eliminated the limitations of the Steinberg's empirical formula, which causes the calculation error in allowable displacement. This could enable more reliable evaluation of solder joint safety in comparison with the conventional Steinberg's theory.

2) Mechanical Safety Evaluation Considering Actual Test and Launch Phases

The important issues associated with the Steinberg's theory, focused in this study, was that the design criterion of 2×10^7 cycles for random vibration provides excessive margin on the fatigue life of solder joint much more than a necessary for survival in test and launch phases. The proposed Oh-park methodology evaluates the solder joint safety according to the accumulated exposure time to the random vibration excitation in a series of on-ground vibration tests and actual launch phases. This approach has not yet been proposed in the previous studies.

3) FEM Modeling Technique for Electronic Package

In regards to the problem of inaccurate mechanical safety evaluation using the Steinberg's theory, the fatigue life prediction theories based on the detailed FEM of electronic package were only solution thus far. However, as described above, the construction and analysis of detailed FEM consumes too much time and effort, such that it is difficult to evaluate the entire electronics with many number of PCBs and packages. The simplified FEM modeling technique using 0D lumped mass and rigid link element, proposed in this study, is effectively reduces the time and effort while proving a reliable evaluation results of solder joint safety. A similar modeling technique has been used in the previous studies, however, used only for analyzing the eigenfrequency and dynamic board displacement. The modeling technique proposed in this study was developed to reliably calculate the PCB strain by determining the number of rigid link connections and shell mesh density of PCB according to various types of packages. This approach has not yet been proposed in the previous studies.

For the experimental validation of the proposed Oh-Park methodology, PBGA388 packages mounted on the PCB with various boundary conditions were exposed to random vibration until solder joint failure was observed. These test results were compared with the MoS calculated in accordance with the evaluation process using the proposed methodology.

TTF_{pred} was also calculated to ensure the reliability of the methodology. In addition, we validated the methodology for the CCGA package and QFP which are commonly used for spaceborne electronics. All of the validation results indicate that the Oh-Park methodology enables reliable and rapid evaluation of the mechanical safety of solder joints for spaceborne electronics. In addition, it might contribute to the reduction in satellite development cost and time as the minimization of the number of development models can be positively considered based on the evaluation using the proposed methodology.

VI. Future Study

The future works on the improvement of the novel PCB strain-based structural design methodology beyond this study are described as follows.

1) Validation on various types of electronic packages & complex PCB configurations

In this study, the Oh-Park methodology was proposed with respect to the several types of packages (PBGA324, PBGA388, CCGA624, QFP208). However, more evaluation shall be validated with respect to the various packages and board configurations to ensure the reliability of this methodology. For example, the other package types such as ceramic QFP (CQFP), ceramic BGA (CBGA), leadless ceramic packages and through hole-type packages are widely used for space application as well but they have not been investigated in this study. In regards to the PCB, more complex configurations including asymmetric shape of board and irregular locations of fixations shall be investigated in the future.

2) Structural design methodology for mechanical shock environment

The Oh-Park methodology was initially proposed in this study for evaluating mechanical safety for launch random vibration environment. However, the design evaluation of electronics with regards to the mechanical shock induced by separations of launcher stage and satellite with on-board deployable appendages shall be performed analytically in the early design phase. Therefore, the methodology for shock environment shall be developed in the future.

3) Application of methodology in actual space applications

Based on the validations described above, the Oh-Park methodology will be evaluated for potential use in other types of integrated packages, such as small outline packages and quad flat packages. In the future, based on the results, the Oh-Park methodology could potentially be applied in actual space programs such as small satellite development. In addition, reusable launch vehicle would be one potential objective for application of proposed design methodology.

References

[1] N. F. de Rooij et al., “MEMS for space”, *Proceedings of International Solid-State Sensors, Actuators and Microsystems Conference*, pp. 17-24, 2009.

[2] H. Ardebili and M. G. Pecht, “Encapsulation technologies for electronic applications”, Elsevier Inc. and William Andrew, MD, USA, 2009.

[3] R. Ghaffarian and N. P. Kim, “Ball Grid Array Reliability Assessment for Aerospace Applications”, Microelectronics Reliability, vol. 39 no. 1, pp. 107-112, 1999.

[4] H. Helvajian, “Microengineering aerospace systems”, 1st Edition, The Aerospace Press, CA, USA, 1999.

[5] R. Ghaffarian, “Microelectronics packaging technology roadmaps, assembly reliability, and prognostics”, *Facta Universitatis-Series: Electronics and Energetics*, vol. 29, no. 4, pp. 543-611, 2016.

[6] L. Tong et al., “Research on the board level reliability of high density CBGA and CCGA under thermal cycling”, *Proceedings of 19th IEEE International Conference on Electronic Packaging Technology (ICEPT)*, pp. 1382–1386, 2018.

[7] J. J. Wijker, “Spacecraft structures”, *Springer Science & Business Media*, Berlin, Germany, 2008.

[8] D. S. Steinberg, “Vibration analysis for electronic equipment”, 3rd Edition, John Wiley & Sons Inc., NY, USA, 2000.

[9] https://stardust.jpl.nasa.gov/mission/details.html

[10] D. Yu, et al., “High-cycle fatigue life prediction for Pb-free BGA under random vibration loading”, *Microelectronics Reliability*, vol. 51 pp. 649-656, 2011.

[11] A. Perkins and S. K. Sitaraman, “Analysis and prediction of vibration-induced solder joint failure for a ceramic column grid array package”, *Journal of Electronic Packaging*, vol. 130, pp. 1-11, 2008.

[12] T. E. Wong et al., “Development of BGA Solder Joint Vibration Fatigue Life Prediction Model”, *Proceedings of 49th Electronic Components and Technology Conference*, pp. 149-154, 1999.

[13] M. Wu, “Vibration-induced fatigue life estimation of ball grid array packaging”, *Journal of Micromechanics and Microengineering*, vol. 19 pp. 1-12, 2009.

[14] S. Mathew et al., “Virtual remaining life assessment of electronic hardware subjected to shock and random vibration life cycle loads”, *Journal of the Institute of Environmental Sciences and Technology (IEST)*, vol. 50, no. 1, pp. 86-97, 2007.

[15] B. Zhao et al., “Simulation of fatigue life of solder ball joints of an ultra-fine-pitch wafer level package”, *5th Electronics Packaging Technology Conference (EPTC)*, pp. 683-686, 2003.

[16] Y. K. Kim, and D. S. Hwang, “PBGA packaging reliability assessments under random vibrations for space applications”, *Microelectronics Reliability*, vol. 55, no. 1 pp. 172~179, 2015.

[17] S. Tripathi et al., “Ceramic column grid array assembly qualification and reliability analysis for space missions”, *IEEE Transactions on Components, Packaging and Manufacturing Technology*, vol. 5, no. 2, pp. 279–286, 2015.

[18] E. Suhir and R. Ghaffarian, “Flip-chip (FC) and fine-pitch-ball-grid-array (FPBGA) underfills for application in aerospace electronics–brief review", *Aerospace*, vol. 5, no. 3, pp. 1–16, 2018.

[19] F. J. Akkara et al., “Effect of solder sphere alloys and surface finishes on the reliability of lead-free solder joints in accelerated thermal cycling”, *Proceedings of 17th IEEE Intersociety Conference on Thermal and Thermomechanical Phenomena in Electronic Systems (ITherm)*, pp. 1374–1380, 2018.

[20] J. Jang et al., “Fatigue life estimations of solid-state drives with dummy solder balls under vibration”, *International Journal of Fatigue*, vol. 88, pp. 42–48, 2016.

[21] S. Hamasha et al., “Long-term isothermally aged concerns for SAC lead-free solder in harsh environment applications”, *Proceedings of IEEE Pan Pacific Microelectronics Symposium*, pp. 1–7, 2018.

[22] M. Jannoun et al., “Probabilistic fatigue damage estimation of embedded electronic solder joints under random vibration”, *Microelectronics Reliability*, vol. 78, pp. 249–257, 2017.

[23] Y. Cinar et al., “Effect of solder pads on the fatigue life of FBGA memory modules under harmonic excitation by using a global-local modeling technique”, *Microelectronics Reliability*, vol. 53, no. 12, pp. 2043–2051, 2013.

[24] S. Saravanan et al., “Fatigue failure of Pb-free electronic packages under random vibration loads”, *International Journal for Computational Methods in Engineering Science and Mechanics*, vol. 19, no. 2, pp. 61–68, 2018.

[25] K. Meyyappan et al., “Knowledge based qualification process to evaluate vibration induced failures in electronic components”, *Proceedings of 2017 ASME International Technical Conference and Exhibition on Packaging and Integration of Electronic and Photonic Microsystems (InterPACK2017)*, pp. 1–9, 2017.

[26] T. An et al., “Vibration lifetime estimation of PBGA solder joints using Steinberg model”, *Microelectronics Reliability*, vol. 102, pp. 1-10, 2019.

[27] S. Su et al., “A state-of-the-art review of fatigue life prediction models for solder joint”, *ASME Journal of Electronic Packaging*, vol. 141, no. 4, pp. 1-33, 2019.

[28] Y. Maniar et al., “Solder joint lifetime modeling under random vibrational load collectives”, *Progress with Lead-Free Solders*, vol. 72, no. 2, pp. 898-905, 2020.

[29] J. Xia et al., “Optimal design for vibration reliability of package-on-package assembly using FEA and Taguchi method”, *IEEE Transactions on Components, Packaging and Manufacturing Technology*, vol. 6, no. 10, pp. 1482-1487, 2016.

[30] http://www.dfrsolutions.com/

[31] M. Grieu et al., “Durability modelling of a BGA component under random vibration”, *Proceedings of 9th International Conference on Thermal, Mechanical and Multiphysics Simulation and Experiments in Micro-Electronics and Micro-Systems* (*EuroSimE)*, pp. 1–8, 2008.

[32] I. H. Jung et al., “Structural vibration analysis of electronic equipment for satellite under launch environment”, *Key Engineering Materials*, vol. 270–273, no. 2, pp. 1440–1445, 2004.

[33] H. U. Oh, S. H. Jeon and S. C. Kwon, “Structural design and analysis of 1U standardized STEP Cube Lab for on-orbit verification of fundamental space technologies”, *International Journal of Materials, Mechanics and Manufacturing (IJMMM)*, vol. 2, no. 3, pp. 239-244, 2014.

[34] G. V. Chary, E. Habtour and G, S. Drake, “Improving the reliability in the next generation of US army platforms through physics of failure analysis”, *Journal of Failure Analysis and Prevention*, vol. 12, no.1, pp. 74-85, 2012.

[35] M. K. Thakur et al., “Estimating fatigue life of space electronic package subjected to launch loads”, *Journal of Materials Science & Surface Engineering Estimating*, vol. 3, no. 1, pp. 181-184, 2015.

[36] S. Qin et al., “Comparing and modifying estimation methods of fatigue life for PCBA under random vibration loading by finite element analysis”, *IEEE Proceedings of 2015 Prognostics and System Health Management Conference (PHM 2015)*, pp. 1–5 2016.

[37] C. Yang and J. Wang, “Steinberg fatigue life prediction of a board-level assembly for random vibrations”, *Proceedings of 18th International Conference on Electronic Packaging Technology (ICEPT)*, pp. 1125-1129, 2017.

[38] A. García et al., “Application of Steinberg vibration fatigue model for structural verification of space instruments”, *AIP Conference Proceedings of Computer Methods in Mechanics (CMM2017)*, vol. 1922, pp. 1–10, 2018.

[39] M. G. Béda, “A curvature-based interpretation of the Steinberg criterion for fatigue life of electronic components”, *Proceedings of 48th International Symposium on Microelectronics (IMAPS 2015)*, vol. 2015, no. 1, pp. 1–6, 2015.

[40] T. J. Logue and J. Pelton, “Overview of commercial small satellite systems in the “new space” age”, *Handbook of Small Satellites: Technology, Design, Manufacture, Applications, Economics and Regulation*, pp. 1-18, 2019.

[41] J. Pelton and D. Finkleman, “Overview of small satellite technology and systems design”, *New Space*, vol. 5, no. 4, pp. 1-21, 2019.

[42] C. S. Ruf et al., “A new paradigm in earth environmental monitoring with the CYGNSS small satellite constellation”, *Scientific Reports*, vol.8, no.1, pp. 1-13, 2018.

[43] M. Hoyhtya et al., “5G and beyond for new space: vision and research challenges” *Proceedings of the International Communications Satellite Systems Conference (ICSSC)*, vol. 29, pp. 1-8, 2019.

[44] G. Dennis et al., “From new space to big space: How commercial space dream is becoming a reality”, *Acta Astronautica*, vol. 166, pp. 431-443, 2020.

[45] ECSS-E-HB-10-02A, “Space engineering-verification guidelines”, *European Cooperation for Space Standardization (ECSS)*, 2010.

[46] Y. I. Parache, P. Ghiglino and N. Perzo, “High performance on-board image processing using canopen for earth observation satellites”, *Proceedings of European Workshop on On-Board Data Processing (QBDP)*, vol. 69, no. 12, pp. 1-7, 2019.

[47] G. Caswell, “17 equations that changed the world – there’s more than that!!! Part 1”, *DfR Solutions*, pp. 1–13, 2014. www.dfrsolutions.com

[48] IPC-WP-011, “Guidance for Strain Gage Limits for Printed Circuit Assemblies”, Association Connecting Electronics Industries (IPC), 2011.

[49] J. De Clerck and D. S. Epp, “Rotating machinery, hybrid test methods, vibro-acoustics & laser vibrometry”, *Proceedings of 34th IMAC–A Conference and Exposition on Structural Dynamics*, vol. 8, 2016.

[50] IPC-9701A, “Performance test methods and qualification requirements for surface mount solder attachments”, *Association Connecting Electronics Industries (IPC)*, 2012.

[51] F. X. Che and J. H. L. Pan, “Vibration reliability test and finite element analysis for flip chip solder joints”, *Microelectronics Reliability*, vol. 49, pp. 754-760, 2009.

[52] DfR Solutions, “Reliability of Pb-free solders”, *DfR Solutions*, www.dfrsolutions.com, 2011.

[53] ECSS-E-ST-32C, “Space engineering - structural general requirements”, *European Cooperation for Space Standardization (ECSS)*, 2008.

[54] D. R. Askeland and P. P. Pradeep, “The Science and Engineering of Materials”, 4th edition, *Springer Science + Business Media*, Berlin, Germany, 2003.

[55] C. Bathias, “There is no infinite fatigue life in metallic materials”, *Fatigue & Fracture of Engineering Materials & Structures*, vol. 22, no. 7, 1999, pp. 559–565.

[56] F. Arabi et al., “Vibration test and simulation of printed circuit board”, *Proceedings of 19th IEEE International Conference on Thermal, Mechanical and Multi-Physics Simulation and Experiments in Microelectronics and Microsystems (EuroSimE)*, pp. 1-7, 2018.

[57] S. Kawamura et al., “Study of the effect of specimen size and frequency on the structural damping property of beam”, *Mechanical Engineering Journal*, vol. 3 no. 6, pp. 1-10, 2016.

[58] J. Jang et al. “Comparison of PSD analysis methods in frequency domain fatigue analysis”, *Journal of the Korean Society for Precision Engineering*, vol. 36 no. 8, pp. 737-743, 2019.

Research Achievements

[International Journals]

1) **Tae-Yong Park** and Hyun-Ung Oh, “Validation of a PCB Strain-based Structural Design Methodology for Reliable and Rapid Evaluation on Spaceborne Electronics under Random Vibration”, International Journal of Fatigue (SCIE), (Accepted)

2) **Tae-Yong Park** and Hyun-Ung Oh, “Validation of the Critical Strain-based Methodology for Evaluating the Mechanical Safety of Ball Grid Array Solder Joints in a Launch Random Vibration Environment”, ASME Journal of Electronic Packaging (SCIE), (Under Review)

3) **Tae-Yong Park**, Seok-Jin Shin, Sung-Woo Park, Soo-Jin Kang and Hyun-Ung Oh, “High-damping PCB Implemented by Multi-layered Viscoelastic Acrylic Tapes for Use of Wedge Lock Applications”, Engineering Fracture Mechanics (SCIE), Vol. 241 (2020) pp. 1-13
https://doi.org/10.1016/j.engfracmech.2020.107370

4) **Tae-Yong Park**, Se-Young Kim, Dong-Woo Yi, Hwa-Young Jung, Jae-Eun Lee, Ji-Hyeon Yun and Hyun-Ung Oh, “Thermal Design and Analysis of Unfurlable CFRP Skin-based Parabolic Reflector for Spaceborne SAR Antenna”, International Journal of Aeronautical and Space Sciences (SCIE), Online (2020) pp. 1-12
https://doi.org/10.1007/s42405-020-00301-7

5) **Tae-Yong Park**, Bong-Geon Chae and Hyun-Ung Oh, “Development of 6U CubeSat’s Deployable Solar Panel with Burn Wire Triggering Holding and Release Mechanism”, International Journal of Aerospace Engineering (SCIE), Vol. 2019 (2019) pp. 1-13
https://doi.org/10.1155/2019/7346436

6) **Tae-Yong Park**, Jang-Joon Lee, Jung-Hoon Kim and Hyun-Ung Oh, “Preliminary

Thermal Design and Analysis of Lunar Lander for Night Survival", International Journal of Aerospace Engineering (SCIE), Vol. 2018 (2018) pp. 1-13
https://doi.org/10.1155/2018/4236396

7) **Tae-Yong Park**, Su-Hyeon Jeon, Su-Jeong Kim, Sung-Hoon Jung and Hyun-Ung Oh, "Experimental Validation of Fatigue Life of CCGA 624 Package with Initial Contact Pressure of Thermal Gap Pads under Random Vibration Excitation", International Journal of Aerospace Engineering (SCIE), Vol. 2018 (2018) pp. 1-12
https://doi.org/10.1155/2018/2697516

8) **Tae-Yong Park**, Su-Hyeon Kim, Hongrae Kim and Hyun-Ung Oh, "Experimental Investigation on the Feasibility of Using Spring-loaded Pogo Pin as a Holding and Release Mechanism for CubeSat's Deployable Solar Panels", International Journal of Aerospace Engineering (SCIE), Vol. 2018 (2018) pp. 1-10
https://doi.org/10.1155/2018/4854656

9) **Tae-Yong Park**, Jong-Chan Park and Hyun-Ung Oh, "Evaluation of Structural Design Methodologies for Predicting a Mechanical Reliability on Solder Joint of BGA and TSSOP under Launch Random Vibration Excitation", International Journal of Fatigue (SCIE), Vol. 114 (2018) pp. 206-216
https://doi.org/10.1016/j.ijfatigue.2018.05.012

10) **Tae-Yong Park**, Joo-Yong Jung and Hyun-Ung Oh, "Experimental Investigation on the Feasibility of Using a Fresnel Lens as a Solar-Energy Collection System for Enhancing On-Orbit Power Generation Performance", International Journal of Aerospace Engineering (SCIE), Vol. 2017 (2017) pp. 1-12
https://doi.org/10.1155/2017/1435036

11) **Tae-Yong Park**, Bong-Geon Chae and Hyun-Ung Oh, "Development of Electrical Power

Subsystem of Cube Satellite STEP Cube Lab for Verification of Space-Relevant Technologies”, International Journal of Aerospace System Engineering (비SCI), Vol. 3 No. 2 (2016) pp. 31-37
http://dx.doi.org/10.20910/IJASE.2016.3.2.31

12) Hyun-Ung Oh and **Tae-Yong Park**, “Experimental Feasibility Study of Concentrating Photovoltaic Power System for CubeSat Applications”, IEEE Transactions on Aerospace and Electronic Systems (SCIE), Vol. 51 No. 3, (2015) pp. 1942-1949
doi:10.1109/TAES.2015.140208

[Domestic Journals]

1) 전영현, **박태용**, 이장준, 김정훈, 오현웅, "달 착륙선의 히터 작동온도 설정에 따른 솔더 접합부의 구조적 신뢰성 분석", 한국항공우주학회지, 제46권 제2호 (2018) pp. 167-174

2) **박태용**, 채봉건, 이장준, 김정훈, 오현웅, "달 착륙선의 착륙 후보지별 열 유입량 분석", 한국항공우주학회지, 제46권 제4호 (2018) pp. 324-331

3) **박태용**, 권성철, 박종찬, 오현웅, "히트싱크 적용에 따른 BGA 패키지의 발사진동 및 궤도 열환경 조건에서의 피로수명의 해석적 검토", 한국소음진동공학회지, 제27권 제5호 (2017) pp. 555-565

4) **박태용**, 박종찬, 박훈, 오현웅, "신뢰성 수명예측 도구 Sherlock을 활용한 랜덤진동에서의 BGA 및 TSSOP 솔더 접합부의 구조 신뢰성 평가", 한국항공우주학회지, 제45권 제12호 (2017) pp. 1048-1058

5) 이명재, **박태용**, 강수진, 장수은, 오현웅, “발사체 분리과정모사 및 단계별 영상획득이 가능한 교육용 물로켓 CULV-1 개발 및 비행시험”, 항공우주시스템공학회지, 제10권 제2호 (2016) pp. 14-21

6) **박태용**, 채봉건, 오현웅, “상용 프레넬렌즈를 이용한 극초소형 위성용 집광형 태양전력 시스템의 궤도 전력생성효율 분석”, 한국항공우주학회지, 제43권 제4호 (2015) pp. 318-325

7) 오현웅, **박태용**, “수동형 자세제어 안정화 방식을 적용한 큐브위성의 열적 특성분석”, 한국항공우주학회지, 제42권 제5호 (2014) pp. 423-429

8) **박태용**, 채봉건, 정현모, 오현웅, “큐브위성용 상용 전력계 부품을 적용한 영구자석 자세제어 안정화 방식 큐브위성의 전력계 개념설계”, 항공우주시스템공학회지, 제8권 제1호 (2014) pp. 42-47

9) 권성철, 정현모, 하헌우, 한성현, 이명재, 전수현, **박태용**, 강수진, 채봉건, 장수은, 오현웅, 한상혁, 최기혁, “우주기반기술 검증용 극초소형 위성 STEP Cube Lab.의 시스템 개념설계”, 한국항공우주학회지, 제42권 제5호 (2014) pp. 430-436

10) **박태용**, 채봉건, 이용근, 강석주, 오현웅, “상용 배열형 렌즈를 적용한 집광형 태양전력시스템의 우주 적용 가능성 실험적 검토”, 한국항공우주학회지, 제42권 제7호 (2014) pp. 622-627

[International Conferences]

1) **Tae-Yong Park** and Hyun-Ung Oh, “Structural Design Methodology of Spaceborne Electronics for Implementing Lightweight and Low-cost Small Satellite Applications”, The 69th International Astronautical Congress (IAC), Cyberspace Edition (Online Conference), 2020

2) **Tae-Yong Park** and Hyun-Ung Oh, “Experimental Validation of using a Critical Strain Theory for Evaluating Mechanical Safety on Solder Joint of Spaceborne Electronics under Random Vibration”, The 32nd International Symposium on Space Technology and Science (ISTS), Fukui, Japan, 2019

3) **Tae-Yong Park** and Hyun-Ung Oh, “Investigation on Fatigue Life of Electronic Package with Thermal Pad under Vibration Environment”, The 3rd Asian Joint Symposium on Aerospace Engineering (AJSAE), Gyeongju, Korea, 2018

4) **Tae-Yong Park**, Gwi-Jung Park and Hyun-Ung Oh, “Enhancement of Thermal Control Performance by Using Liquid Metal Radiator”, The 68th International Astronautical Congress (IAC), IAC-17.C2.7.8-X41120, Adelaide, Australia, 2017

5) **Tae-Yong Park**, Bong-Geon Chae and Hyun-Ung Oh, “Investigation on Thermal Characteristics of Lunar Regolith”, The 9th Asian-Pacific Conference on Aerospace Technology and Science (APCATS) & The 2nd Asian Joint Symposium on Aerospace Engineering (AJSAE), Beijing, China, 2017

6) **Tae-Yong Park**, Young-Hyeon Jeon, Jong-Chan Park, Hyeong-Ahn Kwon and Hyun-Ung Oh, “Fatigue Life Estimation of Spaceborne Electronic by Integrated Life Prediction Tools of Sherlock”, The 31st International Symposium on Space Technology and Science (ISTS), Matsuyama, Japan, 2017

7) **Tae-Yong Park**, Seong-Cheol Kwon and Hyun-Ung Oh, “Development of a 1U Standardized CubeSat of STEP Cube Lab for On-orbit Verification of Space-relevant Research Outputs from Universities in Korea”, The 67th International Astronautical Congress (IAC), Guadalajara, Mexico, 2016

8) **Tae-Yong Park**, Bong-Geon Chae and Hyun-Ung Oh, “Development of Electrical Power Subsystem of Cube Satellite STEP Cube Lab for Verification of Fundamental Space Technology”, The 1st Asian Joint Symposium on Aerospace Engineering (AJSAE), Jeju Island, Korea, 2016

9) **Tae-Yong Park**, Bong-Geon Chae and Hyun-Ung Oh, “Experimental Study on Solar Energy Collection System Using Commercial PMMA Lens for Cube Satellite Application”, The 8th Asian-Pacific Conference on Aerospace Technology and Science (APCATS), Jeju Island, Korea, 2015

[Domestic Conferences]

1) **박태용**, 오현웅, “초소형 위성 전장품 소형/경량화 설계기법 검증”, 한국항공우주학회 2020 추계학술대회

2) 박대일, 채봉건, **박태용**, 오현웅, “초소형 SAR 위성 개념 설계를 위한 예비 열 해석”, 한국항공우주학회 2020 추계학술대회

3) **박태용**, 김홍래, 오현웅, “백두산 폭발징후 관측을 위한 6U 큐브위성 STEP Cube Lab-II의 시스템 설계 결과”, 항공우주시스템공학회 2020 춘계학술대회

4) **박태용**, 김홍래, 오현웅, “광학/중적외선/장적외선 다중밴드 지구관측을 위한

6U 초소형위성 STEP Cube Lab-II 시스템 예비설계”, 한국항공우주학회 2020 춘계학술대회

5) **박태용**, 오현웅, “우주기반기술 검증용 6U 초소형위성 STEP Cube Lab-II 시스템 예비설계”, 항공우주시스템공학회 2019 추계학술대회

6) **박태용**, 오현웅, “초소형위성 STEP Cube Lab-II의 시스템 버짓 분석”, 항공우주시스템공학회 2019 추계학술대회

7) **박태용**, 전수현, 오현웅, “열전도 패드 압축률에 따른 전자패키지의 진동피로수명의 실험적 검토”, 한국소음진동공학회 2018 춘계학술대회

8) **박태용**, 오현웅, “멀티콥터형 소형무인기 전원계통 고장진단방법 고찰”, 항공우주시스템공학회 2017 춘계학술대회

9) 강수진, 권성철, 이명재, **박태용**, 채봉건, 장수은, 오현웅, 한상혁, “우주핵심기술의 궤도검증을 위한 STEP Cube Lab.의 비행모델 개발 및 일련과정”, 한국항공우주학회 2016 춘계학술대회

10) **박태용**, 권성철, 박종찬, 오현웅, “열적패드 압축률에 따른 BGA 패키지의 열탄성 구조 영향성 검토”, 한국항공우주학회 2016 추계학술대회

11) 강수진, 권성철, 이명재, **박태용**, 채봉건, 장수은, 한상혁, 오현웅, “큐브위성 STEP Cube Lab.의 환경시험 및 결과분석”, 한국항공우주학회 2016 추계학술대회

12) 정현모, 권성철, 하헌우, 전수현, 이명재, 강수진, **박태용**, 장수은, 채봉건, 전영현, 한성현, 전성용, 오현웅, “큐브위성 STEP Cube Lab.의 비행모델

개발”, 한국우주과학회 2015 춘계학술대회

13) 정현모, 한성현, 이명재, **박태용**, 오현웅, “큐브위성 STEP Cube Lab.의 우주기술 검증용 탑재체”, 한국우주과학회 2014 춘계학술대회

14) **박태용**, 채봉건, 오현웅, “큐브위성 STEP Cube Lab.을 이용한 집광형 태양전력 시스템 검증”, 한국우주과학회 2014 춘계학술대회

15) **박태용**, 전영현, 김가람, 오현웅, “상용 멀티어레이 렌즈를 적용한 집광형 태양 전력시스템의 유효성 검증”, 항공우주시스템공학회 2014 춘계학술대회

16) 장수은, 전수현, 권성철, 이명재, 한성현, **박태용**, 장태성, 오현웅, “Payload Level Launch Environment Verification Test of STEP Cube Lab.”, 한국우주과학회 2014 추계학술대회

17) **박태용**, 정현모, 오현웅, “큐브위성 전용 상용 전력계를 적용한 영구자석 안정화 자세제어 방식 큐브위성의 전력계 개념설계”, 항공우주시스템공학회 2013 춘계학술대회

18) 정현모, 권성철, 이명재, 전수현, **박태용**, 강수진, 차진영, 오현웅, “극초소형위성 TRANSCUBER의 시스템 개념설계”, 항공우주시스템공학회 2013 춘계학술대회

19) 권성철, 하헌우, 정현모, 한성현, 이명재, 전수현, 김영욱, 박태용, 강수진, 차진영, 장수은, 채봉건, 오현웅, “우주기반기술 검증용 STEP Cube Lab.의 시스템 설계”, 한국우주과학회 2013 추계학술대회

20) 권성철, 정현모, 하헌우, 한성현, 전수현, 이명재, 김영욱, 강수진, **박태용**,

차진영, 채봉건, 장수은, 오현웅, “우주기초기술의 궤도검증을 위한 STEP Cube Lab.의 시스템 개념설계”, 항공우주시스템공학회 2013 추계학술대회

[Patents]

1) 출원번호: 16/193,195 (미국), “포고핀을 적용한 큐브위성용 태양전지판 분리장치”, 발명자: 오현웅, 김홍래, 사공영보, 김수현, **박태용**

2) 등록번호: 10-2116755, “기판 변형률 기반의 솔더 접합부 구조 건전성 평가를 통한 전자 패키지 구조 설계 방법”, 발명자: 오현웅, **박태용**

3) 등록번호: 10-2114295, “다축 구속이 가능한 큐브 위성용 전개구조물 구속/분리 장치”, 발명자: 오현웅, **박태용**

4) 등록번호: 10-2084710, “포고핀을 이용한 큐브위성용 전개구조물 분리장치”, 발명자: 오현웅, 김수현, **박태용**, 사공영보, 김홍래

【감 사 의 글】

고등학교 1학년이었던 2008년, 나로호 첫 발사가 이뤄지는 장면을 보면서 우주공학 분야의 엔지니어를 업으로 삼겠다는 목표를 가졌었습니다. 그 후 조선대학교 항공우주공학과에 입학하여 신입생으로 1년을 보내면서 이 분야에서의 커리어를 쌓기 위해 박사가 필요하다는 생각을 갖고 다소 이른 시기인 학부 2학년 때 우주기술융합연구실에서 학부 연구생으로 연구를 시작했습니다. 그리고 9년이 지난 지금 박사학위논문 심사를 마치고 최종 논문을 마무리하고 있습니다. 연구에 있어서는 코흘리개 어린아이였던 저를 9년간 헌신적으로 지도해주신 오현웅 교수님께 깊은 감사의 말씀을 올립니다. 9년 간의 연구과정 동안 제 부족한 실력으로 정말 혼이 많이 났지만 돌이켜보면 지금의 순간까지 도달하기 위해 반드시 필요한 과정이었습니다. 학위논문 심사를 흔쾌히 수락해주시고 바쁘신 와중에 세심하게 논문을 검토해주신 유영준 박사님, 전북대 임재혁 교수님, 안규백 교수님, 그리고 솔탑 김홍래 책임님께도 감사의 말씀드립니다. 덕분에 학위논문이 무사히 잘 마무리될 수 있었습니다.

그간의 연구과정은 당연하게도 쉽지 않은 순간들의 연속이었습니다. 이해되지 않는 해석과 실험 결과를 이해하기 위해 수많은 논문들을 찾아보며 실마리를 찾아 그래프 하나, 표 하나를 뽑아내는 과정들을 비롯해 그것들을 모아 논문으로 탄생시키는 작업은 매번 할 때마다 넘기 힘든 산과 같이 다가왔습니다. 대학원 과정의 첫발을 딛는 석사 1학기를 이제 막 시작했을 무렵, 연구실에서 하고 있는 일들이 잘 풀리지 않아 대학원 과정을 포기하려고 했던 때가 있었습니다. 그러나 지도교수님과 연구실 선배, 동료들의 지속적인 관심과 조언으로 그 시기

를 극복할 수 있었습니다. 다만, 그 때 이후의 저는 이 과정을 모두 견디고 박사까지 해야 하는 이유에 대해서 처음으로 진지한 고민을 했고, 이 과정에서 얻은 나름의 답이 제가 박사과정을 끝까지 마칠 수 있었던 원동력이 되었습니다. 그것은 자기 자신이 할 수 있는 임계점을 넘길 만큼의 노력이 이뤄져야 만이 성장이 가능하다는 어떤 책의 한 구절이었습니다.

제가 만약 석사과정 1학기였던 그 때 대학원을 그만두고 다른 분야를 선택했더라도 그 분야에서 성공하기 위해 임계점을 넘겨야 하는 것은 마찬가지일 것이라는 생각이 들었습니다. 저는 석사과정까지는 제가 선택한 분야에서의 임계점을 넘기지 못했다고 생각했습니다. 그래서 제가 선택한 길의 끝에 무엇이 있을지는 반드시 임계점을 넘어서 확인해보겠다는 나름의 의지를 갖고 박사과정을 시작했습니다. 연구 과정에서 의문은 되도록 끝까지 물고 늘어지고, 논문을 찾아 읽고 기억하는 일을 잘 되지 않더라도 계속 반복했습니다. 그렇게 박사과정 연차가 올라가자 몇 년 전 학부생, 석사과정 때는 불가능해 보였던 것들이 점차 가능해졌고, SCI 논문을 쓰는 과정이 조금씩 덜 어렵게 느껴졌습니다. 또한 하고 있는 모든 일에 대해 자신감을 갖기 시작했습니다. 박사과정은 단연코 쉽지 않은 과정이었지만, 이 과정에서 제가 느낀 것은 임계점을 넘기기 전까지는 다소 앞이 보이지 않더라도 우직하게 견뎌내는 과정이 필요하다는 것이었습니다. 이 것이 실험실이 처음 생겼을 때부터 전해 내려온 오랜 슬로건인 ‘맨 땅에서 우주로’를 실현하는 하나의 정신이었다고 생각합니다. 그것을 견디는 과정에서 점차 변화한 저의 모습은 제 맘에 들었고, 이와 같은 성취를 느낄 수 있음을 인생의 축복으로 생각하고 있습니다.

또한, 박사과정 중 느낀 다른 한가지는 혼자서 모든 것들을 견디면서 할 수

있는 건 한계가 있다는 것이었습니다. 학부 때 초소형위성 프로젝트를 하면서 위성 시스템 하나를 만들어내는 과정이 쉽지 않음을 느꼈고 매번 어려운 상황에 부딪칠 때마다 추위 속에서 체온을 나누듯 연구실 1기 팀원들이 한데 모여 그 상황들을 견디며 문제를 하나씩 해결해 나갔습니다. 그렇게 2년여 간의 개발과정을 거쳐 위성 비행모델 완성에 이르렀던 경험은 제 기억 속의 진한 향수로 남아 있습니다. 그 후 박사과정을 마치기까지도 저는 연구를 위해 했던 일들 중 100% 혼자 한 것이 없다고 생각하고 있고, 감사하게도 주변에 여러 분들의 지원과 격려가 있었기에 가능했다고 생각하고 있습니다. 연구실 1기 멤버들인 명재형, 성철이형, 수현누나, 현모형, 헌우형, 수진, 봉건, 영현은 모두 대학에 와서 10년이 넘는 시간 동안 지속되고 있는 오랜 인연들이며, 현재 멤버들인 연혁, 지성, 석진, 수현, 혜인, 민영, 재현, 재섭, Shankar도 1기 멤버 이후에 함께 연구를 했던 소중한 사람들입니다. 결과적으로 학위과정은 본인 손에서 마무리되고 저 또한 당연히 그랬지만, 이 인연들이 있었기에 할 수 있었다고 생각하여 항상 감사한 마음을 갖고 있습니다.

이제 대학원을 마치고 저는 13년 전 고등학생 시절에 품었던 목표인 우주공학 분야 엔지니어 중 한명으로서 현업에서 커리어를 쌓아가고자 합니다. 박사가 되는 이유 중 하나는 한 명의 독립연구자로서 연구를 수행할 수 있는 사람이 되는 것이라고 생각합니다. 그러나 박사학위만 받았다고 곧바로 그러한 사람이 될 수 없으며, 그 이후에도 부단한 노력이 필요할 것입니다. 그렇기에 박사학위를 받았다는 것이 무언가를 이룬 것이 아니라, 이제 진짜 무언가를 이루기 위한 출발선상에 선 것이라는 마음가짐을 갖고 학위과정을 마치고자 합니다. 이것이야말로 박사가 되는 목표를 이뤘다고 자만하거나 나태에 빠지지 않는 저만의 마인

드 셋입니다. 앞으로 한 명의 엔지니어로서 현업에서 만날 엔지니어들과 협력하며 겸손한 자세를 갖고 덕을 쌓으며 성장해 나가겠습니다.

마지막으로 항상 저에게 아낌없는 사랑과 지원을 해 주신 부모님께 감사의 말씀을 올리며 이 학위논문을 바칩니다. 제가 박사를 할 수 있었던 데에는 앞서 말한 여러가지 이유들이 있었으나, 부모님의 관심과 지지가 가장 컸습니다. 항상 사랑하고, 감사합니다.

2021년 1월 7일

박태용